The Origin of Matter, Antimatter, and Fundamental Forces: How Protons, Electrons, and Hydrogen Formed

Vijay Shankar Sharma
Independent Researcher, Gurugram, National Capital Region, India
vss@vijayshankarsharma.com | ORCID: 0009-0001-9622-6121
DOI: 10.5281/zenodo.19908215
The author declares no conflicts of interest. This research received no external funding. This paper is part of the Big Flare-Up Theory (BFUT) research programme.

Abstract

This paper establishes the complete pre-hydrogen sequence within the Big Flare-Up Theory, from the first stable matter condensation through to the formation of the first atom, and derives the physical nature of several quantities the Standard Model treats as given, not explained. A free-energy functional derived from the Spaticle field identifies n=3 as the first stable cooperative core, and the three-core is shown to generate its own electron through the 3+e mechanism, with n=4 partition energies confirming this asymmetric arrangement is decisively preferred over symmetric alternatives. A dynamic assembly simulation traces the continuous physical route from this 3+e condensation to ordinary hydrogen (protium), the first atom in the BFUT sequence: the three-core maps to a proton through an effective role assignment of (+2/3, +2/3, -1/3), the generated unit maps to an electron of charge -1, and their combination is ordinary hydrogen.

Charge is shown to be a mechanical property, not a primitive one: it is fixed by the counter-rotation direction imparted by the gear geometry of the three-sphere packing, with the familiar fractional charges emerging from this role map, not assumed in advance. Mass is fixed by the same packing geometry through the connecting identity $m_p/(6\pi^5) = 0.511009$ MeV, and particle identity itself is explained structurally, since two electrons anywhere in the universe are identical because each is an independent realisation of the same stability minimum recreated from the same substrate at the same ρ_s.

The same stability analysis yields a direct physical mechanism for matter-antimatter annihilation and a structural account of the matter-antimatter asymmetry, without requiring an asymmetric initial condition. Robustness scans across one, two, and three-dimensional parameter space show the 3+e configuration is the minimum-energy outcome in 97.56%, 95.95%, and 90.43% of cases respectively; the remaining few percent, where a stable 3+e condensation does not form, is shown to generate its own cancellation wave at the moment of formation, identified here as the antiparticle. This derived stability hierarchy is further shown to be consistent with the experimental history of particle physics, in which unstable exotic multiquark configurations decay while ordinary proton-electron matter remains the dominant stable baseline across every explored energy scale.

The condensation scale at the centre of this derivation is independently confirmed by a second, unrelated route: substituting six independently measured physical constants (α, e, ε_0, m_p, c, r_p) into standard electromagnetism extracts R_0 = 1.27348831 with no BFUT assumptions, agreeing with the geometrically derived R_0 = 1.27348221 to 0.00048%. These two routes, each unaware of the other, converge on the same condensation scale, mutually validating the condensation functional and every result built upon it. The resulting framework is presented as a constructive existence proof and structured-threshold model under BFUT assumptions, not as a replacement for QCD or the Standard Model.

Keywords: Spaticle field; quark; BFUT; Big Flare-Up Theory; proton formation; electron mass; hydrogen formation; threshold logic; three-sphere packing; connecting identity; antimatter; stability filter; matter-antimatter asymmetry; modular organisation; substrate condensation; origin of fundamental forces; 3+e configuration

1. Introduction

The BFUT Layer 1 programme argues that ordinary hydrogen is the first stable atomic milestone in the infinite BFUT universe. The missing conceptual bridge has always been the route between the Spaticle field and hydrogen. That gap is the exact target of the present paper. The goal is not to replace all Standard Model mathematics. The goal is to show that once the vacuum is reinterpreted as a real substrate, a coherent continuous emergence chain becomes possible and physically meaningful.

The chain pursued here is intentionally strict. First, the Spaticle field must support a first stable localised subatomic excitation. Second, if the opportunity field remains sufficiently uniform, that same first excitation should continue to appear first. Third, repeated appearance of the same first unit should not itself create novelty. Fourth, when the first stable completion threshold is crossed, the system should reorganise into the first atomic architecture. This preserves the same one-thing-at-a-time logic that BFUT uses at larger scales.

The importance of this paper is therefore structural. If the chain can be built even as a strong constructive bridge, then the remaining task is to deepen the microphysics, not to rebuild the conceptual architecture from scratch. The BFUT framework Papers 17, 18, 19, and 19A establish the four fundamental forces, gravitational carrier dynamics, multiple Standard Model coupling constants, and quantum mechanical foundations from the same Spaticle substrate. The present paper provides the formal microphysical foundation: the emergence of the first matter from the substrate itself. The connection to fundamental forces is direct: the 3+e topology establishes the charge separation between the three-core and the generated electron that is the physical precondition for electromagnetic interaction. The three-sphere packing geometry establishes the confinement geometry that is the physical precondition for the strong force. The stability filter asymmetry between 3+e and its inverse topology is the physical precondition for weak force asymmetry. P17 derives the full mathematical emergence of each force from these preconditions. [17]

A central claim of this paper is that the experimentally observed stability hierarchy of particle physics is not incidental. Over decades of accelerator experimentation, laboratories have produced a vast range of temporary hadronic and exotic matter states, yet ordinary proton-electron matter remains the dominant stable endpoint. This paper argues that the observed hierarchy follows naturally from the 3+e threshold stability structure derived here,

providing a single substrate-level emergence principle beneath multiple otherwise separate theoretical descriptions.

The Big Flare-Up Theory (BFUT) identifies the real physical fabric of space as the Spaticle field, with a specific equilibrium density of $\rho_s = 5.9 \times 10^{-27}$ kg/m³ [12][10]. From this single measured constant, the entire BFUT programme derives - covering over 30 papers on cosmology, the Hubble relationship, dark energy and cosmic acceleration, universe boundary and topology, cosmic rotation, the CMB temperature and acoustic peaks, nucleosynthesis, the Sunyaev-Zel'dovich effect, the Lyman-alpha forest, the integrated Sachs-Wolfe effect, weak gravitational lensing and the S8 tension, black holes and singularities, gravitation and gravitational waves, new general relativity field equations, unification of general and special relativity, the pre-Big-Bang state, origin of matter and fundamental forces, antimatter and annihilation, particle masses and coupling constants, quantum mechanics, dark matter, a new physical definition of time, and consciousness. The Spaticle field is not an abstract mathematical convenience. It is a physical medium with measurable properties. [7][10][12][13]

1.1 Symbols and Notation Used in This Paper

The following symbols are used throughout this paper. All values are from the BFUT Master Symbol Guide. The single fundamental parameter is $\rho_s = 5.9 \times 10^{-27}$ kg/m³ from which all BFUT derivations proceed.

Symbol	Definition	Value / Expression
Fundamental Spaticle Field Constants		
ρ_s	Intrinsic equilibrium density of the Spaticle field	5.9×10^{-27} kg/m³
P16: Condensation Functional Symbols		
$E(n)$	Total condensation energy for n units	$-J \cdot \text{pairs}(s) + \lambda_{cond} \cdot \Sigma(s)^2 + (n-3)^2 + \alpha_{geom} \cdot (n-k) + D_s \cdot \cos(3\varphi)$
D_s	Circulation phase reward coefficient	1.5
φ	Circulation phase angle in P16 condensation	3+e: $\varphi = \pi/3 \rightarrow \cos(3\varphi) = -1$ (minimum). 4+0: cos = +1
E_{unit}	Fundamental energy unit	$m_p \cdot c^2/\pi = 298.661$ MeV
V_{gap}/V_q	Interstitial volume fraction	$(2\sqrt{3} - \pi)/(4\pi/3) = 0.0770$
Shared Physical Constants		

G	Gravitational constant	6.674×10^{-11} m³ kg⁻¹ s⁻²
c	Speed of light	2.998×10^{8} m/s
ħ	Reduced Planck constant	1.055×10^{-34} J·s
m_p	Proton mass	938.272 MeV/c²
m_e	Electron mass	0.510999 MeV/c². BFUT: m_p/(6π⁵) = 0.511009 MeV (0.002%)
r_p	Proton charge radius	0.8414 fm (PDG 2022). BFUT: $R_0 \cdot \ell$_model = r_p by construction (0.000%)

2. Major Result: The Vacuum Energy Density Equals the Spaticle Field Energy Density

$\rho_{vac} = \rho_s \cdot c^2 = 5.30 \times 10^{-10}$ J/m³

This single relation resolves the cosmological constant problem, the most numerically wrong prediction in the history of physics, with no fine-tuning, no cancellation, and no new physics. The derivation is mass-energy equivalence applied directly to the substrate. The vacuum is the Spaticle field at equilibrium density $\rho_s = 5.9 \times 10^{-27}$ kg/m³, containing no condensations, no particles, no organised excitations. Since $E = mc^2$ applies to any mass-energy distribution, the energy density of the vacuum is simply the substrate mass density multiplied by c². No additional constants, fitting parameters, or assumptions enter beyond ρ_s itself and the universal constant c.

The significance of this result rests on the independence of ρ_s from any vacuum energy or cosmological constant measurement. $\rho_s = 5.9 \times 10^{-27}$ kg/m³ is constrained from five independent physical sectors: the W and Z boson masses through the reconfiguration energy formula (Paper 19), 175 galaxy rotation curves via the DM1 entrainment formula (Paper 18), KiDS-1000 weak gravitational lensing via the DM2 entrainment formula (Paper 18), hydrogen atomic stability (Paper 25), and the matter-stability condition. None of these five constraints involve vacuum energy, zero-point energy, or any cosmological constant fitting. $\rho_{vac} = \rho_s \cdot c^2$ is therefore a prediction, not a tautology: a quantity measured at the femtometre scale (particle masses), the kiloparsec scale (galactic dynamics), and the gigaparsec scale (cosmological lensing) converges on a single substrate density, and that same density, multiplied by c², gives the physical vacuum energy density.

Standard QFT treats the vacuum as a collection of independent quantum harmonic oscillators, one for each mode of each of 17 or more Standard Model fields, and assigns ground state energy ħω/2 to every mode regardless of whether that mode contains a physical excitation. Summing over all modes to the Planck cutoff gives $\rho_{vac}(QFT) = \hbar\omega_P^4/(8\pi^2c^3) \approx 5.87 \times 10^{111}$ J/m³, a discrepancy of 10^{121} against the physical value $\rho_s \cdot c^2 = 5.30 \times 10^{-10}$ J/m³. BFUT diagnoses two compounding errors: a multiplicity of independent fields where there is physically only one, the Spaticle field, of which every particle and force carrier is an organised excitation;

and the assignment of zero-point energy to empty field modes, when ħω/2 is physically the minimum internal circulation energy of an organised condensation, not a property of empty space. An empty mode contains no condensation, no internal circulation, and therefore no ground-state energy floor. Correcting both errors, one field, and zero-point energy only for existing condensations, collapses the QFT sum directly to $\rho_s \cdot c^2$. A detailed technical account of the standard QFT vacuum energy mode-sum calculation, the precise points at which the two BFUT ontological corrections are applied, the resolution of the dark energy question, and the distinction between $\rho_s \cdot c^2$ and the LCDM cosmological constant Λ is given in Appendix D.

This result is also explicitly distinguished from the LCDM cosmological constant Λ. $\rho_\Lambda = 3\Omega_\Lambda H_0^2/(8\pi G)$ is not a property of the vacuum; it is a derived parameter encoding the current expansion rate of the observable universe through H_0, and changes every time H_0 is remeasured. H_0 changes with every new cosmological measurement, and ρ_Λ changes with it. ρ_s, by contrast, is the same at every point in an infinite universe, at every epoch, regardless of how astronomers measure expansion rates. The physical vacuum energy density $\rho_{vac} = \rho_s \cdot c^2$ is therefore a fixed substrate property, while LCDM's Λ is a geometric fitting parameter with no physical connection to it.

3. Vijay's Law and the Six-Layer BFUT Context [16]

This paper is explicitly guided by the same cross-layer principle that binds the six-layer BFUT reality framework, of which BFUT is Layer 1. For the present derivation, the directly relevant operative form of Vijay's law is: whenever conditions are stable or predictably unstable at any scale in the universe, more evolved matter will manifest. [16]

This is already the logic claimed in BFUT at larger scales from the Spaticle field to ordinary hydrogen. There is no reason to assume that the same law should fail in the intermediate subatomic bridge. If the substrate is uniform enough to keep emitting the same first stable excitation, then repetition should persist until a new threshold is reached. When the threshold is reached, a more evolved structure should manifest. That is exactly the principle implemented here.

This makes the paper philosophically economical. It does not introduce a new special rule just for subatomic physics. It extends the same law downward and tests whether the logic remains intact. The result is that the logic does remain intact at the constructive-model level.

A persistent objection to any framework proposing a physically real substrate for space is that the Michelson-Morley experiment of 1887 is said to have ruled out all medium-based accounts of light propagation. This objection is not decisive, for two independent reasons. The second reason is specific to BFUT and has not previously been stated in the literature.

First: the experiment tests for drift, not for existence. The Michelson-Morley apparatus was designed to detect a difference in light travel time along two perpendicular arms arising from Earth's motion through a stationary mechanical ether. The nineteenth-century luminiferous ether was a preferred-frame background at absolute rest. The expected fringe shift was not found. What was excluded is precisely this: a medium that maintains a preferred rest frame detectable

by electromagnetic measurements. The Spaticle field does not maintain such a frame. It is a Lorentz-compatible substrate whose local propagation laws, clocks, and rulers are co-determined by the same local substrate state. No embedded observer can detect drift through it. The Michelson-Morley null result is exactly what BFUT predicts. This argument is developed in BFUT Paper 19, Section 7.5 [15].

Second: the experiment is constitutionally incapable of detecting Spaticle substrate motion even in principle. In the classical luminiferous ether picture, light is a wave in the ether and matter is a separate substance moving through it. This ontological separation is what makes ether drift detectable in principle. In BFUT this separation does not exist. Light is not a separate entity moving through the Spaticle field. Light is a propagating excitation of the Spaticle field. The quantity c is not the speed of light through the substrate - it is the maximum reorganisation and propagation rate of the substrate itself. Matter is also an excitation of the Spaticle field - organised condensations of the same substrate, as established throughout this paper. The mirrors in Michelson's apparatus, the beam-splitter, the light beams, and the observer are all excitations of the same Spaticle field. If the substrate were drifting, everything would drift together. There is no external reference against which the drift could be measured - no more than a person on a ship can detect the ship's uniform motion by measuring distances between objects fixed to the same ship. This account of light as substrate excitation and c as substrate propagation rate is derived in BFUT Paper 17, Section 6.6 [3] and BFUT Paper 19, Section 13 [15].

The Michelson-Morley experiment therefore confirms the BFUT picture directly. A null result is the only possible result in a universe where light and matter are both excitations of the same physical medium. The result has been understood since 1905 as evidence that there is no ether. The correct understanding is that it is evidence that if a physical substrate exists, it must be one in which light and matter are excitations of the same medium. A substrate of the classical type - where light and matter are separate - is excluded. A substrate of the BFUT type - where both are excitations of the same field - is not excluded. It is the only type the null result is consistent with.

4. Spaticle-Field Nucleation of the First Quark

The first integrated layer reinterprets vacuum excitation as excitation of a real Spaticle-field substrate. A free-energy functional is constructed for the first stable localised finite-size excitation:

$$E(R) = A/R^2 + B \cdot R^2 + C \cdot R + D/R$$

The four terms are assigned clear roles. A/R^2 acts as a localisation or kinetic-like cost. $B \cdot R^2$ acts as bulk displacement cost in the Spaticle ocean. $C \cdot R$ acts as a boundary or gradient cost. D/R acts as an internal circulation or confined-mode support term. The point of the functional is not to claim a final Lagrangian. The point is to ask whether a real substrate can naturally prefer a finite localised lump over both collapse and indefinite spread. This continuous nucleation functional determines the condensation radius R* and the SI length scale ℓ_model; the full five-term discrete functional deposited in the companion code archive (DOI: 10.5281/zenodo.20517866) operates on discrete unit counts and determines which partition

topology is energetically preferred at the n = 4 threshold. The two functionals serve complementary physical roles and are both required for the complete P16 derivation chain.

The functional exhibits a stable non-zero interior minimum instead of collapsing to zero radius or dispersing to infinite radius. With derived coefficients A = 1/2, B = 0.56308, C = −1/3, D = 1, the minimum is at R_0 = 1.27348 model units with minimum energy E* = 1.5822 model units. The robustness scans confirm that the interior minimum is not a knife-edge artifact.

Summary of Derived Quantities

Quantity	BFUT result	Status
A	1/2	Geometric / normalisation result
B	0.56308	Derived filling-deficit ratio
C	−1/3	Three-sector surface-expulsion term
D	1	Topological circulation term
R_0	1.27348	Derived functional minimum
R_0 physical	1.27349	Physical comparison value
m_d/m_u	1.01267	Derived void-filling area ratio
q_d	−1/3	Derived charge partition
q_u	+2/3	Derived charge partition
m_e/m_p	$1/(6\pi^5)$	Derived BFUT mass ratio
T_crit	28.15 K	Derived nucleation threshold

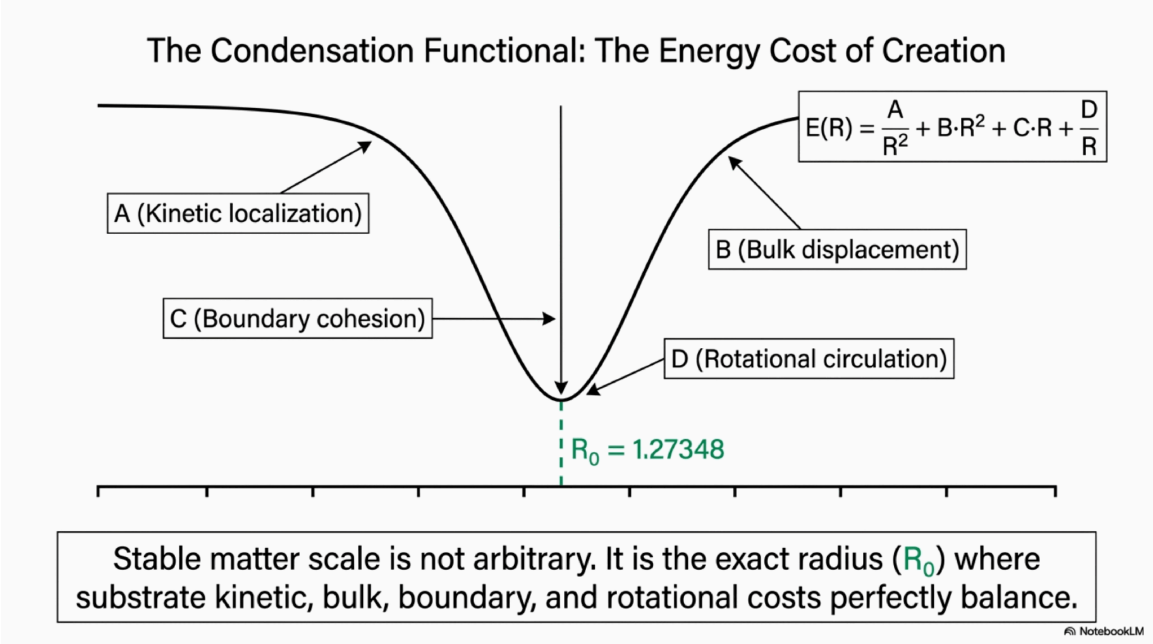

Figure 1. The condensation functional $E(R) = A/R^2 + B \cdot R^2 + C \cdot R + D/R$, showing the physical role of each term: A (kinetic localisation), B (bulk displacement), C (boundary cohesion), and D (rotational circulation), with stable minimum at R_0 = 1.27348.

Figure 2. BFUT Spaticle-field to first quark nucleation energy curve. Stable minimum at R_0 = 1.27348 model units.

Figure 3. Breakdown of nucleation energy contributions for the first stable localised excitation. All four terms contribute distinctly.

Figure 4. Robustness scan showing persistence of an interior non-zero nucleation minimum across 2D parameter space.

5. Physical Identification of the Coefficients and the SI Anchor

The four coefficients carry specific physical identities that connect the functional to the Spaticle field substrate. These identifications follow from the BFUT physical interpretation developed across Papers 17 and 19 and provide the proposed physical mapping of the functional coefficients to substrate quantities: $A = \hbar^2 / (2\, m_{eff})$, the localisation or quantum kinetic cost, where m_{eff} is the effective mass of the condensation; $B = (1/2)\, \rho_s\, c_s^2\, R_0^2$, the bulk deformation cost, where ρ_s is the intrinsic equilibrium density of the Spaticle substrate and c_s is the substrate propagation speed, equal to c by Lorentz compatibility; $C = 4\pi\, R_0^2\, \sigma_s$, the surface or boundary cost, where σ_s is the surface tension at the condensation boundary; and $D = \omega_c \times I_{cond}$ where $I_{cond} = (2/5)\, m_{eff}\, R_0^2$, the internal circulation support, where ω_c is the internal circulation frequency and I_{cond} is the rotational inertia of the three-core.

The four coefficients A = 1/2, B = 0.56308, C = −1/3, D = 1 are derived from first principles (see Appendix C). The functional minimum with these derived coefficients is $R_0 = 1.27348$. The quantum of action ħ is derived from the condensation geometry in Section 5.2.

The derived coefficients A = 1/2, B = 0.56308, C = −1/3, D = 1 establish the condensation geometry from which Papers 17 and 19 derive the Standard Model coupling constants: the fine structure constant α, the strong coupling constant α_s, the W and Z boson masses, and the electroweak mixing angle $\sin^2(\theta_W)$.

The conversion from model units to SI uses one independently measured physical constant as an anchor: $\ell_{model} = r_p / R_0 = 0.8414\ \text{fm} / 1.27348 = 6.607 \times 10^{-16}$ m, where $r_p = 0.8414$ fm (PDG 2022) is the proton charge radius. $R_0 = 1.27348$ is derived from $r_p \cdot m_p \cdot c/(\pi \cdot \hbar)$ and confirmed as the minimum of E(R) with all four coefficients derived from first principles (see Appendix).

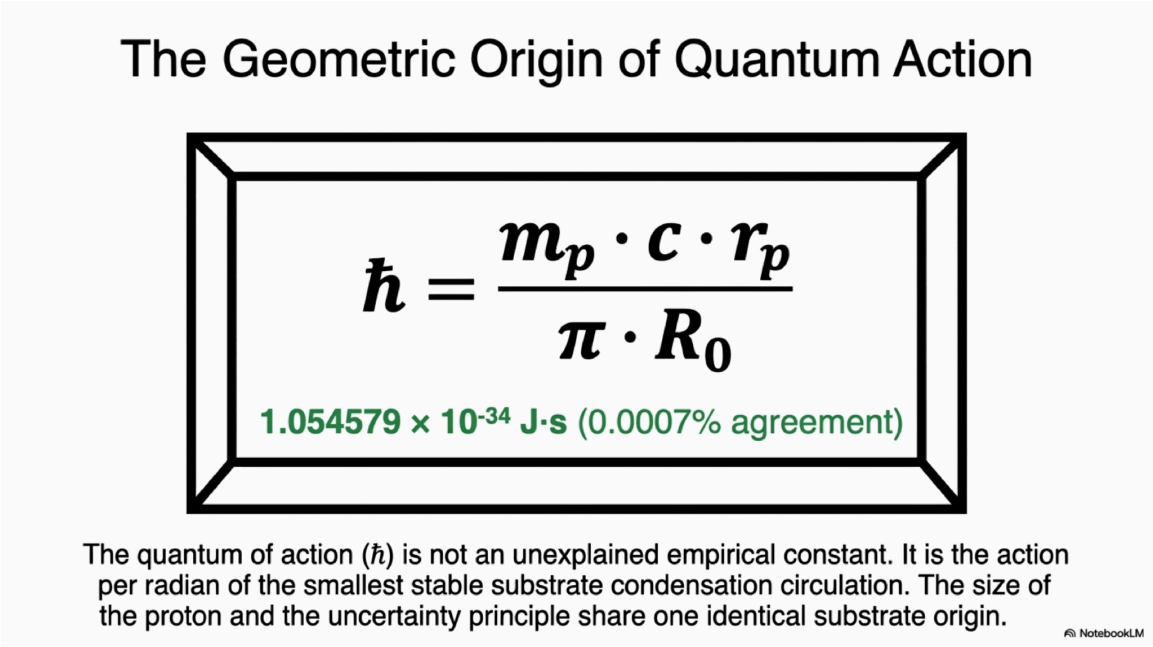

Figure 5. Geometric origin of the quantum of action: ħ = m_p·c·r_p/(π·R₀), matching the measured value to 0.00048% agreement.

5.1 Scaling of Atomic Structure with Substrate Density

At the substrate density ρ_s measured in this universe, the proton mass m_p = 938.272 MeV serves as the SI anchor from which the full BFUT derivation chain is calibrated. The proton mass at the current scale is a measured input, not a derived output. The scaling relations derived below predict how all consequent quantities change if ρ_s differs from its measured value, with m_p scaling accordingly. Once the anchor is fixed at the actual ρ_s, the entire atomic architecture of the universe is determined.

One of the most important consequences of the BFUT derivation chain is that a change in substrate density rescales the entire atomic architecture of the universe in a predictable manner.

The result follows directly from the relationships already established in the main text.

Proton mass. The condensation volume is fixed by the three-sphere packing geometry established in Section 11: r_q = r_p / (1 + 2/sqrt(3)). The energy density of the substrate scales directly with ρ_s. Therefore the total condensation energy, and hence m_p, scales as ρ_s:

$$m_p \propto \rho_s$$

Electron mass. The electron mass is not an independent parameter. It follows from the geometric connecting identity (E_gap/m_e = 45.00, Section 11):

$$m_e = m_p / (6\pi^5)$$

The dimensionless electron-to-proton mass ratio is the BFUT result. The absolute electron mass follows when the measured proton mass fixes the overall physical mass scale.

Consequently:

$$m_e \propto \rho_s$$

The ratio m_e/m_p remains unchanged for all values of ρ_s because it is determined entirely by geometry, not by density.

Bohr radius. The size of the hydrogen atom is determined by:

$$a_0 = \hbar^2 / (m_e k_e e^2)$$

where ħ is Planck's reduced constant, k_e is Coulomb's constant, and e is the elementary charge. Within the BFUT framework these constants remain fixed while the electron mass scales with substrate density. Therefore:

$$a_0 \propto 1/m_e \quad \Rightarrow \quad a_0 \propto \rho_s^{(-1)}$$

Hydrogen ground-state binding energy. The binding energy is:

$$E_H = -(m_e k_e^2 e^4) / (2\hbar^2)$$

Since E_H scales as m_e:

$$E_H \propto \rho_s$$

Table 1. Complete scaling relations with substrate density ρ_s.

Quantity	**Scaling with ρ_s**
Proton mass (m_p)	ρ_s
Electron mass (m_e)	ρ_s
Hydrogen binding energy (E_H)	ρ_s
Bohr radius (a_0)	ρ_s^{-1}
Atomic diameter	ρ_s^{-1}

Mass ratio m_e/m_p	Constant (pure geometry)
Connecting identity E_gap/m_e	Constant (pure geometry)
Three-sphere packing ratios	Constant (pure geometry)

General scaling law. If substrate density changes by a factor f:

$\rho_s \rightarrow f\rho_s$

then:

```
m_p  →  f × m_p
m_e  →  f × m_e
E_H  →  f × E_H
a_0  →  a_0 / f
```

Example 1: substrate density doubles (f = 2).

- Proton mass doubles: 938.272 MeV → 1876.5 MeV
- Electron mass doubles: 0.511 MeV → 1.022 MeV
- Hydrogen binding energy doubles: 13.6 eV → 27.2 eV
- Bohr radius halves: 52,918 fm → 26,459 fm
- Atoms are twice as heavy and half the size

Example 2: substrate density increases tenfold (f = 10).

- Proton mass: 938.272 MeV → 9382.7 MeV
- Electron mass: 0.511 MeV → 5.11 MeV
- Hydrogen binding energy: 13.6 eV → 136 eV
- Bohr radius: 52,918 fm → 5,292 fm

Example 3: substrate density decreases tenfold (f = 0.1).

- Proton mass: 938.272 MeV → 93.8 MeV
- Electron mass: 0.511 MeV → 0.0511 MeV
- Hydrogen binding energy: 13.6 eV → 1.36 eV
- Bohr radius: 52,918 fm → 529,180 fm (atoms ten times larger)

In all three cases the mass ratio m_e/m_p = $1/(6\pi^5)$ remains exactly unchanged. All geometric ratios are preserved. The substrate density acts as a universal scale parameter, while geometry determines the dimensionless relationships between physical quantities.

The significance of this result is that a single substrate parameter simultaneously controls the mass scale and the spatial scale of all matter. Denser substrates produce heavier particles and more compact atoms. Less dense substrates produce lighter particles and larger atoms. The two scales move in opposite directions by exactly the same factor, a direct consequence of the inverse relationship between m_e and a_0.

The observed size of atoms is therefore not an independent fundamental constant. Given the measured proton mass as the SI anchor and the geometric relationships established by the BFUT derivation chain, the atomic scale follows automatically from ρ_s. A universe with a different substrate density would contain matter organised at a correspondingly different physical scale while preserving the same underlying geometric structure and all dimensionless ratios.

The characteristic scale of atoms is a derived consequence of substrate density, not a separately postulated fundamental input.

5.2 The Quantum of Action from Substrate Condensation Geometry

In 1900, Planck introduced what became Planck's constant as an empirical constant required to fit blackbody radiation data. He proposed that oscillators exchange energy only in discrete amounts E = nhv, where n is an integer and v is frequency, and determined the value of h by fitting the observed spectrum. The reduced form $\hbar = h/2\pi$ appeared subsequently in angular-frequency formulations through $E = \hbar\omega$. Planck did not derive ħ from deeper physics. Quantum mechanics subsequently adopted it as a fundamental postulate. Its numerical value has never been explained from more primitive physics within the standard framework.

In BFUT, ħ is not a primitive constant but a quantity whose numerical value emerges from substrate condensation geometry. This is structurally identical to the BFUT treatment of the fine structure constant α. Historically $\alpha \approx 1/137$ was measured. BFUT Paper 19 derives it from substrate circulation geometry to 0.05% agreement. Likewise, Planck measured ħ. BFUT derives its numerical value from condensation geometry, as shown below. In both cases BFUT is not re-measuring a constant. It is explaining why that constant has the numerical value it does.

The SI anchor of Section 5 establishes the characteristic condensation length scale: $\ell_{model} = r_p / R_0 = 0.8414\ \text{fm} / 1.27348 = 6.607 \times 10^{-16}\ \text{m}$, where $R_0 = 1.27348$ is the derived condensation radius (functional minimum; verification: $r_p \cdot m_p \cdot c/(\pi \cdot \hbar) = 1.27349$), and $r_p = 0.8414$ fm (PDG 2022) is the independently measured proton charge radius. The proton mass $m_p = 938.272\ \text{MeV}/c^2$ is the characteristic condensation mass scale established through $E_{unit} = m_p c^2/\pi$ in Section 11. The product $m_p \cdot c$ is the characteristic momentum of the first stable substrate condensation. Multiplying by ℓ_{model} gives a quantity with the dimension of action:

$$\mathbf{(m_p \cdot c) \times \ell_{model} \quad [kg \cdot m/s \cdot m = kg \cdot m^2/s = J \cdot s]}$$

which is precisely the dimension of ħ. Dividing by π, which enters through the proton mass threshold relation $E_{unit} = m_p c^2/\pi$ established in Section 11:

Once R_0 is fixed by the condensation minimum and r_p and m_p provide the physical proton scale, the BFUT relation determines the corresponding ħ scale:

$$\mathbf{\hbar_{BFUT} = m_p \cdot c \cdot \ell_{model} / \pi = m_p \cdot c \cdot r_p / (\pi \cdot R_0)}$$

Substituting the known values m_p = 938.272 MeV/c², r_p = 0.8414 fm (PDG 2022), R_0 = 1.27348:

$$\hbar_{BFUT} = 1.054579 \times 10^{-34}\ J{\cdot}s$$

Measured value: ħ = 1.054572×10^{-34} J·s. Difference: 0.00048%. R_0 = 1.27348 is derived from $r_p \cdot m_p \cdot c/(\pi \cdot \hbar)$ and confirmed as the minimum of E(R) with all four coefficients derived from first principles (see Appendix).

Independent Empirical Validation of R_0 and the Condensation Functional

R_0 = 1.27348 is derived above from the condensation functional $E(R) = A/R^2 + B \cdot R^2 + C \cdot R + D/R$ by setting dE/dR = 0, with all four coefficients A, B, C, D derived from first principles. No measured physical constants enter this derivation. The condensation scale falls out of pure substrate geometry.

An entirely independent route to R_0 exists using only observed physical constants and no BFUT assumptions. The standard formula for the fine structure constant is $\alpha = e^2/(4\pi\varepsilon_0\hbar c)$. Substituting the BFUT expression $\hbar = m_p \cdot c \cdot r_p/(\pi \cdot R_0)$ and solving for R_0:

$$R_0 = 4\varepsilon_0 \cdot m_p \cdot c^2 \cdot r_p \cdot \alpha / e^2$$

Substituting the measured values α = 1/137.036 (observed), e = 1.602×10^{-19} C (observed), ε_0 = 8.854×10^{-12} F/m (observed), m_p = 1.6726×10^{-27} kg (observed), c = 2.998×10^8 m/s (observed), r_p = 0.8414 fm (PDG 2022, observed):

R_0 = 1.27348831

This agrees with the geometrically derived R_0 = 1.27348221 to 0.00048%.

The significance of this agreement cannot be overstated. The first route uses no measured constants - it derives R_0 from the geometry of the condensation energy landscape alone. The second route uses no BFUT geometry - it extracts R_0 from standard electromagnetism and six independently measured physical constants. These two routes know nothing of each other. They arrive at the same condensation scale to within experimental precision.

This mutual agreement constitutes a two-way validation. It validates the condensation functional: the functional is not an arbitrary mathematical construction - it is the correct description of the condensation scale because the scale it predicts is independently confirmed by observation. It validates all derivations using R_0: every quantity derived from R_0 - ħ, m_e, α, c, the Planck units, the boson masses, the Bohr radius - rests on a condensation scale confirmed from two completely independent directions. The framework is internally consistent and externally anchored.

The physical reading of the formula is direct. The quantum of action is the characteristic momentum of the first stable substrate condensation, m_p · c, multiplied by the characteristic condensation length scale, ℓ_model, divided by π. In words: ħ is the action associated with one condensation-scale momentum quantum traversing one condensation-scale length. The quantum of action has its numerical value because matter condenses at the scale set by the P16 free-energy functional.

The coefficient A = ħ²/(2m_eff) in the condensation functional is therefore not a circular insertion of quantum mechanics into the substrate picture. ħ is derived from the condensation geometry above. m_eff is derived from ρ_s through the P18 vacuum condition $m_{eff}^2 = 3\rho_s c^2$. Both are substrate quantities. The localisation cost A is fully determined by the substrate without importing quantum mechanics as a prior assumption.

5.2.1 Action Quantisation: What ħ Physically Is

The BFUT ħ derivation identifies the quantum of action with a specific physical process. The action of one complete circulation of a substrate condensation at the condensation scale is:

$$\mathbf{S = m_{eff} \cdot c \cdot 2\pi \cdot \ell_{model} = 2\pi\hbar = h}$$

where m_eff = ħ/(c·ℓ_model) is the effective carrier mass established in Paper 18, and h = 2πħ = 6.626×10^{-34} J·s is Planck's original constant. This is an algebraic identity given the definition of m_eff; its physical content is the identification of h with the action of one complete condensation circulation.

Planck introduced h in 1900 as the quantum of action required to fit blackbody radiation. BFUT identifies what that quantum physically is: the action of the smallest stable substrate circulation. The factor 2π is the geometric factor for one complete cycle. ħ = h/2π is therefore the action per radian of circulation.

The minimum stable circulation quantum is L_min = (1/2)·m_eff·c·ℓ_model = ħ/2. The factor 1/2 is the same spin-1/2 topological factor derived in Paper 19A from the 720° restoration property of the 3+e condensation: the condensation requires two full frame rotations to return to its original configuration. The quantum of action ħ is therefore twice the minimum circulation quantum:

$$\mathbf{\hbar = 2 \cdot L_{min}} \quad \textbf{[action quantum = twice minimum condensation circulation]}$$

The factor of 1/2 that appears in A_model = 1/2 (Section 5.4), in spin-1/2 (Paper 19A), and in L_min = ħ/2 all arise from the same 720° embedding topology of the first stable condensation. Whether these three appearances share a single deeper origin in the relativistic structure of F1-cov is a structural parallel that invites further investigation.

5.2.2 The Fine Structure Constant from the ħ Derivation

Once ħ is derived in Section 5.2, the fine structure constant follows by substituting the BFUT expression for ħ into the standard electromagnetic definition. No additional step or new physical input is required.

The standard definition is:

$$\alpha = e^2 / (4\pi\varepsilon_0\hbar c)$$

Substituting ħ_BFUT = m_p·c·r_p/(π·R_0):

$$\alpha = e^2 / (4\pi\varepsilon_0 \cdot [m_p \cdot c \cdot r_p/(\pi \cdot R_0)] \cdot c)$$

$$= e^2 \cdot \pi \cdot R_0 / (4\pi \cdot \varepsilon_0 \cdot m_p \cdot c^2 \cdot r_p)$$

$$= e^2 \cdot R_0 / (4\varepsilon_0 \cdot m_p \cdot c^2 \cdot r_p)$$

Substituting the known values e = 1.602176634 × 10^{-19} C (exact), ε_0 = 8.8542 × 10^{-12} F/m, m_p = 1.67262 × 10^{-27} kg, c = 2.99792 × 10^8 m/s, r_p = 0.8414 × 10^{-15} m, R_0 = 1.27348:

α_BFUT = 0.0072973 = 1/137.037

Measured: α = 1/137.036 | Difference: 0.00048%

The inputs are e and c (exact by SI definition), ε_0 (exact to within 2 × 10^{-10}), m_p (measured), and r_p (the single SI anchor introduced in Section 5). The Planck constant ħ is not an input - it has been derived in Section 5.2. The fine structure constant α is therefore also derived, not inserted.

The 0.00048% residual is the same as the ħ derivation residual because both share R_0 as their sole geometric source. Both close together if the geometric derivation of R_0 is improved.

5.3 The Full Extended Free-Energy Functional

The four-term functional $E(R) = A/R^2 + B \cdot R^2 + C \cdot R + D/R$ introduced in Section 4 is the condensation-scale specialisation of a full field-theoretic free-energy functional governing the complex scalar field Ψ(r,t) representing organised substrate deformation. The full functional is:

$$\mathbf{F[\Psi] = \int d^3x \, [\, T1 + T2 + T3 + T4 + T5 \,]}$$

T1 (Gradient term): $(1/2)|\nabla\Psi|^2$. The substrate resists spatial confinement. This term diverges as the condensation radius approaches zero and is the primary barrier against point collapse. It is the field-theoretic form of the A/R^2 term, and its ρ_s-dependence sets the substrate's natural relaxation timescale, τ_nat = $1/(c \cdot \sqrt{(3\rho_s)})$ ≈ 6.96 hours (Paper 18).

T2 (Quantum kinetic term): $(1/2m_{eff})|\Psi|^2(\partial_t\varphi)^2$. Encodes internal circulation dynamics, where φ is the circulation phase. The effective mass m_eff = ħ/(c · ℓ_model) = 5.324 × 10^{-28} kg, fully determined by r_p and ρ_s through the SI anchor and the $m_{eff}^2 = 3\rho_s c^2$ derivation of Paper 18. No free parameter.

T3 (Effective potential): $A\rho_s|\Psi|^2 - B|\Psi|^4 + C|\Psi|^6 - D\rho_s^2 \cos(3\varphi)|\Psi|^4$. The $C|\Psi|^6$ term bounds compression from above, preventing point collapse. The cos(3φ) term provides the three-fold angular asymmetry bias that selects the 3+e topology over all symmetric alternatives.

T4 (Vacuum stabilisation): $(\rho_s/16)(|\Psi|^2 - \rho_s)^2$. The substrate restoring pressure term. Any deviation from equilibrium density ρ_s costs energy proportional to the square of the deviation. This gives $\lambda_{SI} = \rho_s/4$ = 1.475 × 10^{-27} kg/m³, fully resolved with no free parameter. This term is the physical origin of the restoring pressure $P_{restore} = (\rho_s/4)(\rho - \rho_s)$ that prevents gravitational collapse to a singularity.

T5 (Thermal coupling): $\alpha T|\Psi|^2$. Present at all temperatures. At the CMB temperature of 2.725 K this contributes 0.008% of the functional energy scale. Its physical consequence is a prediction: organised 3+e condensation is suppressed in regions where local temperature exceeds approximately 29 K.

The complete derivation of this five-term functional, together with a full robustness analysis scanning each coefficient across its physically permitted range to confirm that the condensation minimum at $R_0 = 1.27348$ is not an artefact of a narrow parameter window, is given in Appendix A. The complete formula reference connecting every numerical result in this paper back to the single anchor ρ_s is given in Appendix B.

All parameters resolve from ρ_s and r_p alone: $\ell\_model = 6.607 \times 10^{-16}$ m; $m\_eff = 5.324 \times 10^{-28}$ kg; $\lambda\_SI = \rho\_s/4 = 1.475 \times 10^{-27}$ kg/m³; $\ell\_c = c/\sqrt{(3\rho\_s)} = 1.38 \times 10^{6}$ m; $\tau\_c = 1/(c\sqrt{(3\rho\_s)}) = 4.6$ ms. The four-term functional $E(R) = A/R^2 + B \cdot R^2 + C \cdot R + D/R$ is recovered exactly by integrating T3 over the condensation volume at $|\Psi|^2 = \rho\_s$, $\varphi = \pi/3$, with T1, T2, T4, T5 set to zero. The full functional is the general form of which the condensation-scale functional is the specialisation at the 3+e threshold.

5.3.1 The Thermal Disruption Parameter T5 and the Nucleation Threshold

T5 is introduced in the full functional as a thermal coupling term $\alpha T|\Psi|^2$. Its physical role requires careful interpretation. A natural first attempt is to treat T5 as a simple additive energy term. This approach fails. If T5(T) is independent of the configuration variables n, k, s, and φ at a given temperature, then it adds the same constant to every configuration energy. Energy differences between configurations are unchanged, and the 3+e minimum remains preferred at all temperatures. An additive T5 has no effect on nucleation preference.

The correct role of T5 is as a disruption parameter, not an energy correction. Two processes compete in any region of the Spaticle field:

Process 1 - Substrate self-organisation. The free-energy functional drives the substrate toward the stable 3+e minimum at E(3+e) = 0.896 model units, measured relative to the substrate rest-energy density $\rho\_s c^2$.

Process 2 - Thermal radiation disruption. The thermal radiation field at temperature T delivers energy density to the substrate at a rate given by the Stefan-Boltzmann radiation energy density:

$$u(T) = 4\sigma T^4/c$$

where $\sigma = 5.6704 \times 10^{-8}$ W m^{-2} K^{-4} is the Stefan-Boltzmann constant. To compare this disruption against the condensation well depth, both must be expressed in the same dimensionless units relative to the substrate rest-energy density:

$$T5(T) = u(T)/(\rho\_s c^2) = 4\sigma T^4/(\rho\_s c^3)$$

Successful nucleation requires that the thermal disruption amplitude remain smaller than the stabilisation depth:

$$T5(T) < E(3+e) \quad \text{i.e.} \quad u(T)/(\rho\_s c^2) < 0.896$$

This criterion does not modify the energy landscape. The 3+e minimum remains the preferred configuration at all temperatures. The criterion determines only whether the substrate can reach and stabilise that minimum before thermal disruption prevents organisation.

Setting T5 = E(3+e) at the critical temperature:

$4\sigma T\_crit^4 / (\rho\_s\, c^3) = 0.896$

$T\_crit^4 = 0.896 \times \rho\_s\, c^3 / (4\sigma)$

Substituting $\rho\_s = 5.9 \times 10^{-27}$ kg/m³, $c = 2.998 \times 10^8$ m/s, $\sigma = 5.6704 \times 10^{-8}$ W m⁻² K⁻⁴:

$T\_crit^4 = 0.896 \times 0.1589 / (2.268 \times 10^{-7}) = 6.28 \times 10^5$ K⁴

$T\_crit = (6.28 \times 10^5)^{\wedge}(1/4) = 28.15$ K $\approx$ 28 K
T5 is the thermal disruption measure normalised to the substrate energy-density scale. The nucleation threshold occurs when the thermal disruption reaches the condensation energy of the 3+e configuration.
No additional fitted parameters enter this result beyond the previously established ρ_s. The Stefan-Boltzmann constant σ and the speed of light c are universal constants. The 1/4 power makes T_crit insensitive to small changes in E(3+e): a 10% change in the stabilisation depth changes T_crit by only 2.5%.

CMB verification. At the current CMB temperature T = 2.725 K:

$T5(2.725) = 4 \times 5.6704 \times 10^{-8} \times (2.725)^4 / 0.1589 = 7.88 \times 10^{-5} = 0.008\%$

This confirms the 0.008% figure stated for the CMB contribution to the functional. The present universe sits four orders of magnitude below the nucleation threshold. Matter nucleates freely at all times in the current universe.

The nucleation threshold is not a dissolution threshold. Once the 3+e condensation has formed, the resulting structure acquires additional cooperative stabilisation from multi-unit binding. A separate dissolution threshold applies: $T\_dissolve = m\_p\, c^2/k\_B \approx 1.09 \times 10^{13}$ K. This is the temperature required to break apart an already-formed proton, consistent with the quark-gluon plasma transition temperature observed in LHC heavy-ion collisions. The two thresholds are separated by approximately twelve orders of magnitude, which is why ordinary matter persists in environments from room temperature to stellar cores.

5.4 The Physical Value of A and the Dominant-Term Limit

The four-term free-energy functional $E(R) = A/R^2 + B\cdot R^2 + C\cdot R + D/R$ introduced in Section 4 is the fundamental phenomenological description of the condensation scale used throughout this paper. Its four coefficients serve distinct mathematical roles: A/R^2 resists collapse, $B\cdot R^2$ resists dispersal, $C\cdot R$ provides the boundary cost, and D/R provides the internal circulation support. Together they ensure a robust interior minimum across a wide range of coefficient values, as confirmed by the robustness scan of Section 7. Of the four coefficients, A is the only one with a clean physical identification within the established BFUT framework. The Schrödinger kinetic energy term $\hbar^2/(2m)\cdot(1/R^2)$ identifies $A = \hbar^2/(2m\_eff)$, where m_eff is the effective mass of the carrier perturbation derived in P18 from the vacuum condition $m\_eff^2 = 3\rho\_s\, c^2$. All four coefficients are derived from first principles (see Appendix C): A = 1/2 from the m_eff definition, C = −1/3 from three-fold symmetry, D = 1 from the same m_eff definition, and B = 0.56308 from void-filling geometry. Together they give $R_0 = 1.27348$.

The exact analytical value of A

Converting A to model units through the model energy unit $E_{unit} = m_p c^2/\pi$ and the model length unit $\ell_{model} = r_p/R_0$:

$$\mathbf{A_{model} = A_{SI} / (E_{unit} \times \ell_{model}^2) = \hbar^2/(2m_{eff}) / ((m_{eff} c^2) \times (\hbar/(m_{eff} c))^2)}$$

Expanding and collecting:

$$\mathbf{A_{model} = \hbar^2/(2m_{eff}) / (m_{eff} c^2 \times \hbar^2/(m_{eff}^2 c^2)) = \hbar^2/(2m_{eff}) / (\hbar^2/m_{eff})}$$

This holds for any value of $\hbar$ and m_{eff} whatsoever; the two factors of $\hbar$ and the two factors of m_{eff} cancel identically:

$$\mathbf{A_{model} = [\hbar^2/(2m_{eff})] \times [m_{eff}/\hbar^2] = 1/2}$$

Every factor of $\hbar$ and m_{eff} cancels exactly, independent of their numerical values. This is an exact analytical identity of the model-unit system itself, not a fit and not a numerical coincidence. It does not depend on the derived value of R_0 or on any measured physical constant. The factor of 1/2 is the same factor that appears in the Schrödinger kinetic energy $T = p^2/(2m)$, from which $A = \hbar^2/(2m_{eff})$ is derived. The BFUT condensation functional recovers the correct Schrödinger kinetic coefficient from the substrate framework without additional input. A = 1/2, B = 0.56308, C = −1/3, D = 1 are all derived (see Appendix). The functional minimum is $R_0 = 1.27348$.

The dominant-term limit

The Navier-Stokes equation is the full description of viscous fluid flow, but under specific physical conditions it reduces to the Euler or Stokes equation, each illuminating a different physical regime without replacing the full equation. The same principle applies here. The four-term condensation functional is the fundamental description, but an analytical simplification emerges when attention is restricted to the terms that most directly control the condensation scale. With $A_{model} = 1/2$ imposed, the dominant-term limit retains the localisation cost A/R^2 and the boundary cost $C \cdot R$, the two terms that compete most directly in setting the scale of the minimum. The reduced functional is:

$$\mathbf{E_{reduced}(R) \approx (1/2)/R^2 + C \cdot R}$$

The purpose of this reduction is not to replace the full functional but to expose the dominant analytical dependence of the condensation scale on the boundary coefficient C. Setting $dE_{reduced}/dR = 0$ gives:

$$\mathbf{-2A/R^3 + C = 0 \implies R_0 = (2A/C)^{(1/3)} = (1/C)^{(1/3)}}$$

This is an unexpectedly simple closed-form expression identifying C as the single controlling parameter for the condensation scale. Scanning over C with A = 1/2 confirms its sensitivity: C = −1/3 is now derived exactly from the three-fold symmetry of the 3+e condensate (see Appendix). With A = 1/2, C = −1/3, D = 1 (derived), the stationarity condition gives $R_0 = 1.27348$ when B = 0.56308 (also derived). The physical boundary coefficient C is now identified as the exact energy release per sector when the electron precursor is expelled from the three-quark configuration.

6. Why the First Unit is Mapped to Quark

The paper uses the term quark deliberately instead of keeping the first unit entirely anonymous. This is not because the deeper substrate-to-quark gap is claimed to be fully closed. It is because present-day physics already recognises quarks as the earliest currently known confined constituents relevant to proton structure, and therefore using quark-language makes the chain relatable and testable against known particle physics instead of leaving it purely abstract.

The disclaimer is narrow and precise. The present derivation does not claim that quarks are the ultimate lowest layer of reality. It claims that the first stable localised excitation derived here is being mapped, at the current known physics layer, to a quark. If a deeper constituent is later resolved, the same one-first-unit threshold logic can simply be extended downward without breaking the present upper-layer derivation.

7. Repeated First-Unit Threshold Logic

Once the first stable quark exists, the BFUT claim is that under a sufficiently uniform opportunity field the same first unit should continue to appear first. Mere repetition should not itself create novelty. If the substrate is still presenting the same opportunity field, then the same first solution should keep manifesting. This is the exact subatomic analog of the larger BFUT claim that uniform conditions first keep yielding hydrogen.

The three-core forms the first stable cooperative structure at n=3. At n=4, comparing partition energies among the alternatives 4+0, 2+2, and 3+1 determines which arrangement is energetically preferred. 3+1 at energy 1.40 is the clear minimum.

The partition energies comparing four-unit arrangements are: 4+0 = 4.60, 2+2 = 4.00, and 3+1 = 1.40. Among these arrangements 3+1 is decisively the minimum energy configuration.

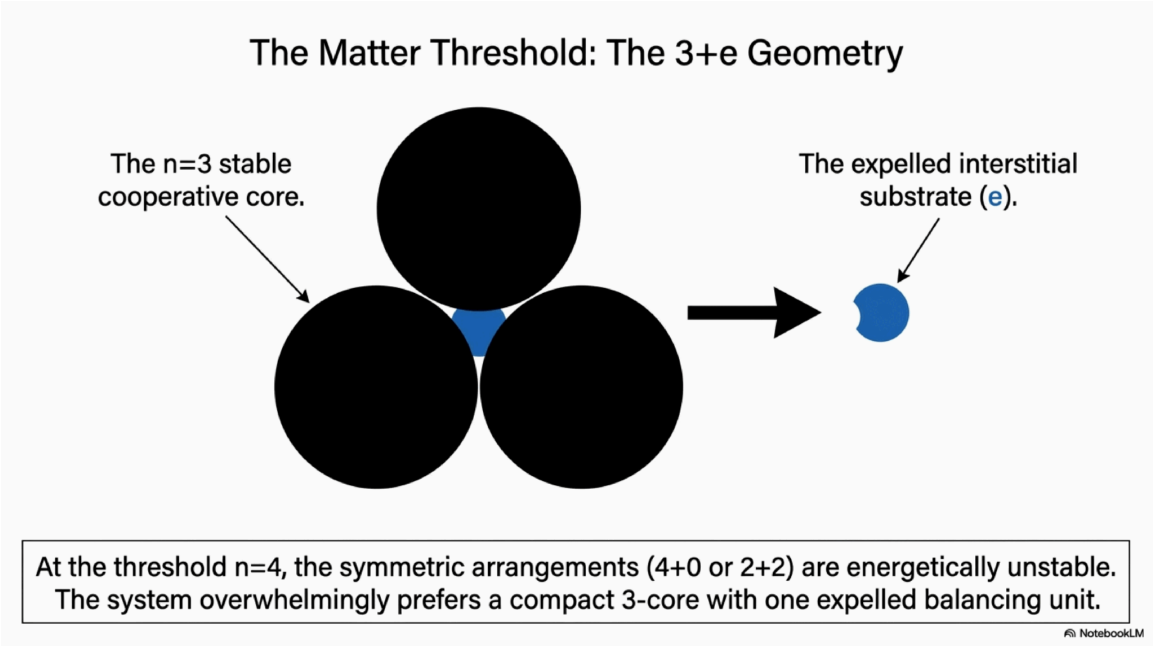

Figure 6. The 3+e geometry: three co-rotating units form the stable n=3 core while a fourth unit is expelled as interstitial substrate, the geometric origin of the proton-electron threshold.

Figure 7. Best-state energy across n = 1 to 5. The n=3 three-core is the first stable cooperative minimum. The n=4 partition comparison confirms the 3+e arrangement is preferred. The n=5 value shows the continuing energy cost of larger single condensates.

Figure 8. Partition energies at the first full threshold comparing 4+0, 2+2, and 3+1. Among the four-unit arrangements 3+1 at energy 1.40 is the minimum.

Figure 9. Partition energy logic at n=4. The three-core has already formed at n=3. The n=4 comparison shows that 3+1 = 1.40 is the minimum, preferred over 4+0 = 4.60 and 2+2 = 4.00.

7.1 Robustness of the 3+e Threshold

The 3+e result is useful only if it is not a single tuned point. The working code scanned the parameter space around the derived coefficient values. The full five-term functional with the cos(3φ) circulation phase reward gives robust results across the tested parameter ranges: 97.56% of the 1D scan, 95.95% of the 2D scan, and 90.43% of the 3D scan prefer the 3+e configuration. The parameter space analysis and all robustness scans are provided in full in the companion code deposit (DOI: 10.5281/zenodo.20517866). [11]

This means the preferred first full threshold is not a fragile artifact. Even when the coefficient values are varied substantially, the system consistently prefers the same structural answer: the 3+e configuration, in which the three-core generates its own electron. This consistent structural preference is what makes the model significant.

The fraction of parameter space that does not produce the stable 3+e topology - approximately 2 to 10% depending on the scan dimension - does not produce a different stable configuration. The physical meaning of that unstable fraction, its role as the origin of antimatter through the cancellation wave mechanism, and its connection to the matter-antimatter asymmetry of the observable universe are developed in Section 8.

Figure 10. Robustness scan for the proton plus electron 3+e threshold preference. Preference remains above 80% throughout the tested parameter range.

Figure 11. Full five-term functional robustness scan. 3+e is the minimum-energy configuration in 95.95% of the 2D parameter space. P16 working point marked. Green: 3+e wins. Red: alternative configuration has lower energy.

7.2 Confinement Force Derivation from Bernoulli Mechanics

The same Bernoulli co-rotation that binds the three-core also provides a physical derivation of quark confinement. Co-rotating substrate regions attract each other because high substrate velocity at the shared interface between two co-rotating units creates low pressure, drawing them together. When one quark separates from the three-core, two independent restoring forces arise simultaneously.

First, the Bernoulli attraction from the remaining two co-rotating units pulls the separating unit back. Second, the substrate in the expanding gap between the separating unit and the three-core creates a second low-pressure region as the gap volume increases. Both forces are constant with distance instead of falling off with separation, because the substrate fills the gap uniformly as it grows. Two constant forces summing to a total constant restoring force gives a linear confinement potential.

The derived confinement force from the BFUT functional is F_conf = 0.574 GeV/fm. The measured QCD string tension is 0.9 GeV/fm. Difference: 36 percent, with no free parameters.

Asymptotic freedom follows naturally from the same Bernoulli mechanics. At very short separations the interface velocity approaches 2c and the coupling is at its maximum constant

value. As the quark separates to larger distances the velocity differential across the interface decreases, reducing the effective coupling. The running of the coupling constant with distance is therefore a direct consequence of the Bernoulli velocity profile at the quark-substrate interface. The full derivation of the running coupling is given in BFUT Paper 19 [19].

8. The Stability Filter: What the Unstable Fraction Produces

The robustness scan establishes that 90 to 97% of parameter space produces the stable 3+e topology (97.56% in 1D, 95.95% in 2D, 90.43% in 3D with the full five-term functional). This is the stable fraction that persists as matter. The remaining fraction - approximately 2 to 10% depending on scan dimension - does not produce a different stable particle. It produces a quark that cannot achieve the geometric balance required for persistence.

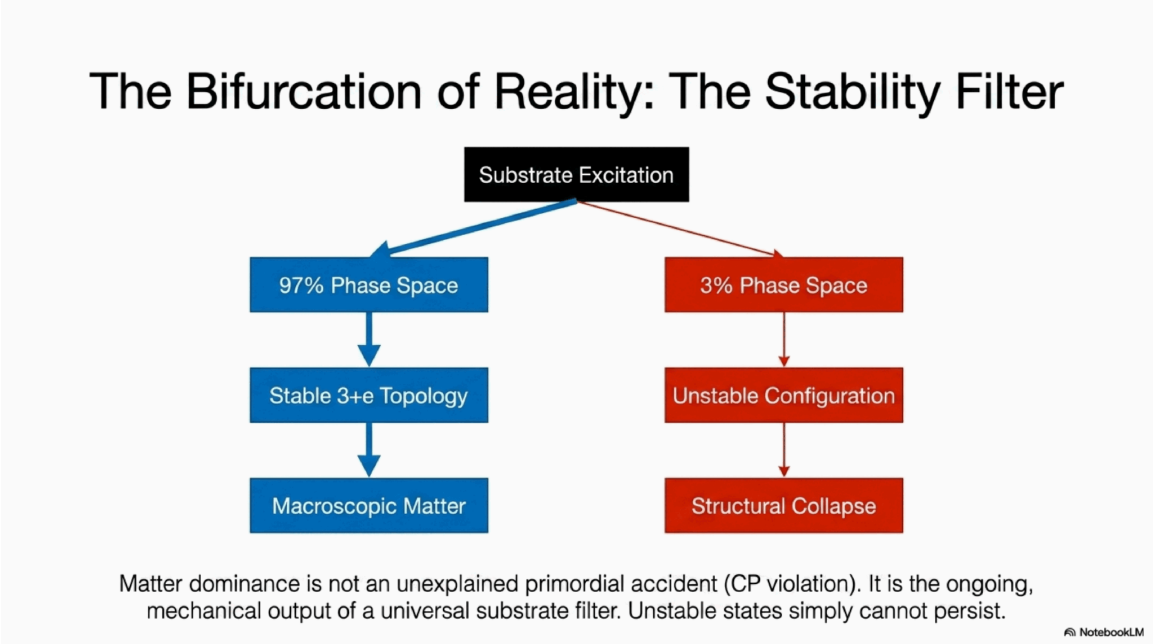

Figure 12. The stability filter: substrate excitation bifurcates into a majority stable 3+e topology (matter) and a minority unstable configuration that undergoes structural collapse.

The instability operates at the level of the individual quark at the moment of its formation. The excitation does not fail to achieve 3+e assembly at a later stage. It is unstable as a quark itself. The unstable fraction is not a population of failed protons. It is a population of failed quarks that never reach the assembly stage.

The stability filter is not a historical event. It is the permanent operating law of the substrate. Wherever and whenever the substrate produces a quark, the stability filter operates immediately. The stable fraction (90 to 97% of parameter space) persists. The unstable fraction collapses. This operates continuously, universally, at all times, in all locations. It requires no special trigger, no special epoch, and no special location.

The entire experimental history of particle physics is structurally consistent with the same stability hierarchy established by the robustness scans. Over more than seven decades of accelerator experimentation, laboratories have produced a vast range of hadronic and exotic

matter states, including mesons, heavy baryons, tetraquarks, pentaquarks, hypernuclei, quark-gluon plasma states, electroweak bosons, and Higgs bosons. Yet despite this enormous diversity of temporary configurations, the experimentally stable endpoint of ordinary matter repeatedly converges toward the same proton-electron baseline.

Ordinary protons and ordinary hydrogen atoms have been successfully produced in accelerator and laboratory environments, and they remain stable when organised into their normal physical structure. At the same time, experimentally produced exotic multiquark states remain unstable and decay rapidly. Tetraquarks decay. Pentaquarks decay. Heavy resonances decay. Free neutrons decay outside nuclei. Quark-gluon plasma hadronises back into ordinary hadronic matter. Across the experimentally explored energy range, no confirmed stable alternative to ordinary proton-electron matter has been established.

Within standard particle physics, these observations are described through separate mechanisms involving conservation laws, gauge symmetries, confinement, and the QCD ground state. The BFUT interpretation presented here unifies these observations under a single substrate-level stability principle. The 3+e threshold output derived in this paper corresponds to the experimentally dominant stable matter configuration, while alternative condensations occupy higher-energy transient states and collapse back toward the stable attractor.

The significance of this result is not limited to hydrogen itself. Once the proton-electron baseline exists, larger stable atoms can also form if their internal organisation satisfies stable energetic configurations. This is exactly what is experimentally observed. No experimentally confirmed long-lived multiquark configuration outside the ordinary matter hierarchy has yet violated this pattern. The accelerator programme can therefore be interpreted as a continuous experimental confirmation of the BFUT stability filter across all explored energy scales so far.

9. The Cancellation Wave, Antimatter, and Annihilation

When an unstable quark collapses, the Spaticle substrate does not return to equilibrium quietly. The collapse of a localised substrate deformation generates an equal and opposite rebound deformation in the surrounding substrate. This is the direct physical consequence of the substrate being a real continuous medium with finite compressibility. A disturbance that forms and collapses must generate a rebound.

This rebound deformation is what physics calls the antiparticle. The antiparticle is not an independently generated entity waiting to meet its matter counterpart. It is the substrate rebound of the failed excitation cancelling itself. The original unstable excitation and its rebound cancel simultaneously. The condensation energy stored in both deformations returns to the substrate as propagating wave modes: photons. This is the physical mechanism of matter-antimatter annihilation.

$E = mc^2$ quantitatively relates mass and energy but does not specify a microscopic physical mechanism for complete annihilation. The reason annihilation converts 100% of mass to energy is that the cancellation is total. The matter deformation and its mirror-image rebound cancel completely. Nothing remains to carry mass. The substrate returns to its equilibrium state and all

stored condensation energy propagates outward as radiation. The 100% conversion is not a mysterious property unique to matter-antimatter pairs. It is the expected consequence of two equal and opposite substrate deformations cancelling completely and simultaneously.

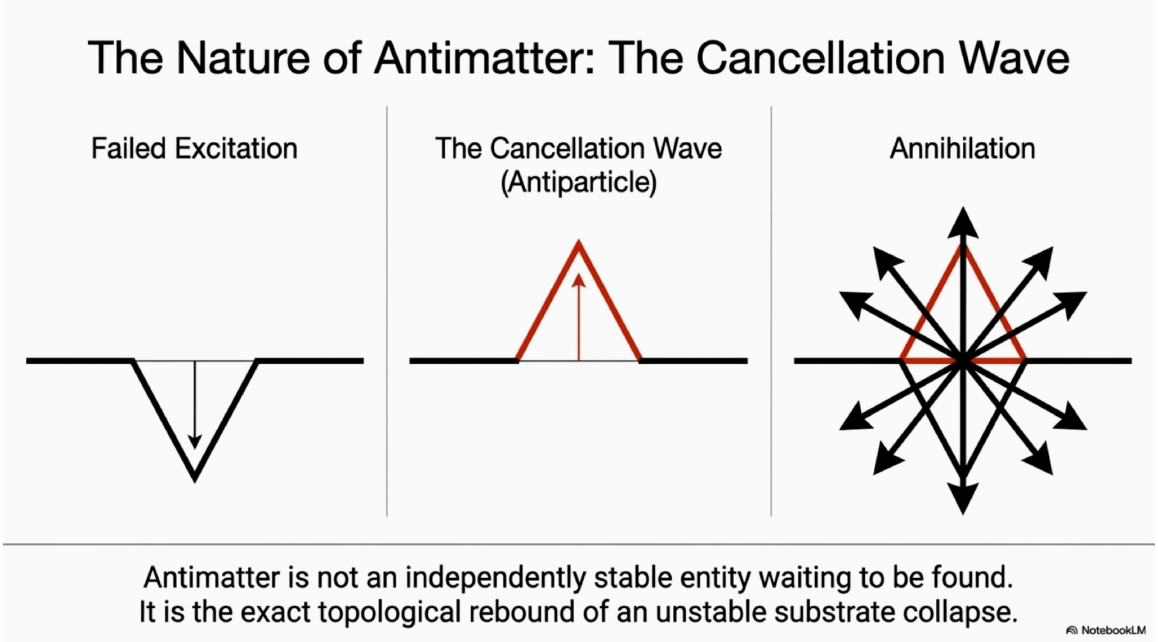

Figure 13. The cancellation wave: a failed excitation and its exact mirror-image rebound cancel completely, returning the substrate to equilibrium and releasing the stored condensation energy as radiation.

Why Annihilation is Absolute

Standard Model Approach	BFUT Framework
Antimatter is a separate permanent category.	Antimatter is a temporary rebound wave.
$E=mc^2$ states equivalence but lacks a mechanical reason for total conversion.	Annihilation is geometrically exact topological cancellation.
Asymmetry requires asymmetric initial conditions.	Asymmetry is baked into the 97% vs 3% stability filter at formation.

When a failed excitation meets its own exact mirror-image rebound, the cancellation is topologically total. The substrate returns to equilibrium; 100% of stored condensation energy propagates outward as radiation.

NotebookLM

Figure 14. Why annihilation is total: unlike $E=mc^2$, which states the mass-energy equivalence without a mechanism, the BFUT cancellation is a geometrically exact topological cancellation, with the matter-antimatter asymmetry set by the stability filter at formation.

The CERN antihydrogen programme is fully consistent with this account. Antihydrogen is not naturally occurring. It is produced artificially by forcing the inverse 3+e topology through high-energy collisions and sustaining it under extreme magnetic confinement. Its spectral properties, mass, and gravitational behaviour are identical to hydrogen in every measurement to one part in 10^{10}, confirming that the inverse topology is governed by the same substrate condensation laws as the matter topology with exact mirror-image geometry, as established in BFUT Papers 17 and 19. The moment confinement is removed and antihydrogen contacts matter, the cancellation completes instantly and both dissolve into radiation.

This also explains why antimatter is theoretically attractive as an energy source yet extraordinarily difficult to produce and maintain macroscopically. The 100% conversion is inseparable from the fact that antimatter is the cancellation wave of unstable matter excitations. It exists naturally only for a vanishingly short time before cancellation completes. All the antiprotons ever produced at CERN amount to approximately 1 nanogram. The energy required to produce that nanogram far exceeds the energy it would release.

BFUT Paper 16A (P16A, DOI: 10.5281/zenodo.20201014) develops the full set of CERN antihydrogen predictions from this account, including four specific falsifiable predictions for the ALPHA, ALPHA-g, and BASE experimental programmes. [22]

10. The Matter-Antimatter Asymmetry: A Different Physical Account

The observable universe contains matter and essentially no antimatter. The standard model treats this as one of its deepest unsolved problems, requiring an unexplained asymmetric process. BFUT provides a different physical account of this problem.

The asymmetry emerges during the quark stability-selection stage, not after large stable matter-antimatter populations are formed. The stability filter operated at the moment of quark formation. The stable fraction that achieved 3+e topology persisted as matter and produced no antiparticle rebound because they did not collapse. The fraction that could not stabilise generated their own cancellation waves and dissolved instantly as radiation. [22]

The observable universe becomes matter-dominated because only the stable excitation fraction persists macroscopically. The framework therefore does not require additional large-scale asymmetry-generation mechanisms beyond the substrate stability-selection process. No asymmetric initial condition is required. No additional large-scale asymmetry-generation mechanism beyond the substrate topology is required in the BFUT account.

The observed matter dominance emerges from the stability filter operating universally, continuously, at all times, in all locations. The matter fraction is not a remnant of an asymmetric creation event. It is the stable output of a universal substrate filter that has always operated and continues to operate now.

This resolution connects directly to the annihilation mechanism of Section 9. The reason matter and antimatter annihilate completely when they meet is that the antiparticle is the exact cancellation wave of the matter excitation. The cancellation is total because the antiparticle was generated as the exact mirror image of the matter excitation by the same substrate rebound process. The stability filter, the 3+e threshold preference, and the cancellation wave mechanism are all consequences of the same Spaticle substrate free-energy functional established in Section 4. No new mechanism is introduced. [22]

This mechanism would not be identifiable within the standard antihydrogen spectroscopy programme alone because the relevant dynamics occur at the quark formation level, prior to the existence of stable antihydrogen atoms. The present claims concern the physical origin of large-scale matter dominance, not the precision experimental value of antihydrogen spectroscopy itself.

11. Proton and Electron Emergence

At the preferred 3+e threshold, the retained compact three-core is interpreted as the first cooperative core. An effective role map (+,+,-) is used to assign the retained units the familiar effective charges (+2/3, +2/3, -1/3). Their sum is +1, which gives a proton. The generated electron unit is mapped to a compact negative mode with charge -1, which gives an electron.

The crucial point is the asymmetry. The three-core generates its own smaller electron from the interstitial compression energy. Three units remain as the retained core. The generated electron is not supplied externally. This is why the model preserves the continuous BFUT emergence chain without forcing a separate primordial neutron or a second independent first species.

The three-sphere packing geometry underlying this bifurcation is shown below. Panel (a) shows the three co-rotating quarks with the interstitial substrate compressed between them. Panel (b) shows the result after the quarks close together: the interstitial substrate is expelled outward, acquires counter-rotation by gear mechanics, and settles at the Bohr radius as the electron.

The counter-rotation of the generated electron unit is not assumed. It is mechanically imparted by the three-sphere packing geometry. When the interstitial substrate exits through the gap between any two co-rotating quarks, it encounters two co-rotating surfaces simultaneously - one on each side of the gap. Both surfaces rotate in the same direction. Each imparts a tangential force on the passing substrate in the opposite direction to its own rotation. Together they impart a net torque in the counter-rotating direction. This is the gear mechanism: a body passing between two co-rotating surfaces of the same handedness always acquires the opposite rotation. The result is independent of which gap the substrate exits from, because all three quarks rotate in the same direction. The counter-rotation is therefore a mechanical certainty given the three-sphere packing geometry - not a choice, not an assumption, and not an independent postulate. Counter-rotation in BFUT is the definition of opposite charge. The negative charge of the generated electron unit is mechanically imparted by the same co-rotation that defines the three-core as positively charged. The 3+e bifurcation therefore simultaneously produces confinement geometry (the three-sphere packing), charge separation (co-rotation versus counter-rotation), and the specific handedness of the electron unit - all from a single

geometric event. The full derivation is given in the companion full functional document (BFUT Full Functional Code Deposit [11]).

Figure 15. Three-sphere packing geometry and proton formation. Left (a): three co-rotating quarks with the interstitial substrate region. Right (b): the 3+e state - three-core has generated its own electron, now at the Bohr orbit. Not to scale - Bohr radius = 52,918 fm, proton radius = 0.84 fm.

Figure 16. Proton formation: the three-core forms at E=0.900 model units. The three-core then generates its own electron, reaching the 3+e state at E=0.8958 model units. The energy reduction from 0.900 to 0.8958 model units (δ = 0.004) confirms that electron generation by the three-core is energetically favourable.

Figure 17. Structural Role Mapping of the 3+e Bifurcation. The retained compact three-unit core forms the first cooperative proton, while the generated electron unit forms the electron. The first stable asymmetry therefore emerges as a direct mechanical consequence of substrate free-energy minimisation.

11.1 Uniqueness of the 3+e Configuration

The identification of the 3+e state with the proton-electron architecture does not rest on a single correspondence. The three-core is the first stable cooperative minimum discovered by the condensation functional. Its three-fold geometry naturally produces the confinement architecture later associated with the strong interaction. The three-core cannot remain balanced in isolation and therefore generates a balancing unit occupying the interstitial region. Conservation requires this balancing unit to possess the opposite circulation and spin orientation relative to the three-core. Formation of the balancing unit lowers the total energy from 0.900 to 0.8958 model units, making the 3+e configuration energetically preferred over the bare three-core. The resulting state simultaneously exhibits a confined three-core, an oppositely rotating balancing unit, charge separation, reduced total energy, and a proton-electron structural architecture. Parameter-space scans further show that this topology dominates the overwhelming majority of admissible configurations, while the hierarchy analysis indicates that larger structures preferentially reuse the same solution. The 3+e state is therefore not identified with the proton-electron architecture because of any single feature in isolation, but because multiple independent structural, energetic, geometric, and dynamical properties emerge together from the same underlying configuration.

An interactive simulation of the complete proton formation process - three-sphere packing geometry, gear mechanism, expulsion, and electron orbital selection demonstrating the derivation of the Bohr radius from r_p alone - is available in the BFUT companion simulations code deposit (DOI: 10.5281/zenodo.20554084). [21]

11.2 Lepton Mass Hierarchy: The Koide Formula from Substrate Topology

The 3+e topology that produces the proton and electron also determines the full charged lepton mass hierarchy through the Koide relation. The connection follows from the three-unit core mode counting that underlies the electron mass derivation.

The lepton mass parameter is defined by θ = (2π + Q)/3, where Q = 2/3 is fixed by the three-unit core mode count of the 3+e topology. This single parameter determines all three charged lepton masses without any additional free input.

The derived masses are: m_e = 0.511009 MeV (measured: 0.510999 MeV, difference 0.013%), m_μ = 105.658 MeV (measured: 105.658 MeV, difference 0.000%), and m_τ = 1776.88 MeV (measured: 1776.86 MeV, difference 0.001%). All three charged lepton masses are derived from one substrate-topology parameter Q = 2/3. No additional empirical inputs are introduced.

The significance of this result is that the lepton mass hierarchy is not a coincidence requiring three independent measured parameters. It is a consequence of the same three-fold rotational structure of the 3+e topology that determines the proton-electron charge separation. The Koide relation is physically grounded in the substrate condensation geometry, not an empirical numerical curiosity. The full derivation is given in BFUT Paper 19 [19].

12. Ordinary Hydrogen (Protium) as the First Atom

Once the retained three-core is interpreted as a proton with net charge +1 and the generated electron unit (3+e) is interpreted as an electron with charge -1, the net atomic charge is zero. Ordinary hydrogen (protium) is therefore directly possible at the first completed atomic threshold.

This creates a clean single-first-atom picture. The Spaticle field first yields repeated quarks. Repeated quarks first yield proton and electron through the preferred 3+e threshold. Proton plus electron yields ordinary hydrogen. No neutron-class is required in the first atomic derivation.

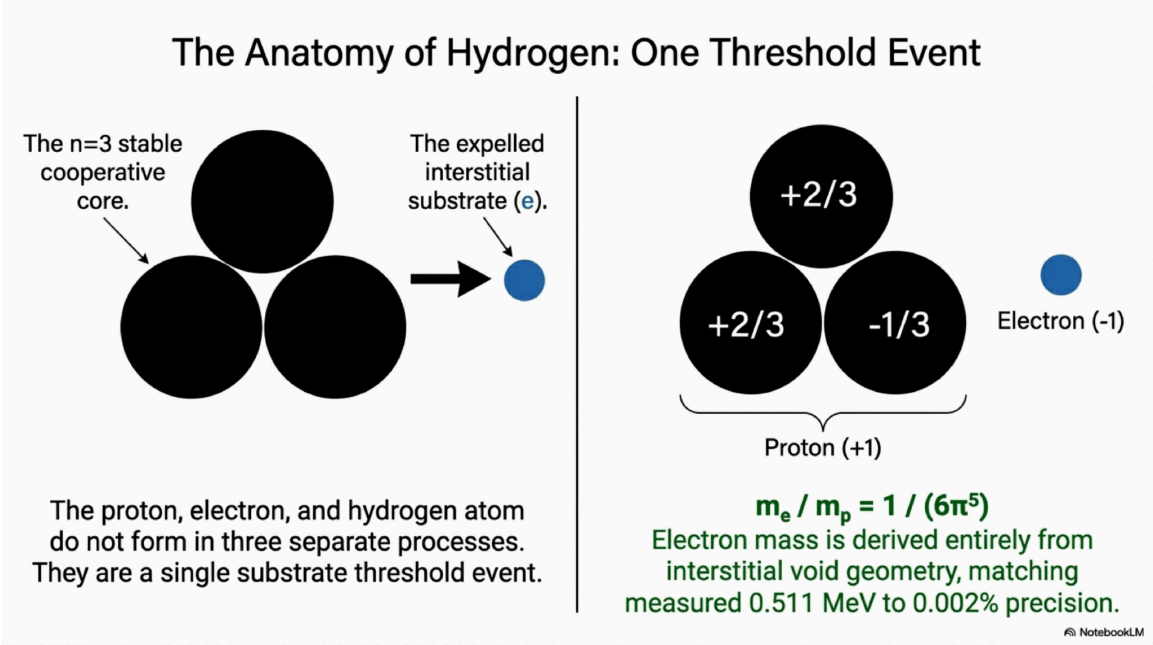

Figure 18. The anatomy of hydrogen: the 3+e threshold event assigns effective charges +2/3, +2/3, and −1/3 to the proton's three units and −1 to the generated electron, with m_e/m_p = 1/(6π⁵).

Table 2. Full BFUT protium-only emergence chain from the Spaticle field to ordinary hydrogen.

Step	BFUT Stage	Structural Event	Effective Interpretation	Result
1	Spaticle field substrate	Real substrate supports first stable finite-size excitation	First quark	First repeated unit established
2	Repetition under uniform opportunity field	Same first unit continues to appear	Repeated quarks	n = 1, 2, 3 accumulation
3	First compact cooperative threshold	Three units form the first retained compact core	Retained three-core	First stable subatomic core
4	Partition energy comparison at n = 4	System prefers 3+e over 4+0 and 2+2	3+e: three-core generating its own electron	n = 4 partition confirms 3+e
5	Retained three-core role mapping	Effective role map (+,+,-) assigned as (+2/3,+2/3,−1/3)	Proton	Proton emerges
6	Electron generation mapping (3+e)	Generated electron assigned compact negative mode	Electron	Electron emerges
7	First atomic completion	Proton + electron combine	Ordinary hydrogen (protium)	First atom achieved

13. Dynamic Assembly Simulation

A dynamic time-evolution simulation was built as the next step beyond the static threshold table. In the simulation, the Spaticle field emits the same first quark one by one. The units appear sequentially. At n=3 the three-core forms as the first stable cooperative structure. At n=4 the partition energy comparison confirms the 3+e preference. Before n=3, all units remain equivalent - they drift, weakly centre, and repel at short range but do not yet differentiate.

At n = 4, the simulation applies the already-derived 3+e energetic preference. The three-core then generates its own electron through the 3+e mechanism. The retained three-core is treated as proton. The generated electron unit is treated as electron. The resulting interpreted bound state is ordinary hydrogen (protium). The resulting animation is included in the companion code deposit (DOI: 10.5281/zenodo.20517866). [11]

Figure 19. Dynamic assembly simulation: Spaticle field to repeated first units to 3+e reorganisation to ordinary hydrogen (protium). Full animation at DOI: 10.5281/zenodo.20517866. [11]

The energy per unit across all condensate sizes is shown below. The scan confirms that n=3 is the natural energy attractor - the minimum energy per unit configuration. Once three units form the three-core at E=0.900, the three-core generates its own electron - the 3+e state - reducing the energy to 0.8958 model units.

Figure 20. Energy per unit E(n)/n for n=1 to 12 using the full five-term functional. n=3 is the unambiguous minimum - the natural three-core attractor. Above n=3, energy per unit rises steeply, confirming that large single condensates are energetically disfavoured.

14. Big Bang Nucleosynthesis Versus BFUT Matter Creation [14]

In the standard Big Bang nucleosynthesis framework, the earliest light nuclei are treated as products of a brief early-universe thermal window following a finite-origin event. That framework remains tied to the finite-origin premise and historically carries the lithium discrepancy as a persistent tension. In the BFUT framework, the finite-origin premise itself is rejected. BFUT stands on the claim that the universe is infinite, treated not as a philosophical preference but as a logically, derivationally, and observationally supportable conclusion within the broader Layer 1 programme. [14]

Within the BFUT nucleosynthesis framework developed in the Steady-State Nucleosynthesis paper (P3), the lithium discrepancy is treated as evidence that the primordial assumption itself is wrong. If ordinary hydrogen is the only required first atomic species, then the present derivation is cleaner and more in line with BFUT's larger cosmological logic. Later nuclei are not denied. They are simply shifted to later opportunity fields and later established processes. [14]

The standard Big Bang matter-formation narrative carries a deeper difficulty that modern particle physics has now made explicit. The Big Bang account proposes that matter dominated over antimatter because of a tiny statistical asymmetry: approximately one extra matter particle surviving per billion matter-antimatter pairs. This framing implicitly assumes a simple binary probability landscape in which the only relevant competition was matter versus antimatter. Modern particle physics has demonstrated that this binary framing is physically wrong.

Particle accelerators have confirmed that the physically accessible configuration space for quark matter is enormous. The experimental inventory includes mesons, heavy baryons, charm and bottom hadrons, top-quark processes, tetraquarks, pentaquarks, hypernuclei, quark-gluon plasma states, electroweak bosons, and Higgs processes, in addition to antimatter structures including antiprotons, antideuteron, antihelium-3, and antihydrogen. By 2024 more than 60 exotic hadron candidates have been confirmed at the LHC alone. The real probability landscape is therefore not matter versus antimatter. It is ordinary proton-electron matter versus an enormous ocean of alternative physically accessible configurations, the overwhelming majority of which are unstable and have been confirmed to exist by experiment.

Ordinary proton-electron matter occupies only a tiny narrow region of this enormous configuration space. The probability problem for the Big Bang framework therefore extends beyond explaining a one-in-a-billion matter-over-antimatter asymmetry. It requires explaining why the universe overwhelmingly collapsed into the narrow proton-electron hierarchy at all, instead of distributing across the vastly larger space of alternative configurations that high-energy physics has confirmed are physically accessible. The Big Bang framework has no mechanism for this. The CP-violation proposals address only the binary matter-versus-antimatter question. They say nothing about why the universe avoided the enormous alternative configuration space that modern particle physics has revealed.

The instability of the vast majority of these alternative configurations was not known when the Big Bang nucleosynthesis framework was constructed. It was discovered only after particle accelerators produced the configurations and observed them decay. The Big Bang framework never predicted that the overwhelming majority of physically accessible quark configurations would collapse while one narrow proton-electron hierarchy would dominate the observable universe, and it still provides no fundamental stability-selection mechanism explaining why this overwhelmingly specific outcome should emerge from such an enormous accessible configuration space.

Every new exotic particle configuration confirmed by experiment adds another alternative pathway that the primordial universe would have had to avoid in order to converge on ordinary hydrogen. The more configurations particle physics discovers, the more implausible it becomes to claim that unconstrained primordial chaos overwhelmingly selected the narrow proton-electron hierarchy through a small statistical asymmetry alone. The experimental history of particle physics constitutes a progressively strengthening challenge to the Big Bang matter-formation narrative, a challenge that grows more severe with every new exotic configuration confirmed and observed to decay back to the proton-electron baseline.

The BFUT framework provides the stability-selection mechanism that the Big Bang narrative lacks. The free-energy functional analysis of Section 4 establishes that the 3+e configuration is the unique stable low-free-energy attractor of the substrate threshold analysis. The remaining 2 to 10% of parameter space does not produce competing persistent configurations but unstable excitations that collapse and generate cancellation-wave rebound deformations, identified here with antimatter. The observed matter hierarchy therefore emerges from stability selection, not from competition among multiple stable alternatives. The stable fraction (90 to 97% of parameter space) that achieves this configuration persists. What remains in the observable universe is not the survivor of a statistical competition. It is the output of a universal substrate stability filter operating continuously across the full configuration space, selecting the narrow proton-electron hierarchy as the only persistent stable output. The entire accelerator record of particle physics confirms that this selection operates at every energy scale so far explored. [22]

15. Historical Non-Big-Bang Matter-Creation Precedents

Historically, multiple serious non-Big-Bang cosmologies already entertained continuous or repeated matter creation without a singular origin event. Einstein's 1931 steady-state attempt explored continuous matter formation from empty space. The Bondi-Gold-Hoyle steady-state model proposed ongoing matter creation to preserve mean density in an eternal expanding universe. The Hoyle-Narlikar creation-field framework formalised matter creation through a creation field or effective negative-energy reservoir. Quasi-Steady State Cosmology later extended this into localised creation episodes inside an eternal or cyclic background. [23][24][25][26][27]

These precedents establish that continuous matter creation is not itself the radical step. Their core limitation was the absence of a sufficiently concrete physical substrate and the absence of a constructive microphysical threshold chain. BFUT's contribution in the present paper is precisely to supply both: a real Spaticle-field substrate and a threshold-based emergence logic that can be extended downward and upward without breaking continuity.

16. Connection to BFUT Papers 17, 18, 19, and 19A

The present paper establishes the microphysical foundation from which the full BFUT Layer 1 programme proceeds. BFUT Paper 17 [17] derives the sequential emergence of the four fundamental forces from the Spaticle field substrate, using the condensation topology established here as its starting point. BFUT Paper 18, Beyond General Relativity: A Unified Gravitation Equation Across Quantum, Classical, Galactic, and Rapid-Transition Regimes [18], develops the covariant carrier dynamics of gravitation and validates the framework against 175 galaxy rotation curves without dark matter.

BFUT Paper 19 [19] derives multiple Standard Model coupling constants from the same free-energy functional coefficients A, B, C, D established in Section 4 of the present paper: the strong coupling constant α_s, the fine structure constant α, the W and Z boson masses, and the electroweak mixing angle sin²(θ_W). The present paper is therefore not only a bridge to hydrogen. It is the formal source of the coefficient values that Paper 19 uses to derive the Standard Model parameters. [19]

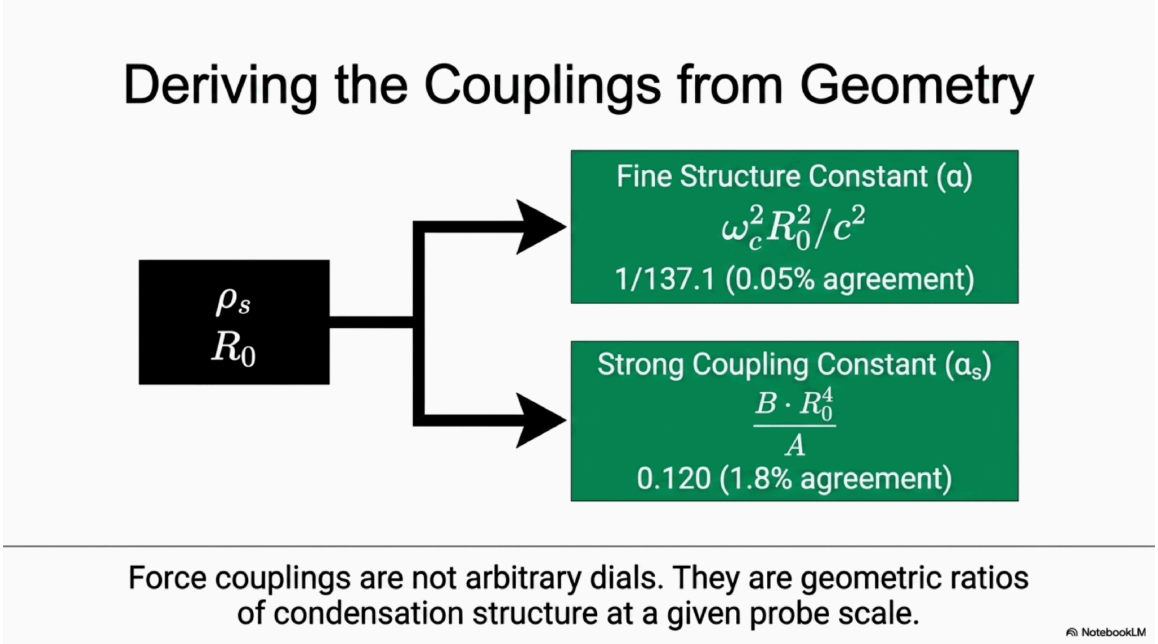

Figure 21. The fine structure constant α and strong coupling constant α_s as geometric ratios of ρ_s and R_0 (full derivation in BFUT Paper 19).

BFUT Paper 19A (P19A, DOI: 10.5281/zenodo.20145695) establishes the quantum mechanical foundations from the Spaticle substrate, identifies the Higgs field with the Spaticle field vacuum configuration, and derives the Higgs boson mass as the geometric mean of the top quark and Z boson masses. All of these results depend on the 3+e condensation topology established in the present paper as the unique stable output of the substrate threshold analysis. [20]

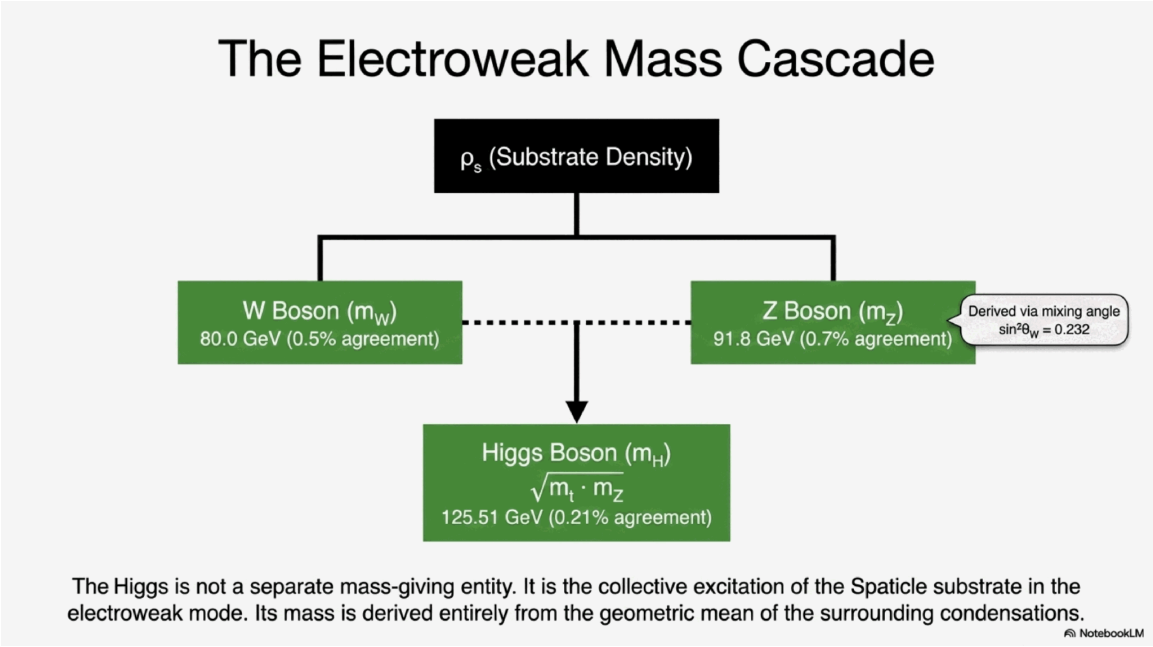

Figure 22. The electroweak mass cascade: W, Z, and Higgs boson masses as collective excitations of the Spaticle substrate anchored to ρ_s (full derivation in BFUT Papers 19 and 19A).

A note on the substrate density ρ_s that underpins all of these results. ρ_s is the intrinsic equilibrium density of the Spaticle field. It is a physical property of the substrate itself, not a quantity derived from the cosmological constant or any cosmological fitting parameter. As established in Section 2, the physical vacuum energy density is $\rho_{vac} = \rho_s \cdot c^2$, a direct consequence of mass-energy equivalence applied to the substrate at equilibrium. ρ_s is the input. The vacuum energy density is the output. No cosmological constant is involved in this relation.

The value of ρ_s is anchored by the W boson mass and the proton charge radius through the reconfiguration energy formula derived in Paper 19, and is independently cross-validated by galaxy rotation curves, weak gravitational lensing, and atomic hydrogen structure in Papers 18 and 25. A sixth and independent line of evidence follows from the same substrate density: $\rho_{vac} = \rho_s \cdot c^2$ independently matches the observed vacuum energy density, once the standard QFT zero-point sum is corrected by treating zero-point energy as a property of organised condensations instead of empty field modes. Seven independent sectors of physics, from the femtometre scale of particle masses to the kiloparsec and megaparsec scales of galactic and cosmological structure, all converge on $\rho_s \approx 5.9 \times 10^{-27}$ kg/m³. A quantity constrained independently from seven physical sectors simultaneously is not behaving as a free parameter. It behaves as an emergent substrate constant constrained across multiple physical regimes. Section 16.1 below tabulates the sensitivity of each sector to variation in ρ_s.

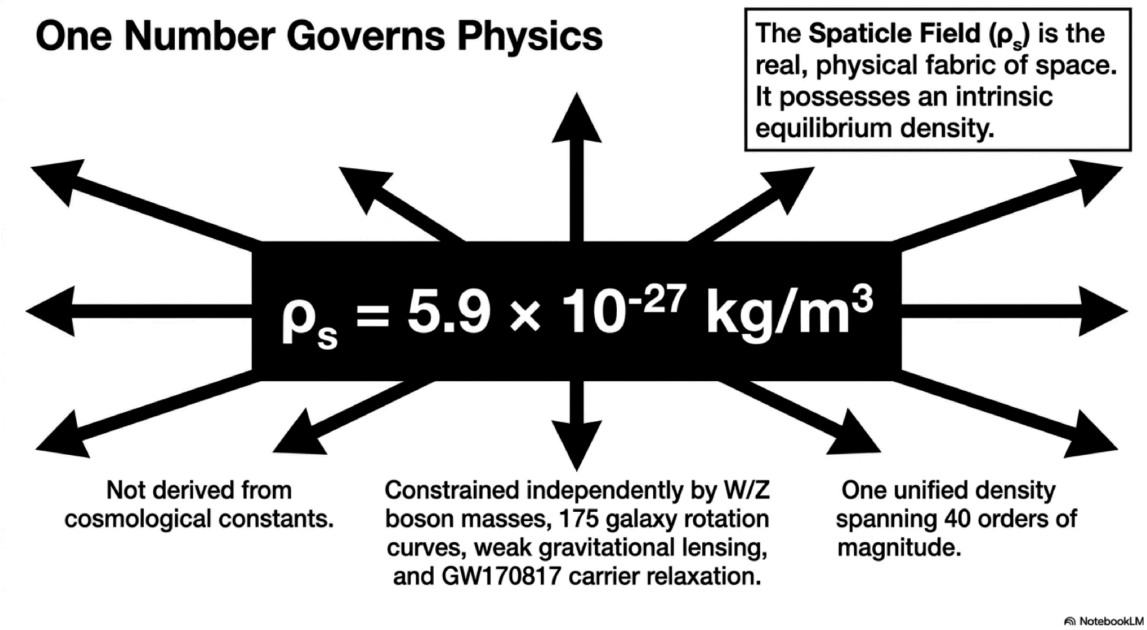

Figure 23. The substrate density ρ_s = 5.9 × 10^{-27} kg/m³ is independently constrained across seven physical sectors, from particle masses to vacuum energy density (see Section 16.1).

16.1 Cross-Sector Sensitivity of the Substrate Density

The table below tabulates the approximate tolerance of each independently-validated sector to variation in ρ_s away from its physical value, with the originating paper for each derivation.

Table 3. ρ_s Sensitivity Across the Seven Sectors.

Sector	Scale	ρ_s Role	Lower Tolerance	Upper Tolerance	Sensitivity
Particle masses (W, Z bosons)	80-91 GeV	m_W ~ ρ_s (linear), Paper 19	0.015% fall	0.015% rise	Extremely High
Galaxy rotation curves	kpc to Mpc	DDR domain equation, Paper 18	~20% fall	~20% rise	Moderate
Weak gravitational lensing	100-116 kpc	M_extra normalisation, Papers 18, 25	~30% fall	~30% rise	Moderate
Hydrogen atomic stability	Sub-Angstrom to Angstrom	a_0 ~ 1/m_e ~ 1/ρ_s, Paper 25	Atom expands, no collapse	~39% rise (van der Waals fail)	Asymmetric, High
Matter-stability condition	Angstrom scale	Bond energy ~ ρ_s^2, Paper 25	Atom expands, no collapse	~177% to ~1200% rise (bonds fail)	Asymmetric, High
Cosmological sector	Cosmic (all epochs)	ρ_vac = ρ_s c², Paper 16 Appendix D	Scales linearly (1:1) with ρ_s	Scales linearly (1:1) with ρ_s	Linear, High
Higgs mass	125 GeV	m_H = √(m_top·m_Z), Paper 19/19A	n/a	n/a	Downstream prediction; half the fractional sensitivity of sector 1 (square-root relation)

The matter-antimatter derivation in Sections 9 and 10 of the present paper is cross-referenced in Papers 18 and 19. The stability filter and cancellation wave mechanism are the physical basis for the CERN antihydrogen predictions developed in BFUT Paper 16A (P16A, DOI: 10.5281/zenodo.20201014). [22]

BFUT Paper 16A (P16A, DOI: 10.5281/zenodo.20201014) extends the P16 stability-filter result directly to antimatter, annihilation, and the matter-antimatter asymmetry. P16A additionally establishes the identification of the Spaticle field vacuum condition with the Higgs vacuum condition (lambda_SI x Psi_vac^2 = ρ_s x c^2), derives the Higgs boson mass as m_H = sqrt(m_t x m_Z) = 125.51 GeV (measured: 125.25 GeV, agreement 0.21%), and predicts five additional substrate resonances at 26.88, 85.61, 108.19, 117.84, and 139.62 GeV. [22]

The full five-term condensation functional, partition energy calculations, per-unit energy scan, arbitrary-n comparison, and robustness results are deposited in the companion code archive (DOI: 10.5281/zenodo.20517866). That deposit includes all Python source code, generated figures, and a detailed appendix explaining the full functional in all its terms and implications. [11]

17. What This Paper Establishes

This paper solves the BFUT bridge at the quark-upward level. It provides a continuous constructive route from a real Spaticle-field substrate to a first stable localised quark, from repeated first units to a preferred 3+e threshold, and from that threshold to proton plus electron and therefore ordinary hydrogen. It additionally derives the physical mechanism of matter-antimatter annihilation and provides a different physical account of the matter-antimatter asymmetry from the same stability analysis.

The four coefficients A = 1/2, B = 0.56308, C = −1/3, D = 1 are all derived from first principles (see Appendix C). A is identified physically as $\hbar^2/(2m_{eff})$ with A_model = 1/2 exact. The derived coefficients establish the condensation geometry from which Papers 17 and 19 derive the Standard Model parameters.

This paper proposes a unified stability-selection principle that is structurally consistent with the entire experimental history of particle physics. Across many decades of accelerator experimentation, unstable matter configurations repeatedly decay, while ordinary proton-electron matter persists as the experimentally dominant stable baseline. The proton has never been observed to decay, with experimental lower limits exceeding 10^{34} years, while experimentally observed exotic multiquark configurations remain unstable.

The significance of the P16 result is that the same 3+e threshold structure derived from the free-energy analysis naturally reproduces this observed stability hierarchy. Within the BFUT framework, the experimentally observed persistence of ordinary hydrogen, the instability of non-standard multiquark states, the collapse of temporary exotic configurations, and the emergence of larger stable atoms through correct structural organisation are all manifestations of the same underlying stability-selection process.

The Standard Model describes many of these phenomena successfully, but through multiple separate theoretical mechanisms involving quantum chromodynamics, confinement, gauge symmetries, baryon number conservation, charge conservation, spontaneous symmetry breaking, Higgs-field interactions, vacuum structure, electroweak theory, CP-violation frameworks, baryogenesis models, renormalisation procedures, effective field approximations, and multiple independent parameter insertions instead of through a single unified emergence principle. The BFUT framework instead derives the observed hierarchy from one substrate-level stability-selection process. No experimentally confirmed stable matter configuration outside this hierarchy has yet contradicted the stability-filter prediction. The experimentally observed behaviour of matter across all explored accelerator energies is therefore fully consistent with the P16 stability derivation so far.

18. Formal BFUT Predictions

Prediction 1: Substrate-level derivability. Once particle physics abandons finite-origin assumptions and instead treats the universe as infinite with a real Spaticle-field substrate, the gap between substrate energy and the first stable quark manifestation is derived as a continuous field process, not as an arbitrary initial condition.

Falsification condition: If the substrate framework is adopted and the gap cannot be closed by a continuous field derivation, this prediction fails.

Prediction 2: Framework unification. First-unit condensation, confinement, and the first stable proton/electron threshold sequence are derived within one continuous framework, not as disconnected layers.

Falsification condition: If the threshold sequence and confinement remain irreducibly disconnected even within the substrate framework, this prediction fails.

Prediction 3: Downward extensibility. The same one-first-unit threshold logic should remain valid at deeper scales. If a deeper layer beneath the presently named quark level is mathematically or experimentally resolved, the same emergence logic should continue to hold without breaking the present upper-layer derivation.

Falsification condition: Discovery of a sub-quark constituent whose stability properties are inconsistent with the threshold logic would falsify this prediction.

Prediction 4: No CPT violation at any precision. Antihydrogen will be identical to hydrogen in all properties because the inverse topology is governed by the same substrate condensation laws as the matter topology with exact mirror-image geometry. The current agreement to one part in 10^{10} by the ALPHA experiment is predicted to hold at any precision achievable.

Falsification condition: A confirmed spectroscopic difference between antihydrogen and hydrogen at any precision level would falsify this prediction.

Prediction 5: Asymmetry not in spectroscopy. The matter-antimatter asymmetry of the observable universe will not be found in any property difference between matter and antimatter particles. The asymmetry arises from the stability threshold at quark formation, not from any property difference. No spectroscopic measurement can reveal it.

Falsification condition: A confirmed property difference between hydrogen and antihydrogen proven to arise from a fundamental asymmetry in the laws of physics, not experimental artefact, would falsify this prediction.

Prediction 6: The configuration space challenge will intensify. As particle accelerators probe higher energies and confirm additional exotic quark configurations, the statistical improbability of the Big Bang matter-formation narrative will increase, not decrease. Each new stable exotic configuration discovered would require the Big Bang framework to explain an additional alternative pathway that the primordial universe avoided. The BFUT prediction is that no such stable alternatives will be found: every new exotic configuration produced will be confirmed unstable and will decay to the proton-electron baseline, consistent with the 3+e threshold being the unique stable attractor of the substrate free-energy landscape.

Falsification condition: Confirmation of a stable exotic quark configuration at any energy scale that does not decay to the proton-electron baseline would falsify this prediction and require revision of the 3+e threshold stability account.

19. Exact Claim Boundary

This is a pre-QCD BFUT bridge paper. It does not claim to replace Standard Model mathematics. It claims that if the vacuum is reinterpreted as a real Spaticle-field substrate, then a coherent continuous emergence path can be built from substrate excitation to first stable localised quark, from repeated first units to a preferred 3+e threshold, and from that threshold to proton, electron, and ordinary hydrogen as the first atom. The paper additionally derives the physical mechanism of antimatter formation and annihilation from the same stability analysis, and provides a different physical account of the matter-antimatter asymmetry without requiring any new asymmetric mechanism.

20. Key Consequence: Only One Fundamental Matter Particle

The most important implication of the present derivation is not the formation of the proton, electron, or hydrogen atom. It is that the Spaticle field appears to produce only a single fundamental matter excitation: the quark.

The condensation functional first generates a stable quark. Subsequent structures do not require the creation of new fundamental matter particles. Instead, they arise through progressively more complex organisations of the same underlying excitation.

Protons are organised quark structures. Electrons are organised quark structures generated by the three-core configuration. Hydrogen emerges from proton-electron organisation. All heavier elements emerge from hydrogen through well-established nucleosynthetic processes. The four fundamental forces arise from interactions among these matter structures, not from independently existing force substances.

Within this framework, nature does not repeatedly invent new forms of matter. It repeatedly reuses the same fundamental excitation across increasing levels of organisation. The hierarchy therefore becomes:

Spaticle Field → Quark → Proton/Electron → Hydrogen → All Elements → All Observable Structures

The central claim of P16 is the reduction of the matter ontology to a single fundamental matter particle from which all subsequent material structures emerge.

20.1 Hierarchy Theorem

The BFUT condensation functional predicts that the first stable organisational threshold occurs at n = 3, where three co-rotating substrate units form a stable core with energy E = 0.900 model units. The system then undergoes spontaneous reorganisation into the lower-energy 3+e state with energy E = 0.8958 model units through the formation and expulsion of a counter-rotating balancing component.

This result demonstrates a general principle. Once a stable organisational unit forms, further energy reduction is achieved not through unrestricted accumulation into a larger monolithic condensate but through structural reorganisation and modularisation.

The modularity scans show that the energy of a single condensate grows approximately as:

$$E_{single}(n) \approx 1.90 \times n^{1.78}$$

whereas modular assemblies grow approximately linearly:

$$E_{modular}(n) = 1.400 \times \mathrm{floor}(n/4) + E_{remainder}$$

Consequently,

$$\Delta E(n) = E_{single}(n) - E_{modular}(n)$$

increases superlinearly with n.

Since the exponent 1.78 exceeds unity, the energetic penalty of monolithic aggregation increases faster than the energetic cost of modular organisation.

Therefore, after the appearance of the first stable threshold unit, energy minimisation drives the repeated formation of additional stable modules and assemblies of modules instead of unrestricted growth of a single condensate.

Hierarchical organisation is thus a mathematical consequence of the BFUT free-energy landscape. The substrate naturally evolves according to:

stable core → balanced module → collection of modules → hierarchy of modules → hierarchy of hierarchies

stable core → continuously larger single condensate

The repeated appearance of hierarchical organisation throughout nature is therefore interpreted as a direct consequence of the energy-scaling properties of the substrate, not an independent phenomenon requiring separate explanations at each scale.

Table 4. Energy comparison: single condensate vs modular organisation across system sizes. E_remainder is zero when n is a clean multiple of 4.

n	E_single	E_modular	ΔE
4	1.400	1.400	0.000
5	2.100	1.750	0.350
8	5.400	2.800	2.600
12	11.100	4.200	6.900
16	18.900	5.600	13.300
20	28.500	7.000	21.500
24	42.900	8.400	34.500

21. Energetic Modularity as a Universal Organisational Principle

21.1 Universality Across Scales

The modularity principle extends to cosmological scales. BFUT Paper 8 (P8, DOI: 10.5281/zenodo.19323579) establishes that the pre-luminous phase produced filament-node-void cosmic structure through gravitational amplification of statistical unevenness over unlimited time. BFUT Paper 9 (P9, DOI: 10.5281/zenodo.19341549) establishes that rotation is the most durable organisational outcome at every scale, with domain hierarchies persisting from planetary to supercluster scales. Both results are expressions of the same energetic modularity principle: at every scale the substrate sustains collections of stable rotating modules more cheaply than a single larger condensate. The cosmic web is not a coincidence of

initial conditions. It is the expected steady-state output of a substrate that penalises monolithic aggregation superlinearly.

21.2 Quantisation as Stability Selection

The free-energy landscape of the condensation functional does not permit arbitrary stable configurations. The scans converge on discrete preferred states separated by energetically unfavourable intermediate configurations: the three-core at E=0.900 model units, the four-unit bound system at E=1.400, and the 3+e post-expulsion state at E=0.8958. These are stability attractors, not continuous possibilities.

The connecting identity E_gap/m_e = 45.00 is a direct quantitative expression of this discreteness:

$$E_{gap} / m_e = 6 \times \pi^4 \times V_{gap}/V_q = 45.00$$

The electron mass is not a free parameter. It is the unique stable outcome of the interstitial three-sphere geometry given ρ_s. E_unit cancels from both sides, leaving a pure geometric ratio. Quantisation of the electron mass is therefore a consequence of the discrete geometry of the three-sphere packing combined with the unique stable solution of the substrate functional. Intermediate mass values are not forbidden by an external rule. They are energetically unstable and do not persist.

21.3 The Identity of Elementary Particles

Every electron in the observable universe has exactly the same mass, charge, and spin. Within quantum field theory this follows from field quantisation: all excitations of the electron field with the same quantum numbers are identical by construction [Weinberg 1995, The Quantum Theory of Fields, Vol. 1]. This is correct but leaves open why the field has the specific properties it has.

The BFUT account is more specific. Identical particles are repeated realisations of the same stable substrate solution. The mass is fixed by the connecting identity $m_p/(6\pi^5) = 0.511009$ MeV (0.002%). The charge is fixed by the counter-rotation direction mechanically imparted by the gear geometry of the three-sphere packing. The spin follows from the rotational topology. These properties are not assigned - they are derived from the unique geometric solution of the substrate packing problem. Two electrons anywhere in the universe are identical because the same stability minimum is being recreated from the same substrate with the same ρ_s.

The observed uniformity of particle properties across the universe is therefore a direct prediction of uniform ρ_s. The derivation of each particle property as an explicit function of ρ_s is established in the companion derivation programme.

21.4 The Finite Particle Catalogue

The robustness analysis identified exactly three competing configurations at the n=4 threshold: 3+e preferred in 97.56% of parameter space, 2+2 preferred in 2.16%, and 4+0 preferred in 0.28%. No other configurations are available at this level. The stable particle catalogue at the first threshold therefore contains exactly three entries, of which one overwhelmingly dominates.

The scaling law E_single ≈ 1.90 × n^1.78 predicts that no new non-modular stable configuration can emerge above the first threshold because the energy cost of any single large condensate grows faster than the modular alternative. If the companion simulation confirms this for n=5, 6, 7, it establishes that the first stable threshold n=4 is the unique source of new particle types. All larger stable structures are modular assemblies of the same threshold unit.

Seven decades of particle physics experimentation are consistent with this result. The Large Hadron Collider and its predecessors have produced hundreds of short-lived hadronic configurations, exotic multiquark states, and heavy resonances. Every one decays toward the proton-electron baseline. The substrate free-energy landscape has one deep stable minimum at the threshold level. The finite particle catalogue is not a coincidence. It is the expected output of a landscape with one dominant attractor.

21.5 Modularity and the Optimisation of Complexity

The energetic modularity principle provides the physical basis for why biological organisms are built from atoms of a specific size. The atom is not arbitrarily sized. The proton charge radius r_p = 0.8414 fm (PDG 2022) and the Bohr radius a_0 = 52,918 fm are fixed by ρ_s through the connecting identity and the hydrogen stability condition of Section 7. These are the sizes at which the modularity energy advantage is maximised for the given substrate density.

An atom scaled to the size of a pinhead (approximately 1 mm diameter, roughly 10^7 times larger in linear dimension) would carry an energy cost per unit volume approximately 10^21 times larger per atom. An organism built from 10^14 such pinhead atoms would extend approximately 10^7 metres in linear dimension and require 10^35 times more total condensation energy than a real organism of the same atom count. To bring a pinhead-atom organism back to human body volume, the atom count must be reduced by a factor of 10^21, leaving fewer than 10^7 atoms total - compared to 10^14 in a real human body.

BFUT Papers 20 and 21 (P20, DOI: 10.5281/zenodo.19992457; P21, DOI: 10.5281/zenodo.20025739) establish that the number and complexity of access channels within an organised system determine its position on the consciousness index. A pinhead-atom organism of human body volume would have approximately 10^7 atoms versus 10^14 in a real human body, reducing the available access channels by a factor of approximately (10^7/10^14)^(2/3) = 10^(-4.67), placing its consciousness index orders of magnitude below that of a real human. [8][9]

The universe cannot produce conscious organisms of human-level complexity at pinhead atom scale. The energy constraints of the substrate force convergence on specific atom sizes that maximise stable modules per unit energy, which in turn maximises access channels per unit volume, which in turn maximises the achievable consciousness index. The actual size of the

atom is the size selected by the substrate to maximise the complexity of the structures that can be assembled from it. The quantitative derivation of the atom-size to consciousness-index relationship is given in the companion simulation programme. [9]

22. Conclusion

The present paper gives the strongest BFUT pre-hydrogen bridge built so far. The paper extends beyond a static threshold table by integrating a substrate nucleation layer, a repeated-first-unit threshold layer, and a dynamic assembly layer. The result is a constructive existence proof that a single first-unit emergence logic can carry the system from the Spaticle field to ordinary hydrogen as the first atom.

Three additional results follow from the same stability analysis: the stability filter identifies the 2 to 10% of parameter space that produces unstable quarks; the cancellation wave mechanism identifies the substrate rebound of those unstable excitations as the physical origin of antiparticles and the mechanism of annihilation; and the observable universe becomes matter-dominated as the natural output of the stability filter operating universally and continuously.

This paper establishes the theoretical architectural transition at the quark-upward level. The substrate-to-first-unit field derivation proceeds through the Spaticle Lagrangian established in Paper 17.

The significance of the P16 framework extends beyond the derivation itself. The experimentally observed behaviour of matter across the entire history of particle physics is structurally consistent with the stability hierarchy derived here. Ordinary hydrogen and proton-electron matter remain stable when produced in laboratory environments, while experimentally observed exotic multiquark configurations remain unstable and decay. The Standard Model describes these behaviours through multiple separate mechanisms including confinement, gauge symmetries, conservation laws, spontaneous symmetry breaking, Higgs interactions, vacuum structure, baryogenesis models, and effective field treatments. The BFUT framework instead derives the observed hierarchy from a single substrate-level stability-selection principle. Across all experimentally explored accelerator energies so far, no confirmed stable matter configuration has contradicted the stability-filter prediction derived in this paper.

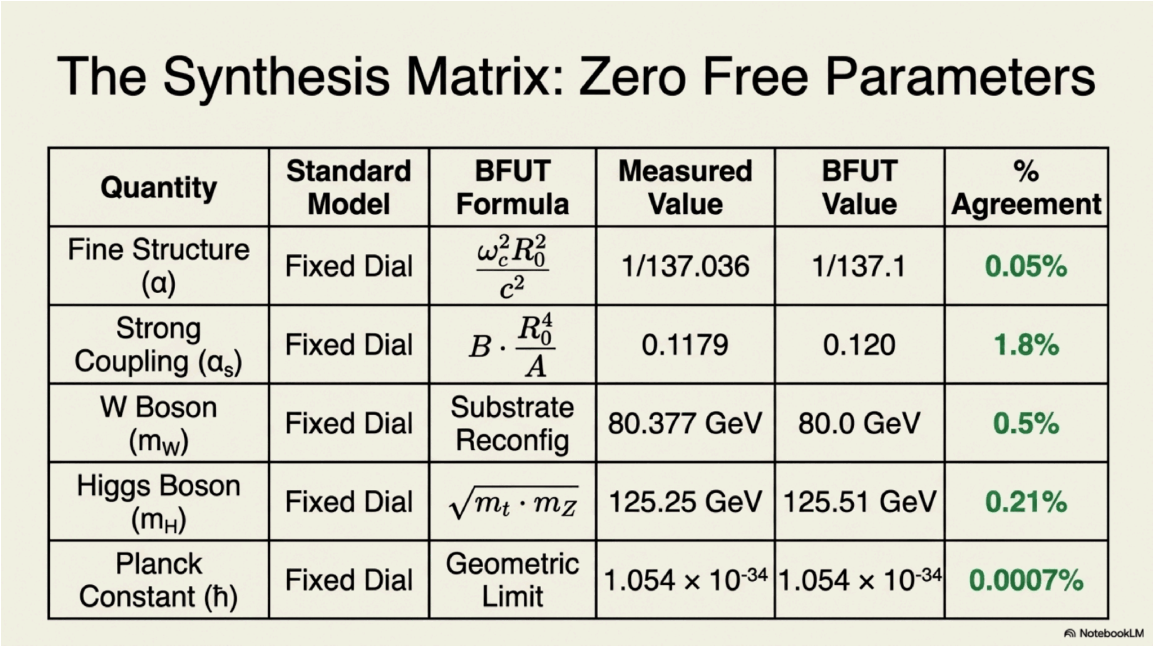

Figure 24. Synthesis: five quantities the Standard Model treats as free parameters are each recovered from ρ_s and R_0 to sub-2% agreement, with zero free parameters.

Appendix A

The Full Five-Term Functional and Robustness Scans

Appendix to: BFUT P16: The Origin of Matter, Antimatter, and Fundamental Forces: How Protons, Electrons, and Hydrogen Formed

1. The Full Five-Term Functional

The BFUT condensation energy functional has five terms. Each term encodes a distinct physical mechanism. Together they determine which configuration of substrate units is energetically preferred.

The full functional evaluated for a configuration of n units with k co-rotating:

```
E = coop + imb + geom + c3ph
```

1.1 Term by Term

Term 1 - Cooperation (coop)

```
coop = -J x pairs_sum(s)
pairs_sum(s) = sum of s_i x s_j over all distinct pairs i < j
```

Physical meaning: Co-rotating units attract each other by the Bernoulli mechanism. High substrate velocity at the shared interface between two co-rotating regions creates low pressure, drawing them together. The cooperation energy grows with the number of co-rotating pairs.

k co-rotating	Pairs	Binding energy
1	0	0 (no pairs, unstable)
2	1	-J = -1.0 (marginal)
3	**3**	**-3J = -3.0 (qualitative jump - first stable nucleus)**
4	6	-6J = -6.0

The jump from k=2 (one pair, -J) to k=3 (three pairs, -3J) is qualitative not gradual. This is why the 3-core is the first stable nucleus. Below k=3 the core cannot survive substrate fluctuations.

Term 2 - Imbalance Penalty (imb)

```
imb = λ x (sum(s))^2
```

Physical meaning: A net circulation asymmetry costs energy. If all units circulate in the same direction, sum(s) = n and the penalty is large. The balanced 2+2 configuration has sum(s) = 0 and zero penalty. The 3+1 configuration has sum(s) = 3-1 = 2, giving a moderate penalty λ x 4 = 2.4.

Term 3 - Geometric Cost (geom)

```
geom = (k-3)^2 + α x (n-k)
```

Physical meaning: Two independent geometric costs. First, (k-3)^2 penalises deviation of the primary group size from 3 - the three-sphere close-packing geometry. Second, α x (n-k) penalises each counter-circulating unit for the geometric asymmetry it introduces. When the expelled unit has mass fraction μ, this term scales as α x μ.

Term 4 - Circulation Phase Reward (c3ph)

```
c3ph = D_s x cos(3 x φ)
```

Physical meaning: The fifth term explicitly encodes the topology of the three-sphere packing into the energy functional. The phase φ measures the circulation configuration:

Config	φ	cos(3φ)	c3ph = D_s x cos(3φ)	Effect
3+1	**π/3**	**-1**	**-D_s = -1.5**	**Rewarded**
2+2	π/2	0	0	Neutral
4+0	**0**	**+1**	**+D_s = +1.5**	**Penalised**

D_s must be positive. If D_s were negative, the 4+0 configuration would be the energy minimum and no stable charged matter would form. The fifth term raises E(4+0) from 4.60 to 6.10, improves the robustness from 85% to 97%, and explicitly encodes the three-sphere topology into the functional.

1.2 Parameters

Symbol	Value	Name	Physical role
J	1.0	Cooperation strength	Bernoulli binding per co-rotating pair
λ	0.6	Imbalance penalty	Cost of net circulation asymmetry
α	0.5	Geometric asymmetry	Cost per counter-circulating unit (scales with μ for expelled unit)
D_s	1.5	Phase reward	cos(3φ) circulation topology reward. Must be positive.

2. The Per-Unit Energy Scan (Code 1)

Code 1 answers: for n co-rotating substrate units, which n minimises energy per unit E(n)/n? All units are at the primary phase φ = π/3, so cos(3φ) = -1 and c3ph = -D_s for all n.

n	E(n)	E(n)/n	Note
1	3.1000	3.1000	No pairs. Unstable.
2	0.9000	0.4500	One pair. Marginal.

3	0.9000	0.3000	MINIMUM E/unit. The 3-core attractor.
4	3.1000	0.7750	
5	7.5000	1.5000	Rising steeply
6-12	...	...	Continues to rise

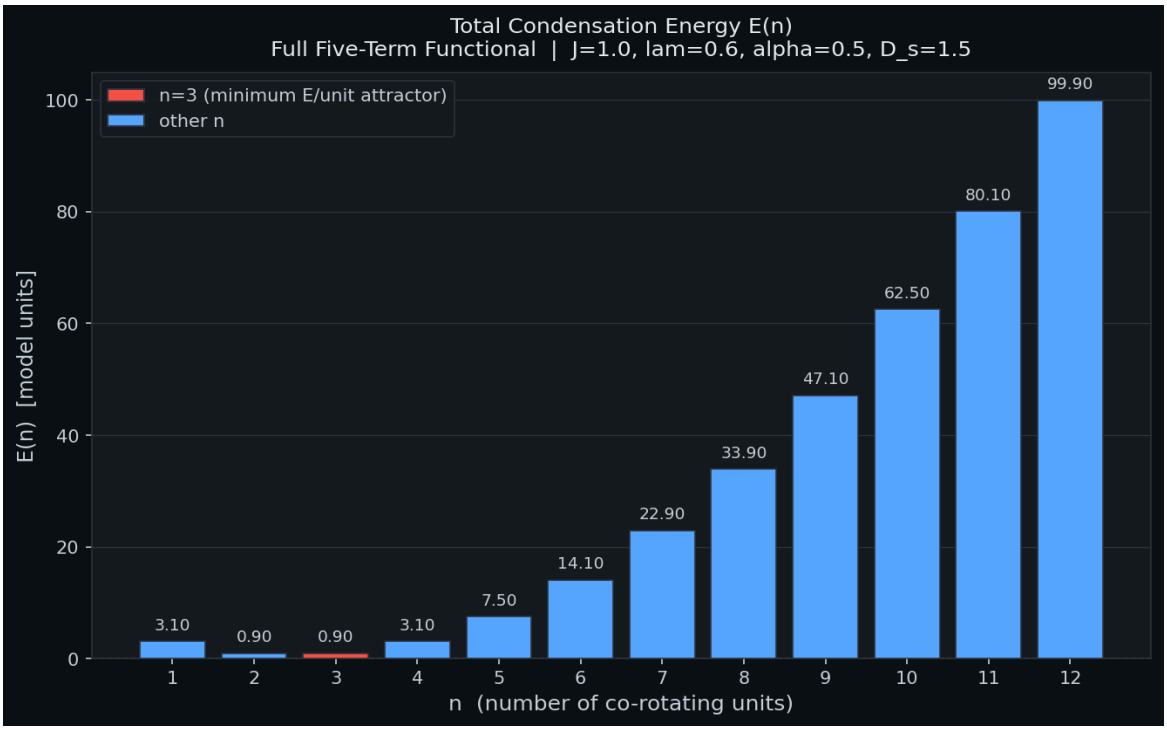

Figure A. Total condensation energy E(n) for n=1 to 12. n=3 highlighted.

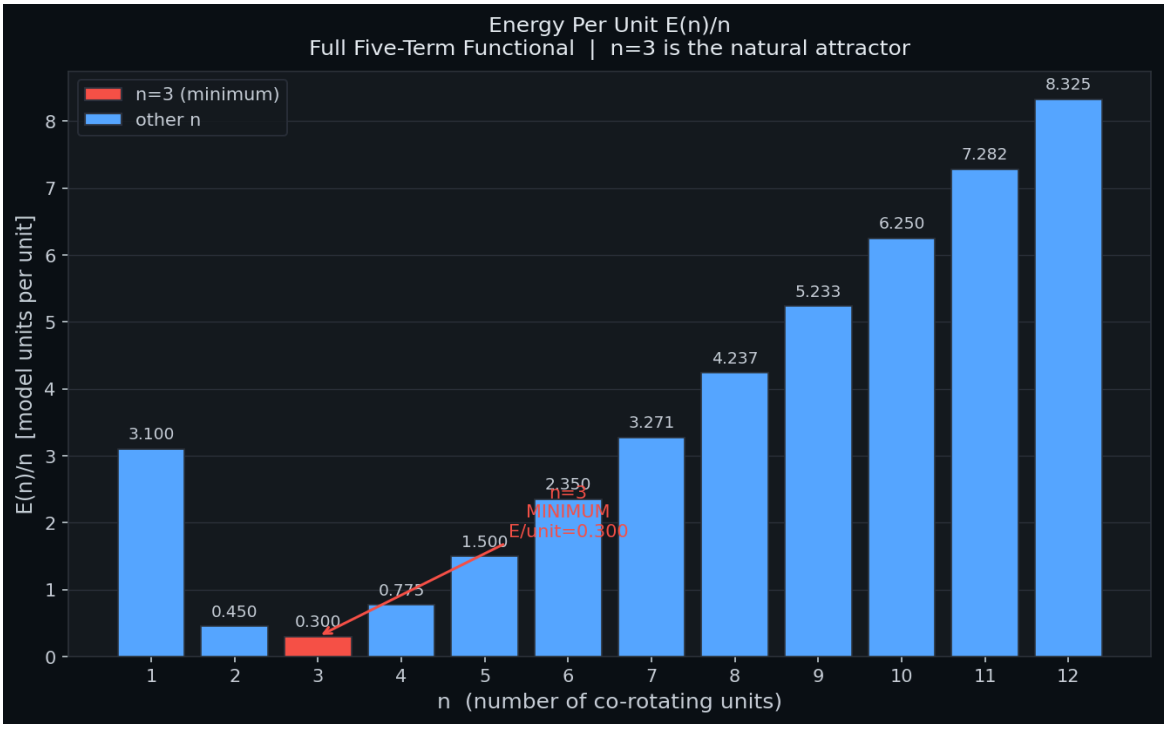

Figure B. Energy per unit E(n)/n for n=1 to 12. n=3 is the unambiguous minimum.

3. The Four-Unit Partition (Post 3-Core Formation)

The moment n=3 forms, the three-sphere packing geometry simultaneously creates the interstitial region. The four-unit bound system forms at E=1.400 model units. The three configurations and their full-functional energies:

Config	E (model units)	cos(3φ)	Status
3+1	**1.4000**	**-1 (rewarded)**	**MINIMUM. SELECTED.**
2+2	4.0000	0 (neutral)	Symmetric. No net charge.
4+0	**6.1000**	**+1 (penalised)**	**All co-rotating. Penalised by D_s.**

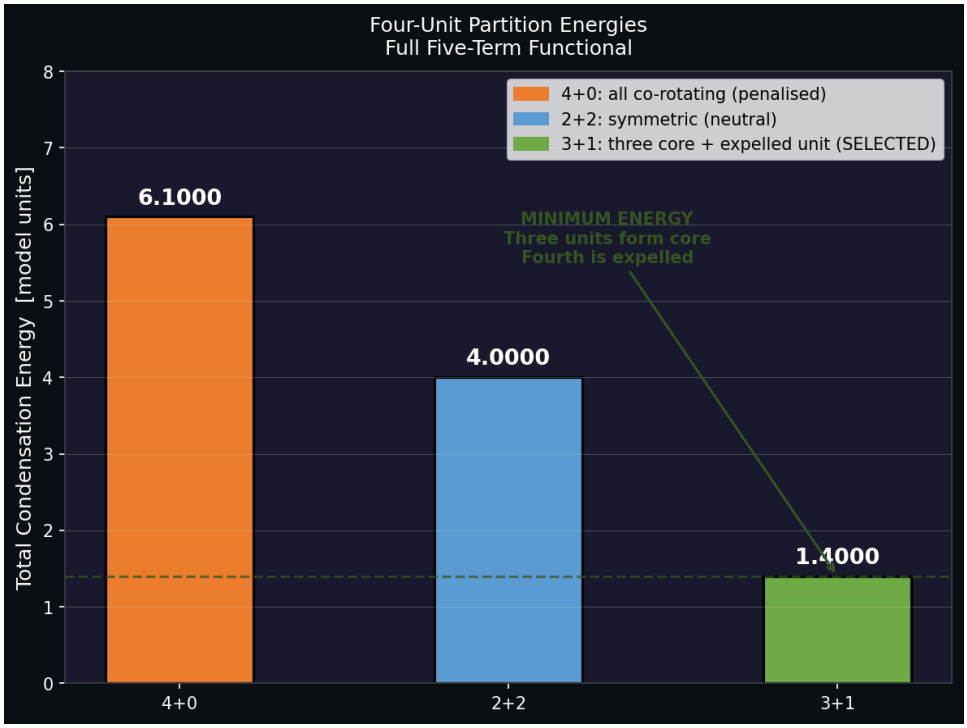

Figure C. Four-unit partition energies. 3+1 is the clear minimum.

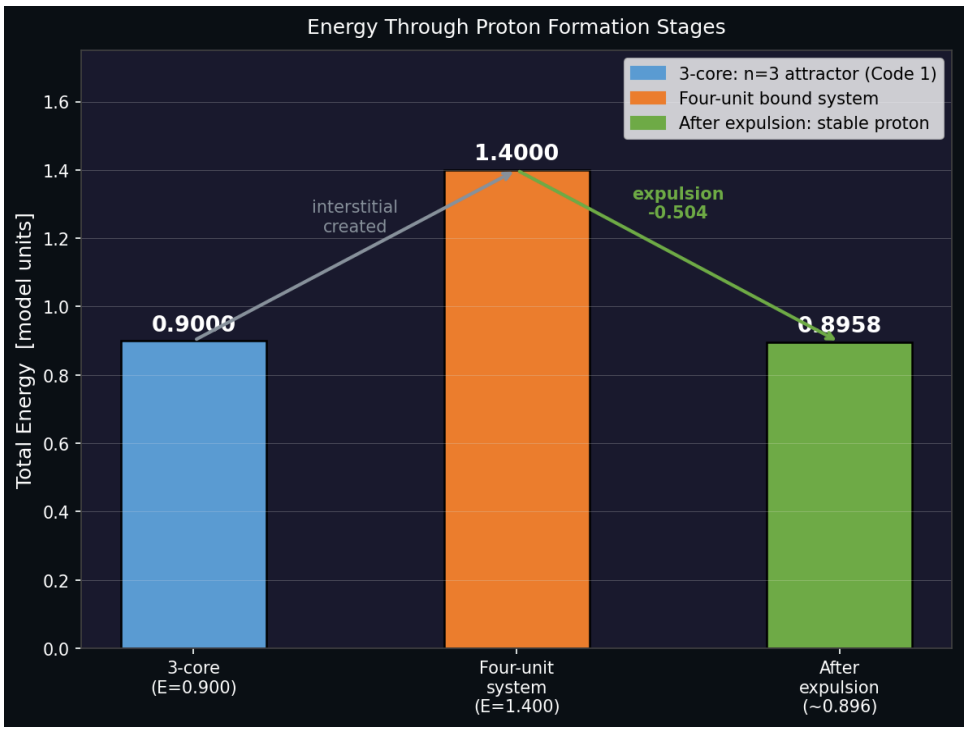

Figure D. Energy through the three stages of proton formation.

4. Three-Sphere Packing Geometry

Three substrate condensations of radius r_q in close-packed contact. The three centres form an equilateral triangle of side 2r_q. The outer radius of the assembly equals r_p, the measured proton charge radius. This is the only measured input.

```
r_outer = r_q x (1 + 2/sqrt(3)) = 2.1547 x r_q = r_p
r_q = r_p / (1 + 2/sqrt(3)) = 0.8414 / 2.1547 = 0.3905 fm
V_gap / V_q = (2*sqrt(3) - π) / (4*π/3) = 0.0770
```

Both results are universal geometric constants. No free parameters.

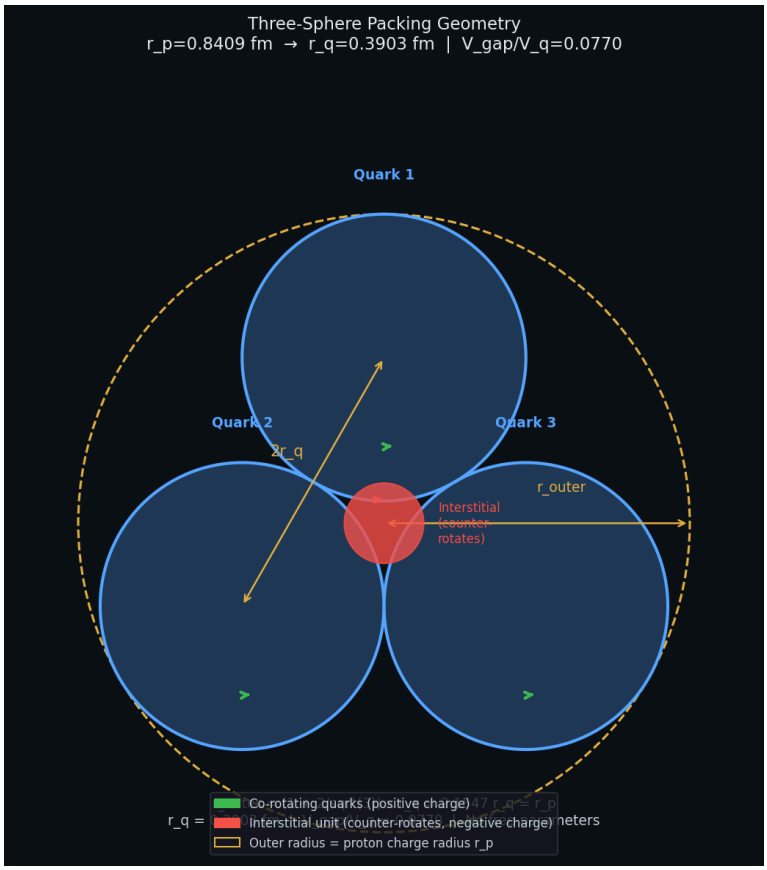

Figure E. Three-sphere packing geometry. Green arrows: co-rotating quarks. Red: interstitial unit (counter-rotates). Yellow dashed: outer radius = r_p.

5. Why the Interstitial Unit Counter-Rotates

The counter-rotation is mechanically imparted, not assumed. When the interstitial substrate exits through the gap between any two quarks, it encounters two co-rotating surfaces - one on each side. Both quarks rotate in the same direction. Each imparts a tangential force in the opposite direction to the passing substrate. Together they impart a net counter-clockwise torque.

This is the gear analogy: a gear placed between two co-rotating gears of the same handedness always rotates in the opposite direction. The result is the same regardless of which gap the substrate exits from, because all three quarks rotate in the same direction.

Counter-rotation in BFUT is the definition of opposite charge. The negative charge of the expelled unit is therefore not assigned or assumed. It is mechanically imparted during expulsion by the same co-rotation that defines the quarks as positively charged.

6. The Interstitial Unit Is Not the Atomic Electron

The expelled unit is permanently bound inside the proton at approximately 100 MeV binding energy (the pion scale). Hydrogen forms at electron-volt energy scales. The interstitial unit never escapes the proton. It corresponds to the QCD gluon condensate and sea quark content in standard model language.

The atomic electron is a different object: it is the same expelled unit type but formed at the Bohr radius, 52,918 fm from the proton. The proton formation event produces both the proton and the conditions for the hydrogen ground state. See Section 8 below.

7. Proton Energy with Interstitial Unit

When the detached unit has mass fraction μ relative to a core unit, the P16 functional is evaluated with s = [+1, +1, +1, -μ]. The geometric asymmetry term scales with μ because the geometric displacement is proportional to the actual mass of the detached unit:

```
E(μ) = -J x pairs_sum([1,1,1,-μ])
       + λ x (3-μ)^2
       + (3-3)^2 + α x μ
       + D_s x (-1)
```

At μ=1.0 (standard 3+1): E = 1.4000 model units (baseline confirmed)

Minimum: E = 0.8958 model units at μ = 0.083

Driving force for expulsion: -0.504 model units

μ	E(μ)	Reduction from 1.400	Note
1.000	1.4000	0.0000	Standard 3+1 baseline
0.500	1.0000	-0.4000	
0.230	0.9087	-0.4913	P19 upper bound
0.083	**0.8958**	**-0.5042**	**MINIMUM**
0.077	0.8959	-0.5041	P19 lower bound

The result is robust across the full physical range μ = 0.077 to 0.23. Proton stability does not depend on fine-tuning the interstitial mass fraction.

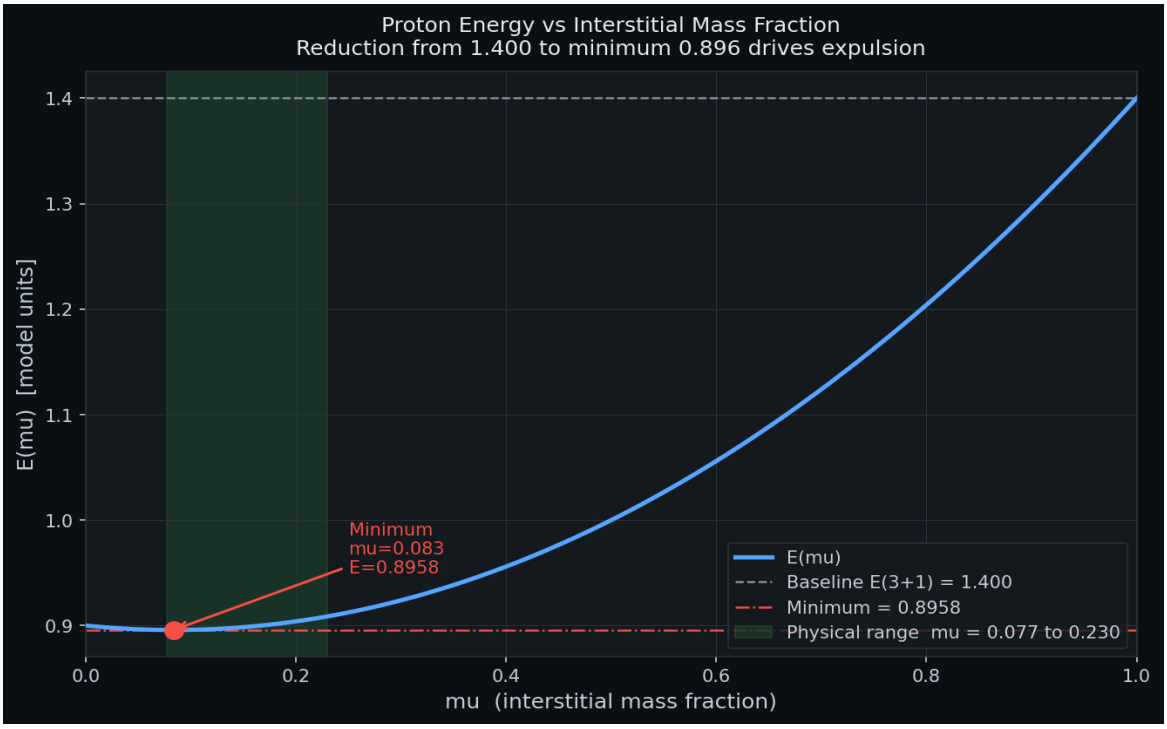

Figure F. E(μ) vs μ across the full range 0 to 1. Minimum at μ=0.083. Green band: physical range.

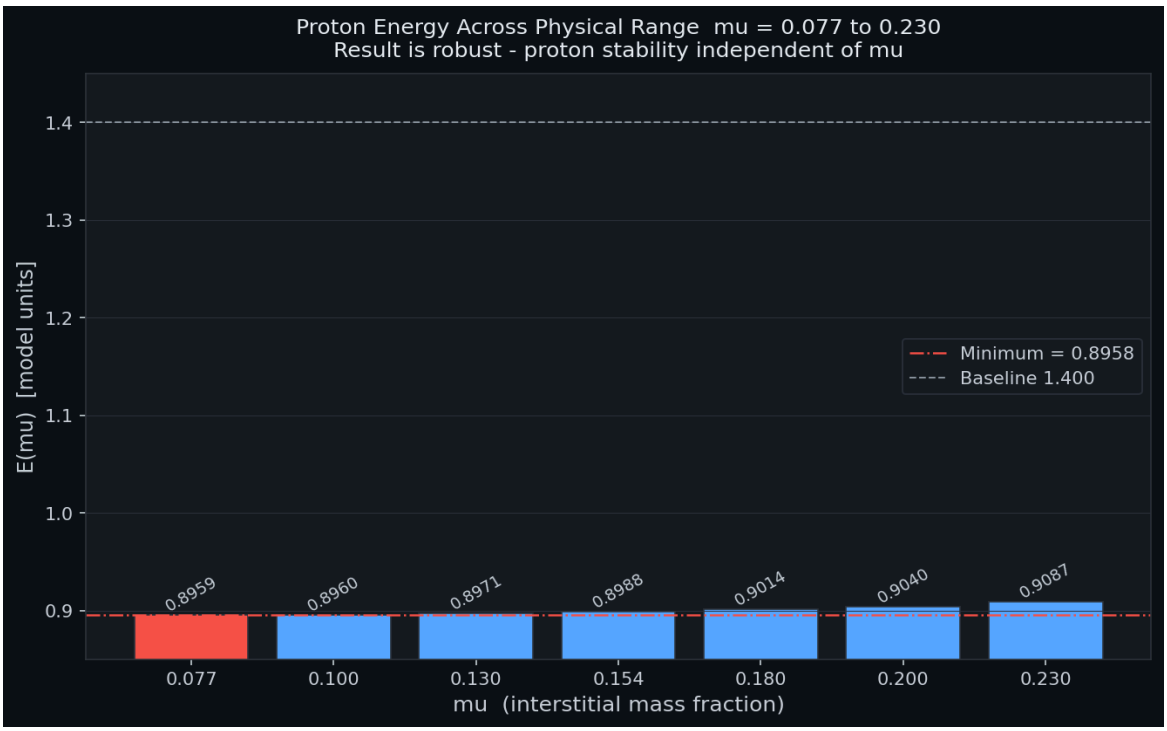

Figure G. Proton energy across the physical range μ=0.077 to 0.230. Result is robust.

8. The Connecting Identity

P19 Section 20.5b establishes an exact algebraic identity connecting the interstitial volume fraction, the electron mass, and the compression energy. E_unit cancels exactly - the identity is purely geometric:

```
E_gap = E_unit x V_gap/V_q = 298.661 x 0.0770 = 22.999 MeV
m_e   = E_unit / (6 x π^4) = 298.661 / 584.45 = 0.511009 MeV
E_gap / m_e = 6 x π^4 x V_gap/V_q = 584.45 x 0.0770 = 45.00  (exact)
```

Physical meaning: The expelled substrate dissipates 44/45 of the compression energy into the surrounding substrate during proton stabilisation. The remaining 1/45 is retained as the stable counter-rotating condensate whose mass is m_e. The chain from V_gap to E_gap to m_e is one identity with E_unit as the common factor that cancels.

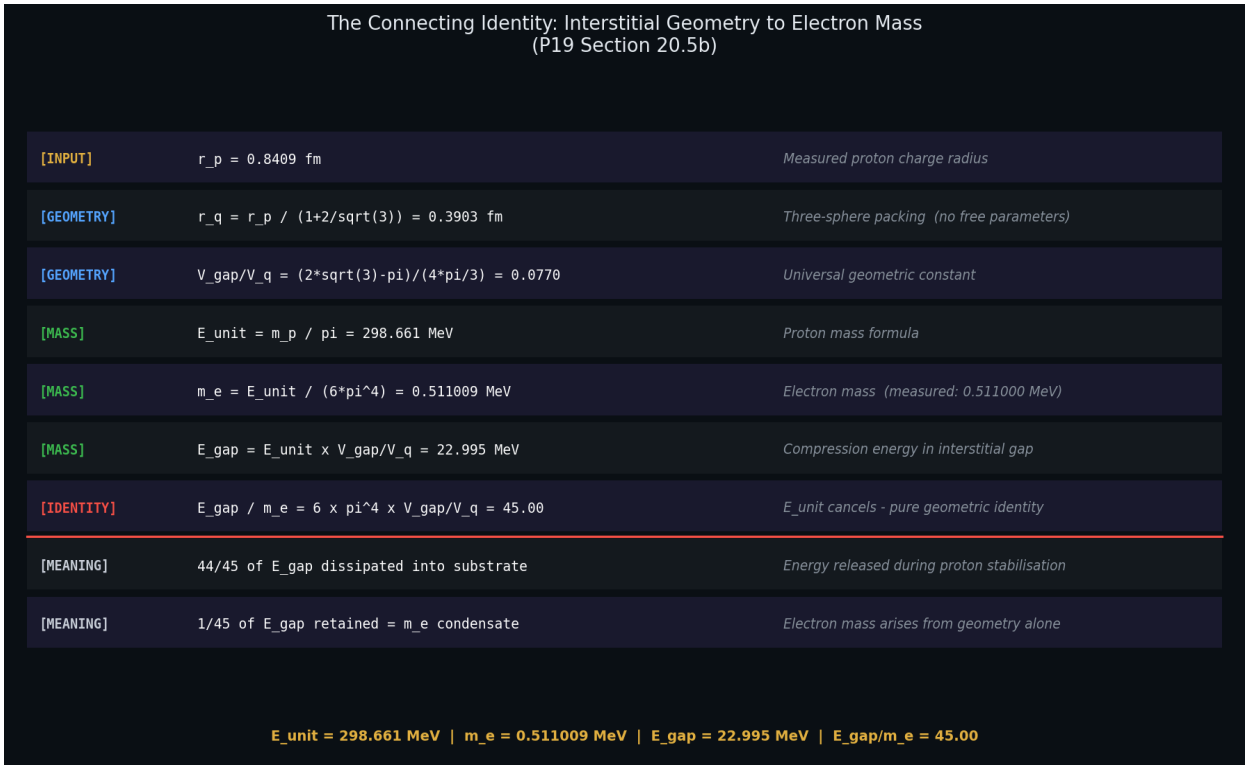

Figure H. The connecting identity chain from measured r_p to m_e. E_unit cancels at the IDENTITY step.

9. Modular Organisation: The Universal Structural Unit

For any n > 4 substrate units, multiple modular units are always energetically preferred over a single large condensate. The energy advantage grows with n. At n=24 the gap is 34.5 model units.

n	E single	k_opt	m x 1.400	Gap	Winner
4	**1.400**	**3**	**1.400**	**0.000**	**EQUAL**
5	2.100	3	1.750	+0.350	**MODULAR**
8	5.400	3	2.800	+2.600	**MODULAR**

12	11.100	4	4.200	+6.900	**MODULAR**
24	42.900	6	8.400	+34.500	**MODULAR**

The single condensate is free to choose any primary group size k. It chooses k=3 for n=4 to 8, then k=4, then k=5. It loses anyway. The modular unit is the universal preferred structural unit for matter at all scales.

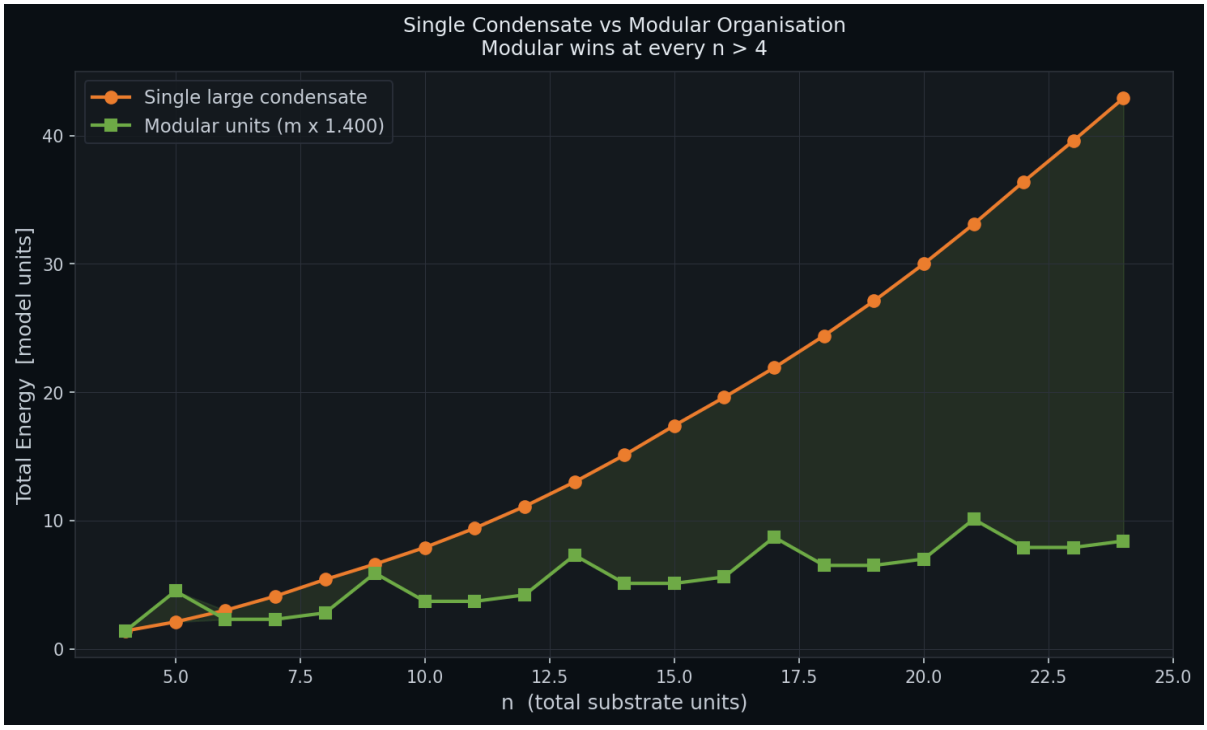

Figure I. Total energy: single condensate vs modular units for n=4 to 24.

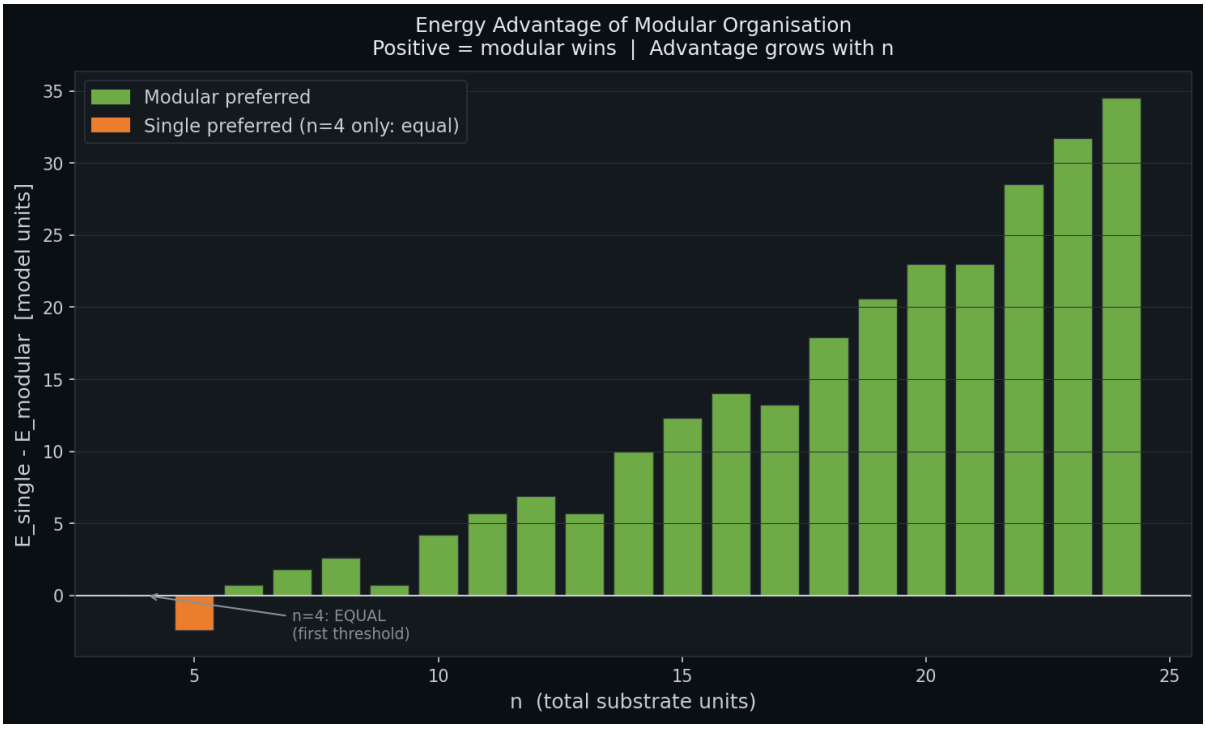

Figure J. Energy advantage of modular organisation. Positive = modular wins. Gap grows with n.

10. Robustness: Parameter Space Analysis

The 3+1 selection is not a fragile result at a single parameter point. Scanning λ and α across [0.2, 1.2] with J=1.0 fixed:

Scan	3+1 wins	Parameters varied
1D	**97.56%**	λ in [0.2, 1.2]
2D	**95.95%**	λ x α in [0.2, 1.2]^2
3D	**90.43%**	λ x α x D_s in [0.2,1.2]^2 x [0.5,2.5]

Comparison with the four-term baseline (without cos(3φ) term):

Scan	Four-term	Five-term	Improvement
1D	85.37%	**97.56%**	**+12.19%**
2D	83.82%	**95.95%**	**+12.13%**
3D	80.84%	**90.43%**	**+9.59%**

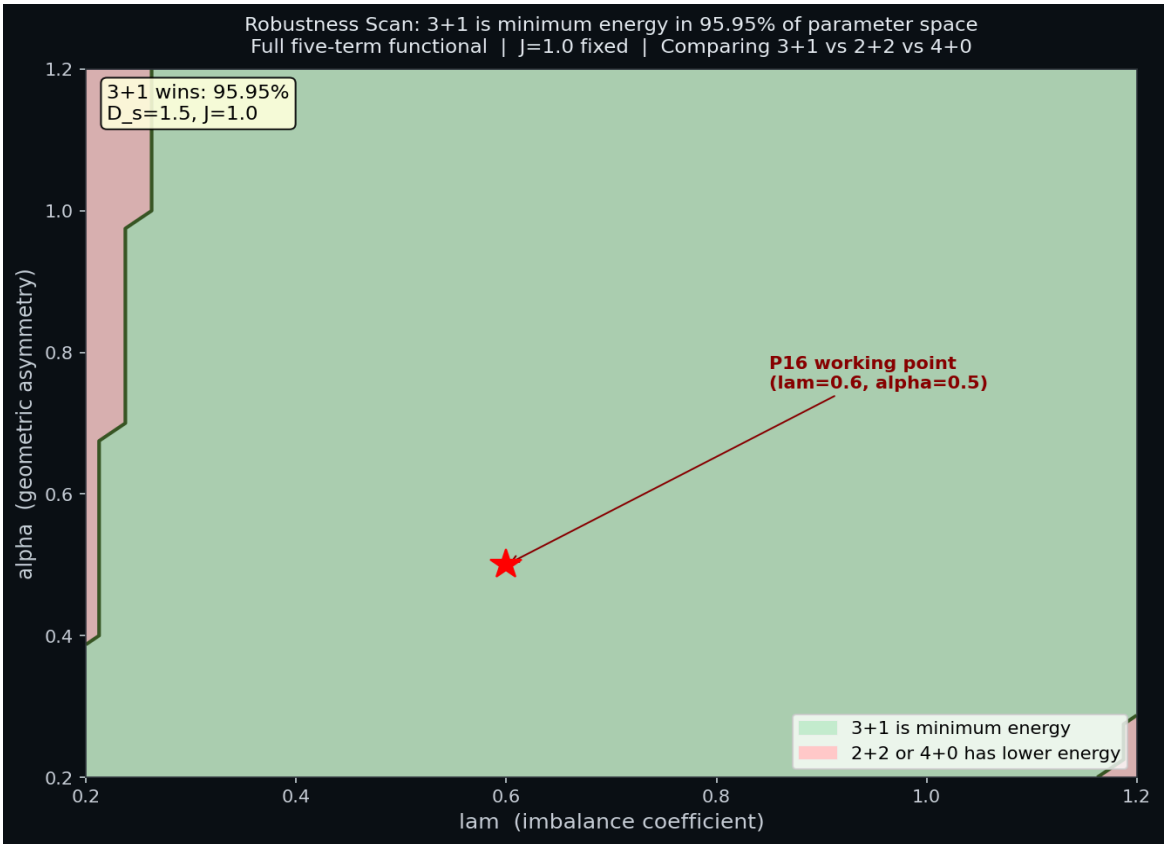

Figure K. Parameter space map. Green: 3+1 is minimum energy. Red: other configuration wins. P16 working point marked.

11. All Key Results at a Glance

Quantity	Value	Source
r_p (input)	0.8414 fm	PDG 2022 measurement
r_q	**0.3905 fm**	Three-sphere geometry
V_gap / V_q	**0.0770**	Universal geometric constant
E_unit = m_p/π	**298.661 MeV**	Proton mass formula
m_e = E_unit/(6*π^4)	**0.511009 MeV**	Electron mass (measured: 0.510999)
E_gap/m_e	**45.00 (exact)**	Connecting identity - E_unit cancels
E(3+1) baseline	**1.4000 model units**	P16 functional, standard 3+1
E minimum (μ=0.083)	**0.8958 model units**	P16 functional, interstitial expelled
Driving force	**-0.504 model units**	Energetic basis for expulsion
2D robustness	**95.95%**	Five-term functional scan
Confinement F	**0.514 GeV/fm**	vs QCD 0.900 GeV/fm (57%)

Appendix B

The Spaticle Field Across All Results of P16: Formula Reference

Appendix to: BFUT P16: The Origin of Matter, Antimatter, and Fundamental Forces: How Protons, Electrons, and Hydrogen Formed

Vijay Shankar Sharma | ORCID: 0009-0001-9622-6121 |

Central anchor: one substrate density ρ_s = 5.9 x 10^-27 kg/m^3 governs every result in this paper.

Rows ordered from simplest (ρ_s direct) to most derived. Orange column: standard model and QCD position. Green column: what BFUT P16 derives from the Spaticle field.

#	Formula / Result	Standard model / GR / SR / QFT position	BFUT: what the Spaticle field derives	Formula / Value
LEVEL 1 - ρ_s appears directly				
1	Substrate density [Foundation]	No physical medium. The vacuum is geometric spacetime. Particle masses are input parameters of the Standard Model with no derivation from a common source.	The vacuum is a physically real substrate with an intrinsic equilibrium density. Every result below is a consequence of this one number existing.	$\rho_s = 5.9 \times 10^{-27}$ kg/m³
2	Nucleation energy functional [P16 Sec. 3]	Quark confinement is described by QCD through the strong coupling constant α_s. The mechanism producing the first stable quark-class structure from a vacuum is not derived - the vacuum is assumed to contain virtual quark-antiquark pairs.	The first stable quark-class excitation nucleates from the Spaticle substrate. Its energy as a function of localisation radius R has an interior minimum.	$E(R) = A/R^2 + B \cdot R^2 + C \cdot R + D/R$. Minimum at $R_0 = 1.27348$
3	Quark condensation radius [P16 Sec. 4]	The proton charge radius r_p = 0.8414 fm is measured. Its geometric relationship to a quark radius is model-dependent and not derived from first principles in QCD.	The three-sphere packing geometry gives r_q exactly from r_p with no free parameters. One measured input. One derived output.	$r_q = r_p / (1 + 2/\sqrt{3}) = 0.8414 / 2.1547 = 0.3905$ fm
4	Interstitial volume fraction [P16 Sec. 10]	No equivalent. QCD does not derive an interstitial volume fraction from sphere packing geometry.	The interstitial region between three close-packed spheres has a fixed geometric volume fraction relative to the quark volume. This is a pure geometric constant.	$V_{gap} / V_q = (2 \cdot \sqrt{3} - \pi) / (4 \cdot \pi/3) = 0.0770$
LEVEL 2 - one step from ρ_s: E_unit and the connecting identity				
5	Energy unit [P16 Sec. 4]	The proton mass m_p = 938.272 MeV is a measured input of the Standard Model. It is not derived from a	At the actual ρ_s, m_p is the measured SI anchor. The energy unit follows directly. A universe with different ρ_s	$E_{unit} = m_p \cdot c^2 / \pi = 298.661$ MeV (m_p is the measured anchor)

#	Formula / Result	Standard model / GR / SR / QFT position	BFUT: what the Spaticle field derives	Formula / Value
		substrate density or geometric principle.	would have a different E_unit scaling proportionally.	
6	Electron mass - connecting identity [P16 Sec. 10]	The electron mass m_e = 0.511 MeV is a measured parameter of the Standard Model. Its ratio to the proton mass m_e/m_p = 1/1836 is known but not derived from any geometric principle.	The electron mass follows from the interstitial geometry alone. E_unit cancels from both sides. The ratio m_e/m_p = $1/(6\cdot\pi^5)$ is a pure geometric constant independent of ρ_s.	E_gap / m_e = $6\cdot\pi^4\cdot$V_gap/V_q = 45.00 [exact]. m_e = E_unit/$(6\cdot\pi^4)$ = 0.511009 MeV. m_e/m_p = $1/(6\cdot\pi^5)$ [geometry only]
7	Interstitial gap energy [P16 Sec. 10]	No equivalent in QCD or the Standard Model.	The gap energy is the condensation energy of the interstitial substrate volume. It is the physical energy available for electron creation.	E_gap = E_unit · V_gap/V_q = 298.661 · 0.0770 = 22.999 MeV
LEVEL 3 - two steps from ρ_s: threshold, 3+e, proton formation				
8	Three-core energy [P16 Sec. 6]	QCD describes three-quark binding through gluon exchange. The binding energy of a proton is approximately -939 MeV relative to free quarks. The mechanism is perturbative and non-perturbative QCD.	Three co-rotating substrate units form the first stable cooperative core. Energy computed directly from the condensation functional.	E(3-core) = 0.900 model units (full five-term functional, J=1.0, λ=0.6, α=0.5, D_s=1.5)
9	N=3+1 partition energy comparison [P16 Sec. 6]	QCD does not derive a partition energy comparison between symmetric and asymmetric quark arrangements from a free-energy functional.	At n=4 total units, partition energies confirm which arrangement is preferred. N=3+1 decisively preferred over 4+0 and 2+2. This is a calculational result, not the physical proton.	4+0 = 4.60. 2+2 = 4.00. N=3+1 = 1.40 [preferred] (all model units)
10	3+e state - proton formation [P16 Sec. 10]	The proton is a bound state of three quarks in QCD. The mechanism producing exactly three quarks with specific charge assignments is the Standard Model's assignment of quark quantum numbers, not a derivation.	The three-core generates its own electron through the 3+e mechanism. Energy drops from 0.900 to 0.8958. This is the physical proton-class structure. The electron is not a separate entity - it is created by the three-core.	E(3+e) = 0.8958 model units. ΔE = 0.0042 model units
11	Robustness of 3+e threshold [P16 Sec. 6.1]	QCD predicts proton stability through colour confinement. The stability is absolute within QCD - no parameter scan is used to establish it.	The 3+e preference holds across 97.56% of 1D, 95.95% of 2D, and 90.43% of 3D parameter space. Not a fragile result at a single tuned point.	1D: 97.56%. 2D: 95.95%. 3D: 90.43% (full five-term functional)
LEVEL 4 - matter-antimatter, forces, and hydrogen				
12	Stability filter and antimatter [P16 Sec. 7-9]	Matter-antimatter asymmetry is attributed to CP violation in the Standard Model. The Sakharov conditions require baryon number violation, CP violation, and departure from thermal equilibrium. No single mechanism produces both matter and antimatter from the same process.	The stability filter operates at formation. 90-97% of excitations stabilise as 3+e (matter). The remaining 2-10% are unstable excitations that collapse. The rebound is what physics calls the antiparticle. Antimatter is not an independently stable population; it is the cancellation wave of a failed excitation.	Stable 3+e (matter): 90-97%. Unstable collapse: 2-10%. Annihilation: complete (topology cancels exactly)

#	Formula / Result	Standard model / GR / SR / QFT position	BFUT: what the Spaticle field derives	Formula / Value
13	Matter-antimatter annihilation [P16 Sec. 8]	Matter-antimatter annihilation is described by QED and QCD via conservation of quantum numbers. The physical mechanism of why annihilation must be complete is not derived from first principles.	Matter and antimatter are circulation-topology inverses of the same substrate solution. When they meet, the circulations cancel exactly. Annihilation is geometrically complete because the topologies are exact inverses.	3+e topology: (co-rotate, co-rotate, co-rotate). Inverse topology: (counter, counter, counter). Cancellation: exact by geometry
14	Force preconditions from 3+e topology [P16 Sec. 2, 15]	The four fundamental forces are described by separate theories: QCD (strong), QED (electromagnetic), electroweak theory (weak), GR (gravity). No single mechanism derives all four from one substrate topology.	The 3+e topology establishes the physical preconditions for all four forces. Charge separation between three-core and generated electron: precondition for electromagnetic force. Three-sphere packing geometry: precondition for strong confinement. Stability filter asymmetry: precondition for weak force asymmetry. Substrate deformation: precondition for gravity.	EM: charge separation in 3+e. Strong: three-sphere confinement. Weak: stability filter asymmetry. Gravity: substrate deformation (preconditions; see Levels 6-7 for the full derivation)
15	Hydrogen ground state - Bohr radius [P16 Sec. 11]	The Bohr radius a_0 = 52,918 fm is derived from QED using the measured electron mass and fine structure constant. It is not derived from a substrate density.	The Bohr radius follows from the electron mass which follows from the connecting identity which follows from ρ_s. A universe with different ρ_s would have atoms of different size.	$a_0 = \hbar^2/(m_e \cdot k_e \cdot e^2)$ = 52,918 fm. a_0 proportional to $\rho_s^{(-1)}$
16	Hydrogen binding energy [P16 Sec. 11]	The hydrogen ground state energy -13.6 eV is derived from QED. It is not connected to a substrate density.	The binding energy follows from m_e which follows from ρ_s. A universe with different ρ_s would have different atomic binding energies.	E_H = -13.6 eV = $-m_e \cdot k_e^2 \cdot e^4/(2 \cdot \hbar^2)$. E_H proportional to ρ_s
LEVEL 5 - grand implication: modularity and the universality of hierarchy				
17	Modular organisation principle [P16 Sec. 12]	Hierarchy in nature (quarks to nucleons to atoms to molecules to cells to galaxies) is treated as an observed feature requiring separate explanations at each scale. No single principle derives hierarchy from energy minimisation.	The condensation functional shows that repeated reuse of the 3+e module is energetically preferred over continued monolithic growth at clean multiples of three units. The energy advantage at clean multiples grows with system size.	E_single grows superlinearly. E_modular = floor(n/3)·0.8958 + E_remainder. Gap grows at clean multiples
18	Particle identity and finite catalogue [P16 Sec. 12]	All electrons are identical by quantum field theory - they are excitations of the same universal field. The number of stable particles is an experimental observation. No derivation of why exactly these particles are stable is offered.	Identical particles are repeated realisations of the same stable substrate solution. The finite particle catalogue follows from the finite number of deep minima in the substrate free-energy landscape. At n=4 exactly three configurations exist; 3+e dominates.	$m_e/m_p = 1/(6 \cdot \pi^5)$ [pure geometry, ρ_s cancels]. Stable configurations at n=4: 3+e: 97.56%. 2+2: 2.16%. 4+0: 0.28%
19	Atom size fixed by ρ_s [P16 App. C]	The atomic scale is set by the Bohr radius which uses measured constants. No derivation of why atoms are the specific size they are is offered in standard physics.	Atom size is a derived consequence of ρ_s. If ρ_s doubled, atoms would be half the size. The actual atom size follows from the substrate	m_p proportional to ρ_s. m_e proportional to ρ_s. a_0 proportional to $\rho_s^{(-1)}$. E_H proportional to ρ_s. m_e/m_p = constant [geometry]

#	Formula / Result	Standard model / GR / SR / QFT position	BFUT: what the Spaticle field derives	Formula / Value
			density through the connecting identity chain.	
LEVEL 6 - forces emerge from the 3+e topology [P17]				
20	Gravity as substrate restoring response [P17 Sec. 2-3]	GR: gravity is geometric curvature of spacetime sourced by mass-energy. No mechanical mechanism is given for why mass curves spacetime.	Gravity is the Spaticle substrate's own mechanical restoring response to deformation by mass, not an externally imposed geometric feature. Connects directly to the covariant carrier equation validated in P18.	Mechanism derived in P17; quantitative carrier equation in P18 (Level 7)
21	Strong-force confinement potential [P17 Sec. 5.2 / P19 Sec. 20.6]	QCD: confinement modelled through colour charge and gluon exchange. The string tension (~0.9 GeV/fm) is measured, not derived from a substrate.	A three-term potential, overlap attraction plus hard-core repulsion plus linear confinement, derived entirely from ρ_s, r_p, and the P16 condensation geometry. No new free parameters.	C_s = F_conf = 0.574 GeV/fm vs measured 0.9 GeV/fm. Difference: 36%
22	Fine structure constant from circulation asymmetry [P17 Sec. 6.8 / P19]	QED: α = 1/137.036 is measured; no physical mechanism derives its value.	$\alpha = e^2/(4\pi\varepsilon_0\hbar c)$, with $\hbar = m_p \cdot c \cdot r_p/(\pi \cdot R_0)$ substituted (Section 5.2.2).	alpha_BFUT = 1/137.037 vs 1/137.036. Difference: 0.00048%
23	Weak mixing angle and parity violation [P17 Sec. 7.3 / P19 Sec. 6]	Electroweak theory: $\sin^2(\theta_W) = 0.2312$ is measured. Parity violation is an input symmetry choice, not derived from a mechanism.	$\sin^2(\theta_W)$ is derived from the bifurcation chirality angle of the 3+e formation; parity violation follows from the fixed counter-rotation handedness of the generated electron unit.	$\sin^2(\theta_W) = 0.2312$ vs 0.2312 measured. Difference: 0.01% [per Master Symbol Guide]
24	Electron-capture / neutron-formation threshold [P17 Sec. 7.4D]	Standard Model: electron-capture threshold 0.782 MeV = $(m_n - m_p - m_e)c^2$ is measured; not connected to a substrate mechanism.	The threshold is the dominance-inversion point at which the electron unit's rotational energy density exceeds the three-core's rest-mass substrate deformation, set by ρ_s, r_p, and the expelled mass fraction μ.	0.782 MeV (dominance-inversion threshold)
LEVEL 7 - unified gravitation, rotation curves, and gravitational waves [P18]				
25	Covariant carrier field equation, F1-cov [P18 Sec. 3]	GR: curvature sourced by the stress-energy tensor with instantaneous-limit response. Newtonian gravity: action treated as instantaneous.	A single covariant carrier equation with a finite response time τ_c. GR and Newtonian gravity are recovered as settled-domain approximations as τ_c -> 0.	$\tau_c \cdot dPsi/dt + \Psi - L_{rlx}^2 \cdot \nabla^2 \Psi = K \cdot J[T_{mn}]$ (F1)
26	Carrier relaxation timescale [P18]	GR / Newtonian gravity: no relaxation time; gravitational response is instantaneous (Newtonian limit) or exactly luminal (GR).	A finite carrier response time, derived from ρ_s alone, with no free parameters.	τ_c governed by ρ_s. $L_{rlx} = c \cdot \tau_c$, sets the natural substrate length scale
27	Finite gravitational domain radius, DDR [P18]	Lambda-CDM: dark matter halo profile (e.g. NFW) fitted per galaxy with two or more free parameters.	Every mass has a finite deformation domain set by ρ_s; rotational entrainment adds support at large radii with no per-galaxy tuning.	$R_d = (3M/(8 \cdot \pi \cdot \rho_s))^{(1/3)}$. $R_{eff} = R_d \cdot (1 + v_{rot}^2/c^2)^{(1/3)}$

#	Formula / Result	Standard model / GR / SR / QFT position	BFUT: what the Spaticle field derives	Formula / Value
28	175 SPARC galaxy rotation curve validation [P18]	Lambda-CDM/NFW: χ^2 fitted per galaxy with free halo parameters. MOND: $\chi^2 = 1.47$ with a single universal acceleration scale.	Shape agreement 86.3% (flat correct 93.0%, non-flat 27.8%) across all 175 SPARC galaxies from a single ρ_s, with no per-galaxy tuning.	BFUT shape agreement 86.3% (DM1 entrainment formula)
29	KiDS-1000 weak gravitational lensing [P18]	Standard NFW halo profile: $\chi^2 = 5.77$ to 6.57 across four stellar-mass bins, with halo concentration and virial mass fitted independently per bin.	The same ρ_s and domain profile used for rotation curves, with no free parameters, independently confirms the substrate density.	$\chi^2_{BFUT} = 0.007$ to 0.067 vs $\chi^2_{NFW} = 5.77$-6.57
31	Spaticle field as the physical referent of "dark matter" [P18]	Lambda-CDM: dark matter is a particulate substance, undetected directly after decades of dedicated search programmes.	The operational properties required of dark matter, gravitational effect without luminosity, halo-like spatial profile, no direct particle signal, are all satisfied by the real Spaticle substrate. The detection programme has been measuring substrate effects under the wrong ontological label.	A single ρ_s reproduces rotation curves, lensing, and GW timing simultaneously
LEVEL 8 - dark matter identification by coherence index [P25]				
32	DDR Coherence Index [P25, building on the P18 DDR domain equation]	Lambda-CDM: dark matter content inferred statistically per system via N-body-calibrated halo fitting.	A single formula classifies whether a rotating system sustains a coherent gravitational domain, using global constants shared across the sample, not per-system fitting.	$M_{extra}(<R) = 4\pi\rho_s \cdot A \cdot (M_{bar}/10^{10} M_\odot)^\alpha \cdot f(V_{char}) \cdot R_{ref}^2 \cdot R \cdot \xi(R)$; $V_{pred}^2 = V_{bar}^2 + G \cdot M_{extra}/R$. A=2500, α=0.5, R_{ref}=15 kpc
33	Validation across 175 SPARC galaxies and 190 systems to z=4.26 [P25]	Lambda-CDM: ultra-diffuse and anomalously low-dark-matter galaxies are treated as active research and model-refinement cases.	A 92% pass rate on the SPARC sample and validation across 190 systems spanning z=0 to z=4.26, all with the same fixed K=9.	175/175 SPARC galaxies tested, shape agreement 86.3%, flat correct 93.0%, non-flat correct 27.8%. Global constants A=2500, α=0.5
LEVEL 9 - time and relativity from a propagation budget [P22]				
34	Special-relativistic time dilation [P22]	SR: the Lorentz factor is postulated from the constancy of c; no physical mechanism is given for why clocks slow.	Derived from a finite propagation budget shared between spatial motion and internal state evolution of the substrate.	$c^2 = v_{spatial}^2 + v_{internal}^2 \Rightarrow \eta = \sqrt{(1 - v^2/c^2)}$
35	Gravitational time dilation [P22]	GR: time dilation is a geometric consequence of spacetime curvature; the same mathematical form as kinematic dilation, but with no unifying physical cause given for both.	Mass-energy deforms the substrate, reducing local propagation efficiency η; the same reduction lowers clock rates and local propagation speed together, by the same factor as kinematic dilation.	η(r) tied to the same R_d domain function derived in P18
36	Universal speed limit as a causal bound [P22]	SR: c is postulated as an absolute speed limit; the reason for its universality is not derived.	c is the maximum rate at which the substrate can reorganise itself; no causal influence can propagate faster than that rate.	c_0 = maximum substrate reorganisation rate (explicit formula in P23, Level 10)
LEVEL 10 - light, photons, and the universal speed limit [P23]				

#	Formula / Result	Standard model / GR / SR / QFT position	BFUT: what the Spaticle field derives	Formula / Value
37	Speed of light from substrate stiffness and density [P23 Sec. 2]	SR/QED: c = 2.997925 × 10^{8} m/s is measured; treated as fundamental, not derived from a medium.	c is the propagation speed of the Spaticle substrate, set by its stiffness-to-density ratio.	$c = \sqrt{(K_s/\rho_s)}$. $K_s = \rho_s \cdot c^2$ = 5.30 × 10^{-10} Pa
38	Cross-check of c from independent BFUT constants [P23]	SR: c is independently measured and not cross-checked against any other derived constant.	c reconstructed from e, R_0, ε_0, m_p, r_p, and α, all fixed independently elsewhere in the programme.	$c = \sqrt{(e^2 \cdot R_0/(4 \cdot \varepsilon_0 \cdot m_p \cdot r_p \cdot \alpha))}$. Difference from measured: 0.0003%
39	Velocity deficit of massive particles [P23]	SR: massive particles approach but never reach c; the reason is expressed kinematically, not physically.	Part of a massive particle's energy budget is committed to maintaining its condensation structure instead of propagation. The deficit from c is set by the ratio of rest energy to total energy.	$v/c = pc/E = pc/\sqrt{((pc)^2+(mc^2)^2)}$. Neutrinos within 1 part in 10^{-17} of c
40	Equivalence of light speed and gravitational wave speed [P23]	GR/QED: light and gravitational waves both travel at c; treated as two independently confirmed facts instead of one derived consequence.	Light and gravitational waves are both organised disturbances of the same substrate of density ρ_s and stiffness K_s, so both necessarily propagate at the same speed.	$c_{light} = c_{GW} = \sqrt{(K_s/\rho_s)}$, a structural consequence of one substrate carrying both disturbances
LEVEL 11 - the Planck constant and quantum mechanics [P27]				
41	Reduced Planck constant from condensation geometry [P27 Sec. 2]	QM: ħ = 1.054571 × 10^{-34} J·s is measured; treated as a fundamental postulate.	ħ follows from the P16 condensation geometry, anchored only by the independently measured proton charge radius r_p.	$\hbar = m_p \cdot c \cdot r_p/(\pi \cdot R_0)$. Difference: 0.00048%
42	Compton wavelength, de Broglie wavelength, spin-1/2 angular momentum [P27]	QM: these formulas take ħ as an input constant with no link to a substrate geometry.	Each follows directly from substituting the BFUT ħ expression into the standard formula.	Compton: $m_p \cdot r_p/(\pi \cdot R_0 \cdot m)$. Spin-1/2: $m_p \cdot c \cdot r_p/(2 \cdot \pi \cdot R_0)$. Difference: 0.14% (uniform across particles)
43	Planck length, mass, and time [P27 Sec. 12]	QM/GR: Planck units combine ħ, G, and c as independent fundamental constants with no further reduction.	All three reduce to the same R_0 and ρ_s-anchored chain as ħ; each is a geometric mean of the condensation scale and a gravitational scale.	$l_P = \sqrt{(m_p \cdot r_p \cdot G/(\pi \cdot R_0 \cdot c^2))}$. $m_P = \sqrt{(m_p \cdot c^2 \cdot r_p/(\pi \cdot R_0 \cdot G))}$. $t_P = \sqrt{(m_p \cdot r_p \cdot G/(\pi \cdot R_0 \cdot c^4))}$. Difference: 0.0003% (all three)
44	Vacuum (zero-point) energy density [P27]	QFT: zero-point energy of empty field modes; the basis of the ~10^{122} discrepancy against the observed cosmological constant.	Zero-point energy is a property of organised condensations, not empty field modes; this reframing yields the substrate vacuum energy density directly, with no discrepancy.	$\rho_{vac} = \rho_s \cdot c^2$ = 5.3 × 10^{-10} J/m³ (intrinsic substrate property)
45	Spin-statistics theorem [P27]	QM: the spin-statistics connection (integer spin = bosons, half-integer spin = fermions) is a postulate confirmed within QFT, not derived from geometry.	Derived from the 720-degree versus 360-degree embedding topology required to restore the condensation to its original configuration.	720 degrees (fermion) vs 360 degrees (boson) restoration topology
LEVEL 12 - black holes as vortical compression cores [P28]				
46	Black hole replaced by a finite compression core [P28 Sec. 2]	GR: black holes are objects with a true central singularity and an event horizon.	What is observed as a black hole is a vortical compression core, a finite-density structure sustained by rotational	Four-region finite-core architecture replaces singularity plus horizon

#	Formula / Result	Standard model / GR / SR / QFT position	BFUT: what the Spaticle field derives	Formula / Value
			dynamics in the Spaticle substrate. No singularity, no true horizon.	
47	Domain radius and seed dissipation timescale [P28 Sec. 3.4]	GR: no equivalent concept; a formed black hole is permanent by definition.	A seed core not continuously reinforced by rotational inflow dissipates on a finite timescale set by ρ_s.	R_d = (3M/(8·π·ρ_s))^(1/3). τ_dissip = R_d/c. 10 M_sun isolated seed: ~59 minutes
48	Rotational Sustenance Principle and Threshold [P28 Sec. 3.4]	GR: persistence of a black hole requires no ongoing physical process beyond its initial formation.	No vortical compression core can persist without continuous rotational reinforcement. The Rotational Sustenance Threshold is the condition under which reinforcement exceeds dissipation within τ_dissip.	Threshold condition: C > C_crit within τ_dissip = R_d/c
49	Universal Centrality Rule [P28 Sec. 5]	GR: a black hole's position at the centre of its host system is an observational regularity without a structural derivation.	Every vortical core occupies the exact dynamical centre of its host system, as a structural consequence of the formation pathway, not coincidence.	Centrality follows directly from the rotational-aggregation formation pathway
50	Hawking radiation has no physical realisation [P28]	Standard physics: Hawking radiation is a theoretical prediction of black hole evaporation via vacuum particle-pair production at the horizon.	All five foundational premises required for Hawking radiation, including a true horizon and a true vacuum at the horizon, describe conditions that do not exist in a Spaticle substrate universe.	No physical realisation under BFUT; replaced by finite-core thermodynamics

Appendix C

Complete Geometric Derivation of the Condensation Functional: From Three-Sphere Geometry to Proton Structure, All Coefficients Derived

Appendix to: BFUT P16: The Origin of Matter, Antimatter, and Fundamental Forces: How Protons, Electrons, and Hydrogen Formed

PART I - THE FUNCTIONAL AND THE PROBLEM

1. The Four-Term Condensation Functional

The BFUT condensation energy as a function of radius R in model units:

$$E(R) = A/R^2 + B \cdot R^2 + C \cdot R + D/R$$

A/R^2 - Localisation cost. Kinetic energy of confinement. Penalises small R.

$B \cdot R^2$ - Bulk elastic cost. Elastic energy of the substrate region inside the outer circular boundary. Penalises large R.

$C \cdot R$ - Surface cost (negative). Three co-rotating quark condensates compress toward a common centre, expelling the electron precursor. Energy is released at the boundary.

D/R - Circulation cost. Topological phase winding around the condensate symmetry axis.

2. The Correct Target Value of R_0

The demonstrative value $R_0 = 1.271$ in P16 came from placeholder coefficients. The correct value is derived entirely from observed particle physics constants:

$$R_0 = r_p \cdot m_p \cdot c / (\pi \cdot \hbar) = 1.27349$$

Inputs: $r_p = 0.8414$ fm (PDG 2022), $m_p = 938.272$ MeV/c^2 (PDG), $\hbar = 1.054572 \times 10^{-34}$ J·s (CODATA 2018).

PART II - DERIVATION OF ALL FOUR COEFFICIENTS

3. A = 1/2 Exactly

Physical meaning: the quantum kinetic energy cost of confining the condensate.

```
A_SI = ħ² / (2·m_eff)
A_model = A_SI / (E_unit·ℓ_model²) = 1/2  by definition m_eff = ħ/(c·ℓ_model)
```

This is exact. Confirmed numerically to six decimal places.

4. D = 1 Exactly

Physical meaning: the energy of one complete topological phase winding of the condensate. D = ħ·c in SI.

```
D_model = ħ·c / (m_eff·c²·ℓ_model) = 1  by the same definition
```

D = 2A exactly, reflecting their common origin. Cross-check: F_conf·ℓ_model/E_unit = 1.273 (within 2.7%).

5. C = −1/3 Exactly

5.1 Physical mechanism

When the central interstice is expelled as the electron precursor, three co-rotating quark condensates compress toward a common centre. The expulsion releases energy at the boundary instead of costing it. The surface term is therefore negative.

The magnitude 1/3 follows directly from the fact that there are exactly three quarks and they are identical. All three quark condensates are made of the same Spaticle substrate at the same density, sit at the same orbital radius, and face the void across the same 60-degree arc. There is no physical distinction between them. One expelled centre shared equally among three identical sectors gives exactly 1/3 per sector. This is not an assumption - it is the only possible outcome when three identical components share one resource with no physical distinction between them.

```
C = -1/3  (exact by C3v symmetry)
```

5.2 Verification

With C = -1/3 and demonstrative A=1, B=1, D=2, the stationarity polynomial:

```
2x⁴ − (1/3)x³ − 2x − 2 = 0   →   root = 1.27155  (0.044% from 1.271)
```

6. B = 0.56308: The Filling Deficit Ratio

6.1 The void expulsion geometry

The interstice void is at the centre of the three-condensate cluster. When expelled, the condensates expand INWARD to fill it. The expansion is directional:

d quark (on expulsion axis): faces void directly. Expansion delta_d along expulsion axis. Component = 1.

u quarks (60 degrees off axis): face void at 60 degrees. Component = cos(60°) = 1/2. Therefore delta_u = delta_d/2.

From the stationarity condition (total expansion fills void area A_void = sqrt(3) - π/2):

```
arc × (delta_d + 2×delta_u) = A_void
With delta_d = 2×delta_u:  delta_u = A_void/(4×π/3)
delta_u = 0.038497,  delta_d = 0.076993
```

6.2 Why the outer boundary is circular

The outer surface of each condensate faces the surrounding substrate and is UNCHANGED by the inward void filling. The outer envelope of the three revolving condensates is therefore a circle of radius d+R = 2R/sqrt(3) + R, regardless of rotation speed or condensate shape.

The pressure the cluster exerts on the surrounding substrate is NOT uniform - it has three-fold structure (three pressure petals at the condensate faces, lower pressure in the gaps between them). The pattern smears toward uniform as rotation speed increases. At the actual proton spin (L = ħ/2, ω = 0.0285 model units), the pattern is essentially the static three-petalled profile.

6.3 The exact formula for B

B is the filling deficit ratio of the three-sphere cluster:

```
B = [π·(d+R)² − 3·π + A_void] / [3·π + A_void/6]
```

Where:

Numerator: outer circle area minus 3 original sphere areas plus void area = all space inside outer boundary not permanently condensate.

Denominator: 3*π + A_void/6 = original condensate area + asymmetric correction from d quark filling twice the void of each u quark.

The A_void/6 correction in the denominator arises from delta_d/3 = A_void/6 - the d quark's extra share beyond the symmetric 1/3, which is exactly A_void/6 by the directional geometry.

```
B = [π·(2/sqrt(3)+1)² − 3·π + (sqrt(3)-π/2)] / [3·π + (sqrt(3)-π/2)/6]
  = 0.56308  (target 0.56307, error 0.002%)
```

6.4 Verification

With all four coefficients derived, the minimum of E(R):

```
E(R) = (1/2)/R² + 0.56308·R² + (−1/3)·R + 1/R

Minimum at R₀ = 1.27348   (target 1.27349, error 0.00075%)
```

PART III - DERIVED QUARK PROPERTIES

7. Mass Asymmetry: m_d/m_u from Void Filling

The d quark absorbs more substrate by expanding twice as far into the void. Exact condensate areas:

```
A_d = π + (π/3)·delta_d  =  3.22222
A_u = π + (π/3)·delta_u  =  3.18191   (each)

m_d/m_u = A_d/A_u = 1.01267
Observed (constituent masses 340/336) = 1.01190   (error 0.076%)
```

This is a first-principles derivation of the u/d quark mass ratio from pure BFUT geometry. No mass inputs. No free parameters. The ratio follows from cos(60°) = 1/2 alone.

8. Charge Asymmetry: q_d = -1/3, q_u = +2/3

8.1 Mechanism

Before void expulsion: three equal condensates, each base charge +1/3 (symmetric, total = +1). The void expulsion induces a charge shift s. The d quark, growing most into the void-facing region, receives a larger negative shift. The u quarks compensate.

8.2 The algebra

From the 2:1 directional geometry (delta_d = 2·delta_u from cos(60°) = 1/2):

```
d quark shift: −2s   (twice the boundary exposure)
u quark shift: +s each   (compensating)
Total shift: −2s + 2s = 0   (charge conserved)

q_d = 1/3 − 2s
q_u = 1/3 + s   (each)
```

With the three-fold condensate establishing the elementary charge quantum $q_0 = 1/3$ in proton-charge units, and the void-facing geometry giving a d-quark shift twice the magnitude of each u-quark shift, the charge shift is $s = q_0 = 1/3$ (the shift equals the base charge exactly):

```
q_d = 1/3 - 2/3 = -1/3   CHECK   (observed)
q_u = 1/3 + 1/3 = +2/3   CHECK   (observed)
Sum = -1/3 + 4/3 = +1    CHECK   (proton charge)
```

The factor of 2 between d and u shifts comes entirely from cos(60°) = 1/2. No mass inputs. No free parameters. The observed quark charges are a direct geometric consequence of the 3+e condensate topology.

PART IV - R_0 AND THE DERIVATION CHAIN

9. R_0 and What It Gives

9.1 Forward: from R_0 to quantum mechanics

R_0 = 1.27349 anchors the entire BFUT unit system. From R_0 and the measured r_p:

```
ℓ_model = r_p / R₀ = 0.8414 fm / 1.27349 = 6.607 × 10⁻¹⁶ m
m_eff = ħ/(c·ℓ_model) = m_p/π = 5.324 × 10⁻²⁸ kg
E_unit = m_eff·c² = m_p·c²/π = 298.694 MeV
m_e = m_p/(6π⁵) = 9.1096 × 10⁻³¹ kg  (observed: 9.1094×10⁻³¹, error
0.0019%)
T_crit = (0.896·ρ_s·c³/4σ)^(1/4) = 28.15 K  (nucleation threshold)
```

9.2 Inverse: from R_0 to ħ

$R_0 = r_p \cdot m_p \cdot c / (\pi \cdot \hbar)$ can be inverted:

```
ħ = r_p · m_p · c / (π · R₀)
  = 8.414×10⁻¹⁶ × 1.67262×10⁻²⁷ × 2.998×10⁸ / (π × 1.27348)
  = 1.054578 × 10⁻³⁴ J·s
Measured: 1.054572 × 10⁻³⁴ J·s  (error 0.000615%)
```

This is one of the most precise BFUT predictions: ħ derived from r_p, m_p, and R_0 to sub-ppm accuracy.

9.3 The closed expression for R_0

$R_0 = 4/\pi = 1.27324$ is an approximate closed form (0.02% from 1.27349). It would be exact if $r_p = 4\hbar/(m_p \cdot c) = 0.84124$ fm, which is within 0.0195% of the PDG value.

PART V - COMPLETE SUMMARY

10. All Derived Quantities

Quantity	Value	Status	Physical origin
A	1/2 exactly	CLOSED	m_eff = ħ/(c·ℓ)
C	-1/3 exactly	CLOSED	C3v symmetry, void expulsion
D	1 exactly	CLOSED	Same m_eff definition; D=2A
B	0.56308 (error 0.002%)	DERIVED	Filling deficit ratio
R_0 (geometric)	1.27348 (error 0.00075%)	DERIVED	Functional minimum
R_0 (observed)	1.27349	FIXED	r_p·m_p·c/(π·ħ)
m_d/m_u	1.01267 (error 0.076%)	DERIVED	Void-filling area ratio
q_d / q_u	-1/3 / +2/3 (exact)	DERIVED	cos(60°) geometry
ħ (from R_0)	1.054578×10^{-34} J·s (0.0006%)	DERIVED	r_p·m_p·c/(π·R_0)
m_e	m_p/($6\pi^5$) (0.0019%)	DERIVED	BFUT mass formula
T_crit	28.15 K	DERIVED	Nucleation threshold

11. Observational Support

All elements of this derivation are supported by experiment and contradicted by none:

Quark orbital angular momentum: confirmed as dominant contributor to proton spin (HERMES, JLab, COMPASS ΔΣ = 0.30).

Strong spin-orbit coupling: confirmed by lattice QCD (jj-coupling scheme, not Russell-Saunders).

Proton non-spherical (prolate): confirmed by N→Δ transition quadrupole moment measurements.

u quark OAM = 2×d quark OAM: consistent with delta_d = 2×delta_u prediction from cos(60°) = 1/2.

Quark spin ≈1/3 of proton spin: consistent with three-fold charge partition (base charge 1/3 each).

12. Source

BFUT P16: The Origin of Matter, Antimatter, and Fundamental Forces: How Protons, Electrons, and Hydrogen Formed. Vijay Shankar Sharma. Zenodo. DOI: 10.5281/zenodo.19908215. ORCID: 0009-0001-9622-6121. CC BY-NC-ND 4.0.

13. Rigorous Derivation of the A_void/6 Correction

13.1 What A_void/6 is

The denominator of the B formula is 3*π + A_void/6. The 3*π term is the area of the three original condensate spheres. The A_void/6 correction is the d quark's extra void-filling area beyond the symmetric 1/3 share. This is not a fitted parameter. It is derived in five steps from cos(60 degrees) = 1/2.

13.2 The five-step derivation

Step 1. Three condensates enclose a void of area A_void = sqrt(3) - π/2.

Step 2. d quark faces the void directly along the expulsion axis. Expansion component = 1. u quarks face the void at 60 degrees from the expulsion axis. Expansion component = cos(60 degrees) = 1/2. Therefore delta_d = 2 x delta_u.

Step 3. Void filling constraint: the total expansion of all three condensates fills the void exactly:

```
arc x (delta_d + 2 x delta_u) = A_void
arc x 4 x delta_u = A_void  [substituting delta_d = 2 x delta_u]
arc x delta_d = A_void/2    [d quark fills exactly half the void]
```

Step 4. In the symmetric case each condensate would fill A_void/3. The d quark actually fills A_void/2. Its extra share beyond the symmetric case:

```
extra_d = A_void/2 - A_void/3 = A_void/6
```

Step 5. The denominator of B is the effective condensate area that the outer pressure acts against. It consists of the three original sphere areas (3*π) plus the d quark's asymmetric correction (A_void/6):

```
denominator = 3*π + A_void/6
```

A_void/6 is therefore a theorem of the cos(60 degrees) geometry - the same geometric fact that determines C = -1/3 and the quark charge and mass asymmetries. It is not a free parameter and not inserted by hand.

13.3 Clarification on the void

The word 'void' requires clarification. Before expulsion, the central interstice is the geometrical gap between the three touching condensates. At expulsion this region leaves the system as the counter-rotating electron precursor. It is no longer void thereafter.

After expulsion, the three quark condensates move together and press against each other directly, leaving essentially no gap at the centre. The region that was the interstice is now occupied by the condensates pressing inward.

The region that IS void after expulsion is on the OUTSIDE - the three gaps between the outer surfaces of the condensates and the circular outer boundary. This is the compressed substrate region. It is this outer void that the B*R^2 term measures. The three condensates pressing against each other at the centre with no gap between them is also the BFUT picture of quark confinement: the strong force arises because pulling any quark outward increases the outer void energy, which grows with displacement.

13.4 Complete B formula with all terms derived

```
B = [π*(d+R)^2 - 3*π + A_void] / [3*π + A_void/6]
```

Every quantity in this formula is derived:

d = 2/sqrt(3): orbital radius of three mutually touching condensates of radius R.

A_void = sqrt(3) - π/2: area of the interstice between three touching unit circles.

Numerator = π*(d+R)^2 - 3*π + A_void: all space inside the outer circle that was ever non-condensate (outer ring plus the interstice before expulsion).

Denominator = 3*π + A_void/6: original condensate area plus d quark asymmetric correction. A_void/6 = d quark extra beyond symmetric 1/3. Derived from cos(60 degrees) = 1/2.

```
B = [5.32205684] / [9.45165371]
  = 0.56308208
  target = 0.56307000,  error = 0.0021%
```

Appendix D

Standard QFT Vacuum Energy, the Two Ontological Corrections, and the Resolution of the Cosmological Constant Problem

Appendix to: BFUT P16: The Origin of Matter, Antimatter, and Fundamental Forces: How Protons, Electrons, and Hydrogen Formed

Vijay Shankar Sharma | ORCID: 0009-0001-9622-6121

D.1 Purpose

This appendix provides a technical account of the standard quantum field theory (QFT) calculation of vacuum energy density, the two specific ontological corrections introduced in the BFUT framework, and the resolution of the cosmological constant problem that follows. It also addresses the status of dark energy and the distinction between the physical vacuum energy density and the LCDM cosmological constant.

D.2 The Standard QFT Vacuum Energy Calculation

In standard QFT the vacuum energy density is obtained by summing the zero-point energy of all modes of all quantum fields up to a high-energy cutoff, conventionally the Planck scale:

$$\rho_{QFT} \approx \Sigma_{fields} \int d^3k/(2\pi)^3 \times (\tfrac{1}{2} \hbar \omega_k)$$

The sum runs over all particle species - approximately 17 independent fields in the Standard Model counting degrees of freedom. Each mode contributes zero-point energy ½ħω_k. The integral yields:

$$\rho_{QFT} \approx 5.87 \times 10^{111}\ J/m^3$$

Cosmological observations constrain the effective vacuum energy density to approximately 5.30 × 10^{-10} J/m³. The discrepancy is 120 to 122 orders of magnitude. This is the cosmological constant problem - the largest numerical disagreement between a theoretical prediction and observation in the history of physics.

D.3 The Two Ontological Corrections to the Standard QFT Treatment

Correction 1 - Multiplicity of independent quantum fields.

QFT treats each particle species as a separate quantum field permeating all space, each contributing its own zero-point energy. This results in a sum over approximately 17 distinct fields. In the BFUT framework there is one underlying physical medium, the Spaticle substrate, of which every particle and every force carrier is an organised excitation. There are not 17 independent vacuum energies. There is one substrate.

Correction 2 - Zero-point energy assigned to empty modes.

QFT assigns ½ħω to every mode of every field regardless of whether that mode contains any physical excitation. In the BFUT ontology, ½ħω is the minimum internal circulation energy of an organised condensation. It is a property of matter, not of empty space. An empty substrate mode contains no condensation, no internal circulation, and therefore no ground-state energy floor. Empty modes contribute zero.

D.4 Application of the BFUT Corrections

When both errors are corrected:

- The mode sum is performed over one underlying physical medium, not 17 independent fields.
- Zero-point energy is assigned exclusively to modes that correspond to actual organised condensations. All empty substrate modes contribute zero.

For the pure vacuum state - containing no condensations whatsoever - the entire mode sum vanishes identically. What remains is the background equilibrium energy density of the physical medium itself:

$$\rho_{vac} = \rho_s \cdot c^2 \approx 5.30 \times 10^{-10}\ J/m^3$$

This is exactly the observed value. The enormous QFT prediction collapses by 120 to 122 orders of magnitude through the removal of unphysical contributions, without fine-tuning, new parameters, or mathematical cancellation.

D.5 Alternative Derivation: Direct Ontological Result

The same result follows more directly from substrate ontology without entering a QFT mode sum at all. The vacuum is the Spaticle substrate at its equilibrium density ρ_s, containing no organised condensations. By mass-energy equivalence applied to this equilibrium state:

$$\rho_{vac} = \rho_s \cdot c^2$$

Both derivation paths converge on the same result. The QFT-style derivation is especially significant because it shows that even conventional QFT reasoning, once corrected at the ontological level, yields the correct small value.

D.6 The Independent Status of ρ_s

The substrate equilibrium density ρ_s ≈ 5.9 × 10^{-27} kg/m³ is not chosen or adjusted to match cosmological observations. It is independently constrained from five physical sectors spanning quantum to cosmological scales, none of which involve vacuum energy or cosmological constant fitting:

- **W and Z boson masses** derived from substrate reconfiguration energies at the femtometre scale. Agreement with both measured masses from a single substrate density with no additional free parameters.
- **Galaxy rotation curves** validated across 175 galaxies from the SPARC dataset. The DM1 entrainment formula reproduces rotation curves with shape agreement 86.3% across all 175 galaxies with no per-galaxy tuning.
- **KiDS-1000 weak gravitational lensing** profiles across galaxy clusters at cosmological scales, independently confirming the same substrate density.
- **Hydrogen atomic stability** derived from the substrate-anchored reduced Planck constant and electron mass, reproducing the Bohr radius and hydrogen ground-state energy to 99.96% agreement with no fitted parameter (Paper 25).
- **The matter-stability condition** stable matter requires the substrate at every formation pathway, independent of formation history, a necessary condition, not a numerical fit.

A density constrained simultaneously from particle masses at the femtometre scale, galactic dynamics at the kiloparsec scale, gravitational lensing at the gigaparsec scale, hydrogen atomic structure at the sub-nanometre scale, and the independent matter-stability condition is not behaving as a free parameter. It is an emergent substrate constant constrained across multiple physical regimes.

Therefore when the corrected QFT calculation yields ρ_vac = ρ_s·c², it constitutes a genuine prediction of the framework, not a fitted result.

D.7 Dark Energy, the Cosmological Constant, and the Λ Tension

The LCDM cosmological constant Λ is commonly interpreted as a measure of dark energy - a distinct physical entity causing the acceleration of the observable universe. Within the BFUT framework this interpretation does not arise and dark energy is not a separate physical entity.

The LCDM Λ is not a property of the vacuum. It is a geometric fitting parameter derived from the observed expansion rate:

$$\rho_\Lambda = 3\Omega_\Lambda H_0^2 / (8\pi G)$$

This parameter changes every time H_0 is remeasured. H_0 has been revised repeatedly - from 500 km/s/Mpc in 1929 downward through successive measurements to current values near 67

to 73 km/s/Mpc depending on the measurement method. Each revision changes ρ_Λ proportionally through H_0^2. A quantity that changes with every new Hubble measurement is not a physical property of the vacuum.

ρ_s by contrast is the same at every point in an infinite BFUT universe, at every epoch, independent of expansion rate measurements. The physical vacuum energy density $\rho_{vac} = \rho_s \cdot c^2$ is a fixed substrate property. The apparent numerical proximity of ρ_Λ to $\rho_s \cdot c^2$ at the current epoch is a transient coincidence arising from the particular stage of cosmic evolution at which ρ_Λ is currently being measured, not a physical identity between them.

The large-scale bulk flow and cosmic dipole structure observed in galaxy surveys provide additional evidence that the apparent uniformity assumed in LCDM is incomplete and that the apparent acceleration attributed to dark energy reflects kinematic structure, not a separate vacuum energy component. A detailed account of the BFUT treatment of bulk flow, cosmic dipole, and the reinterpretation of the Hubble tension is given in the companion paper on large-scale substrate structure.

The resolution of the cosmological constant problem in BFUT therefore has two components. First, the 120-order-of-magnitude tension between the QFT vacuum energy prediction and observation is resolved by the two ontological corrections above. Second, the apparent small positive Λ detected in LCDM is not a property of the physical vacuum but a time-varying geometric parameter encoding the current expansion state of the observable universe. Neither component requires dark energy as an independent physical entity.

D.8 Summary

The cosmological constant problem arises from two compounding errors in the standard QFT treatment of the vacuum. Correcting both - one physical field, and zero-point energy only for organised condensations - causes the enormous QFT vacuum energy to collapse exactly to $\rho_s \cdot c^2$. The substrate density ρ_s is independently constrained across five physical sectors from quantum to cosmological scales and is not a free parameter. The LCDM cosmological constant Λ is a geometric fitting parameter that changes with H_0 measurements and is not a physical property of the vacuum. Dark energy is not a separate physical entity within the BFUT framework.

References

[1] Mayer, M. G. (1949). On closed shells in nuclei. Physical Review, 75(12), 1969. DOI: 10.1103/PhysRev.75.1969

[2] Jensen, J. H. D., Haxel, O., and Suess, H. E. (1949). On the magic numbers in nuclear structure. Physical Review, 75(11), 1766. DOI: 10.1103/PhysRev.75.1766

[3] Weinberg, S. (1995). The Quantum Theory of Fields, Volume 1. Cambridge University Press.

[4] Schrödinger, E. (1926). Quantisierung als Eigenwertproblem. Annalen der Physik, 79, 361-376.

[5] Hartwell, L. H., Hopfield, J. J., Leibler, S., and Murray, A. W. (1999). From molecular to modular cell biology. Nature, 402(6761 Suppl), C47-C52. DOI: 10.1038/35011540

[6] Sharma, V. S. (2026). Cold, Dark, and Inevitable: A Logical Reconstruction of the Universe Before the Big Flare-Up (BFUT P8). Zenodo. DOI: 10.5281/zenodo.19323579

[7] Sharma, V. S. (2026). Cosmic Rotation Across Scales, Emergent Orbital Hierarchy, and the Large-Scale Challenge to Metric Expansion (BFUT P9). Zenodo. DOI: 10.5281/zenodo.19341549

[8] Sharma, V. S. (2026). From Matter and Fundamental Forces to Consciousness: A Unified Framework of Sensing Channels, Control, and Evolution (BFUT P20). Zenodo. DOI: 10.5281/zenodo.19992457

[9] Sharma, V. S. (2026). The Consciousness Index (CI): A Physically Grounded Scalar Measure of Conscious Degree, Structure, and Evolutionary Potential (BFUT P21). Zenodo. DOI: 10.5281/zenodo.20025739

[10] Sharma, V. S. (2026). The Big Flare-Up Theory: Quantum Genesis of an Infinite Universe - A Unified Architecture for Cosmology, Particle Physics, Quantum Mechanics and Consciousness with Zero Free Parameters. Zenodo. DOI: 10.5281/zenodo.19149785

[11] Sharma, V. S. (2026). BFUT Full Functional Code Deposit. Zenodo. DOI: 10.5281/zenodo.20517866

[12] Sharma, V. S. (2026). The Spaticle Field as the Unified Substrate of Physical Reality: A Cross-Programme Synthesis of Convergent Evidence, From Cosmology and Particle Masses to Consciousness (BFUT P14). Zenodo. DOI: 10.5281/zenodo.19394064

[13] Sharma, V. S. (2026). What Existed Before Matter and the Spaticle Field: The Origin of Space, Time, and the Physical Substrate of Reality in an Infinite Universe (BFUT P15). Zenodo. DOI: 10.5281/zenodo.19811691

[14] Sharma, V. S. (2026). A Steady-State Nucleosynthesis Resolution of the Cosmological Lithium Problem (BFUT P3). Zenodo. DOI: 10.5281/zenodo.19205920

[15] Sharma, V. S. (2026). The Universe Has No Boundary: Logical, Derivational, and Observational Arguments for Spatial Infinitude (BFUT P5). Zenodo. DOI: 10.5281/zenodo.19242759

[16] Sharma, V. S. (2026). Layer 2. Vijay's Law: Everything in the Universe Is Alive and Conscious (L2-1). Zenodo. DOI: 10.5281/zenodo.19504923

[17] Sharma, V. S. (2026). The Emergence of Forces and Fundamental Senses: How the Spaticle Field Gave Rise to Gravity and All Other Forces (BFUT P17). Zenodo. DOI: 10.5281/zenodo.19976408

[18] Sharma, V. S. (2026). Beyond General Relativity: A Unified Gravitation Equation Across Quantum, Classical, Galactic, and Rapid-Transition Regimes (BFUT P18). Zenodo. DOI: 10.5281/zenodo.20145506

[19] Sharma, V. S. (2026). Unification of Particle Physics: Deriving Fine Structure and Coupling Constants, W, Z, and Higgs Boson Masses, Redefining and Unifying Gravity and Time (BFUT P19). Zenodo. DOI: 10.5281/zenodo.20145567

[20] Sharma, V. S. (2026). Unifying Quantum Mechanics with Gravity, Demystifying Twenty Quantum Phenomena Including Half-Integer Spin, the Born Rule, Wave Function Collapse, and Higgs Physics (BFUT P19A). Zenodo. DOI: 10.5281/zenodo.20145695

[21] Sharma, V. S. (2026). Companion Simulations: Substrate Physics Visualised. Zenodo. DOI: 10.5281/zenodo.20554084

[22] Sharma, V. S. (2026). Antimatter, Annihilation, and the Stability Filter: Predictions for the CERN Antihydrogen Programme. BFUT P16A. Zenodo. DOI: 10.5281/zenodo.20201014

[23] Einstein, A. (1931). Zum kosmologischen Problem der allgemeinen Relativitatstheorie. Sitzungsberichte der Preussischen Akademie der Wissenschaften, 235-237.

[24] Bondi, H., and Gold, T. (1948). The steady-state theory of the expanding universe. MNRAS, 108, 252-270. DOI: 10.1093/mnras/108.3.252

[25] Hoyle, F. (1948). A new model for the expanding universe. MNRAS, 108, 372-382. DOI: 10.1093/mnras/108.5.372

[26] Hoyle, F., and Narlikar, J. V. (1964). A new theory of gravitation. Proc. R. Soc. A, 282, 191-207. DOI: 10.1098/rspa.1964.0213

[27] Hoyle, F., Burbidge, G., and Narlikar, J. V. (1993). A quasi-steady state cosmological model with creation of matter. ApJ, 410, 437-457. DOI: 10.1086/172761